Tumors of the Central Nervous System

6

Kar-Ming Fung, Zhongxin Yu, and Kalliopi Petropoulou

Normal Anatomy and Development

Knowledge of normal neuroanatomy and neurodevelopment is critical to proper diagnosis. A few normal structures may be mistaken as tumor particularly on frozen sections.

The external granular layer (Fig. 6.1a) is a layer of small neurons that covers the external surface of fetal/infant cerebellum. It is quite prominent at the time of birth but is almost completely regressed by the ninth postnatal month. It should not be misinterpreted as medulloblastoma or lymphocytic infiltration in younger infants. The internal granular layer is also composed of small neurons. Without a size comparison, these cells may be mistaken for medulloblastoma or other small blue cell tumors in minute specimens or cytologic preparations. Conversely medulloblastoma cells, particularly those with smaller nuclei, can be mistaken as internal granular cells. Purkinje cells are rather large and should not be mistaken as rhabdoid cells (Fig. 6.1b). Other normal structures that can be mistaken for neoplastic tissue include the posterior pituitary and the pineal gland which may be mistaken as glial neoplasm and normal choroid plexus being mistaken as choroid plexus papilloma. These misinterpretations are likely to be committed when the specimen is minute and communication between the pathologist and the neurosurgeon is poor.

K.-M. Fung, M.D., Ph.D. (✉) • Z. Yu, M.D.
Department of Pathology, University of Oklahoma Health Sciences Center, BMSB 451, 940 Stanton Young Blvd., Oklahoma City, OK 73104, USA
e-mail: karming-fung@ouhsc.edu

K. Petropoulou, M.D.
Department of Radiology, State University of New York (SUNY) Upstate, Syracuse, NY 13210, USA

Overview and Classification

Tumor of the CNS is not uncommon in the pediatric age group and some of these entities occur only rarely in adults (Table 6.1). While meningiomas are very common in adults, it is uncommon in children and almost nonexistent in infants. The most common pediatric tumors in descending order of frequency are pilocytic astrocytoma, diffuse astrocytomas, medulloblastomas, and craniopharyngiomas. Ependymal neoplasms and schwannomas are the most frequent infratentorial tumors. Most tumors occur in the brain with a supratentorial-to-infratentorial ratio of approximately 2-to-1. Malignant CNS neoplasms represent 16.6 % of all malignancies in the pediatric age group. In general, the incidence is higher in males than females and among white compared to black children. The incidence is 36.2 per million between infancy and 7 years of age and 21.0 per million between 7 and 10 years of age. As a group, they are the second most frequent malignancy and most common solid tumor in pediatric patients. About 2,200 new cases are diagnosed annually in the United States. Among CNS malignancies, astrocytic tumors account for 52 %, while medulloblastoma and primitive neuroectodermal tumor (PNET), other gliomas, and ependymomas accounted for 21, 15, and 9 %, respectively [2].

In contrast to adults, there is a high occurrence of malignancies in the cerebellum and brain stem in young children. About 40 % of all thalamic tumors arise in patients under 18 years old and account for 2–5 % of all intracranial tumors in children [3]. About two third or pediatric thalamic tumors are high grade in histology [4]. Tumor of the spinal cord represents about 9.9 % and extramedullary tumors are slightly more common than intramedullary tumors [5]. Astrocytomas are most common and comprise 70 % of tumors arising in the spinal cord of children. In contrast, ependymoma is the most common spinal cord tumor in adults [6]. Although hemangioblastoma is common in adults [6], it is uncommon in children other than those affected by von Hippel Lindau syndrome. Myxopapillary ependymoma and paraganglioma

D.M. Parham et al. (eds.), *Pediatric Malignancies: Pathology and Imaging*,
DOI 10.1007/978-1-4939-1729-7_6, © Springer Science+Business Media New York 2015

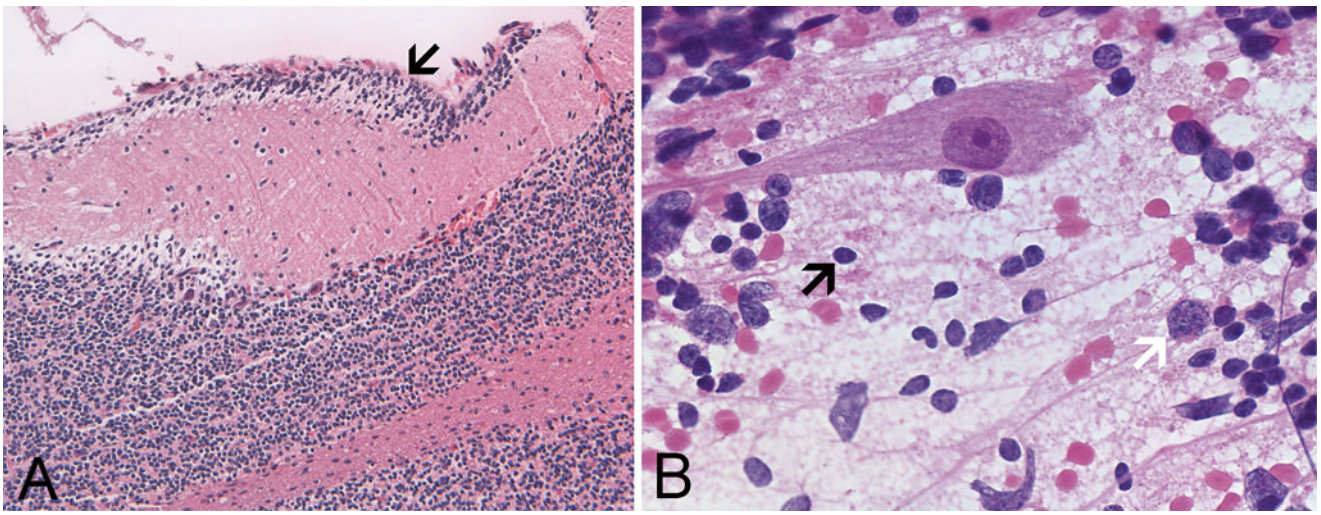

Fig. 6.1 Normal anatomy: (**a**) The external granular layer (*arrow*) is a transient structure that is present in infants, and much less commonly, toddlers. It should not be mistaken as evidence of meningitis or neoplastic changes. (**b**) In this cytologic preparation, the large cell is a Purkinje cell. The smaller cells (*black arrow*) are internal granular cells. They are monotonous and almost always appear in form of naked nuclei. Medulloblastoma cells, for comparison here, are larger and more variable in size (*white arrow*)

Table 6.1 WHO classification and grades of tumors

Tumor	I	II	III	IV
Astrocytic tumors				
Subependymal giant cell astrocytoma[a]	■			
Pilocytic astrocytoma[a]	■			
Pilomyxoid astrocytom[a] a		■		
Diffuse astrocytoma[b]		■		
Pleomorphic xanthoastrocytoma		■		
Anaplastic astrocytoma			■	
Glioblastoma[a]				■
Giant cell glioblastoma				■
Gliosarcoma				■
Gliomatosis cerebri[b]			■	
Oligodendroglial tumors				
Oligodendroglioma		■		
Anaplastic oligodendroglioma			■	
Oligoastrocytic tumors				
Oligoastrocytoma		■		
Anaplastic oligoastrocytoma			■	
Ependymal tumors				
Subependymoma	■			
Myxopapillary ependymoma[a]	■			
Ependymoma[a]		■		
Anaplastic ependymoma[a]			■	
Choroid plexus tumors				
Choroid plexus papilloma[a]	■			
Atypical choroid plexus papilloma[a]		■		
Choroid plexus carcinoma[a]			■	
Other neuroepithelial tumors				
Astroblastoma[c, d]				
Angiocentric glioma[c]	■			
Choroid glioma of the third ventricle		■		

Table 6.1 (continued)

Tumor	I	II	III	IV
Neuronal and mixed neuronal-glial tumors				
Gangliocytoma[a]	■			
Ganglioglioma[a]	■			
Anaplastic ganglioglioma[a]			■	
Desmoplastic infantile astrocytoma and ganglioglioma[a]	■			
Dysembryoplastic neuroepithelioma[a]	■			
Central neurocytoma		■		
Extraventricular neurocytoma		■		
Cerebellar liponeurocytoma		■		
Paraganglioma of the spinal cord	■			
Papillary glioneuronal tumor[b]	■			
Rosette-forming glioneuronal tumor of the fourth ventricle[b]	■			
Dysplastic gangliocytoma of the cerebellum (lhermitte-Duclos disease)[b, e]	■			
Pineal tumors				
Pineocytoma[a]	■			
Pineal parenchymal tumor of intermediate differentiation[a]		■	■	
Pineoblastoma[a]				■
Papillary tumor of the pineal region[b]		■	■	
Embryonal tumors				
Medulloblastoma[a]				■
CNS primitive neuroectodermal tumor (PNET)[a]				■
Atypical teratoid/rhabdoid tumor[a]				■
Tumors of the cranial and paraspinal nerves				
Schwannoma	■			
Neurofibroma[a]	■			
Perineurioma	■	■	■	
Malignant peripheral nerve sheath tumor (MPNST)[b]		■	■	■

(continued)

Table 6.1 (continued)

Tumor	I	II	III	IV
Meningeal tumors				
Meningioma	■			
Atypical meningioma		■		
Anaplastic/malignant meningioma			■	
Hemangiopericytoma		■		
Anaplastic hemangiopericytoma			■	
Hemangioblastoma	■			
Tumors of sellar region				
Craniopharyngioma[a]	■			
Granular cell tumor of the neurohypophysis	■			
Pituicytoma	■			
Spindle cell oncocytoma of the adenohypophysis	■			
Miscellaneous tumors of the CNS				
Primary malignant lymphoma of the CNS[d]				
Histiocytic tumors[a, d]				
CNS germ cell tumors[a, d]				

[a]These tumors are common in children. Some of them, such as medulloblastoma and pilocytic astrocytoma, occur mostly in infants and children. Others, such as glioblastoma, are also common in adults
[b]These tumors can be seen in the second decade of life but are uncommon in younger patients. They also have significant incidence in adults
[c]The incidence of these tumors is very small. However, cases have been reported in the pediatric age group
[d]WHO has not established a grading system for these tumors
[e]As per WHO, it is not clear whether this is neoplastic or hamartomatous. If neoplastic, it corresponds histologically to WHO grade I
Modified from the WHO classification of tumors of the central nervous system [1]

(rare in children) are two entities that are mostly limited to the filum terminale.

The incidence of congenital brain tumors is reported to be 11 per million live births with medulloblastoma as the most frequent one in one study [7]. In another study, teratoma is the most frequent followed in descending order by glioblastoma, intracranial lipoma, choroid plexus papilloma, craniopharyngiomas, and others [8].

Overview of Diagnostic Imaging Approach

While computed tomography (CT) provides excellent demonstration of acute intracranial hemorrhage or calcifications, the superb soft tissue resolution and direct multiplannar imaging capability of magnetic resonance imaging (MRI) make it the modality of choice. Different excitation and relaxation sequences with or without gadolinium provide a comprehensive delineation of tumors in terms of extent and relationship with surrounding tissue. Fluid attenuation with image recovery (FLAIR) and T2-weighted sequences provide valuable estimation on the extent of edema and differentiation of solid from cystic components. Gradient echo sequences are sensitive to susceptibility artifact and can detect tiny amounts of blood products and, though slightly less effectively, calcification in the brain parenchyma and tumor bed. CT, however, remains a key modality in evaluation of the bony calvarium.

Proton magnetic resonance spectroscopy (MRS) detects important metabolites like choline, creatine, *N-acetyl-aspartate* (NAA), lactate, and lipid which form the major peaks and shed light on the tumor composition. Choline reflects membrane turn over; creatine reflects energy metabolism; NAA is a marker of neuronal cells; lactate is detected in necrotic tumor or ischemic/infarcted brain; and a lipid peak reflects myelin breakdown and necrosis. Tumors almost invariably are associated with decreased NAA/creatine ratio, increased choline/creatine ratio, and increased lactate. Increased choline/NAA ratio is often seen in cellular tumor due to the increase in cell membranes. Increased lactate peak is suggestive of necrosis and tumor aggressiveness [9, 10]. While MRS is useful in separating residual tumor from post radiation changes and from tumor progression with necrosis, it is sensitive but not specific and must be interpreted in conjunction with MRI. For example, pilocytic astrocytoma typically shows an elevated lactate peak [11] which is otherwise a hallmark of more aggressive tumors such as glioblastoma.

Diffusion based MRI techniques include diffusion-weighted imaging (DWI) which evaluates microscopic water diffusion within tissues and thus provides information on the degree of cellularity of a lesion. DWI distinguishes reliably between cystic and solid masses when both are hyperintense on T2-weighted sequences. The most notable example is the differentiation of an arachnoid cyst from epidermoid. DWI has also proven helpful in distinguishing brain tumors with necrosis from abscess. DWI along with the calculated apparent diffusion coefficient (ADC) maps have recently been utilized to assess tumor cellularity in an attempt to differentiate between different brain tumors [12, 13]. Diffusion tensor imaging (DTI) demonstrates the relation between tumor and adjacent white matter tracts that may be infiltrated or displaced by tumor. DTI is a useful tool for stereotactic surgical planning.

Perfusion-weighted imaging (PWI) can be performed either with CT or with MRI. CT perfusion though is deemed inappropriate for children because of the involved radiation exposure. Perfusion weighted imaging of a brain tumor reflects the degree of angiogenesis and abnormal neovascularity with leaky vessels. Different perfusion techniques are available and include dynamic susceptibility contrast enhanced (DSC), arterial spin label (ASL), and dynamic contrast enhanced (DCE) techniques. DSC echo planar imaging is utilized most commonly to acquire data from which maps of relative cerebral blood flow (rCBF), relative cerebral volume (rCBV), and mean transit time (MTT) are calculated. rCBV is the most useful parameter in the evaluation of brain tumors [14] because increased angiogenesis and neovascularity are features of tumors with higher aggressiveness. Currently, the most common application of perfusion

MRI is to define the area of the tumor with highest perfusion (CBV) and thus the highest histologic grade [15] for biopsy. PWI may also help in distinguishing between post-radiation injuries from tumor recurrence [16].

Intraoperative Consultation, Immunohistochemistry, and Molecular Pathology

Cytologic preparation and frozen section are the two arms in intraoperative diagnosis. The authors prefer to do a squash preparation by pressing a piece of representative tissue about 1 mm cube in volume between two microscopic glass slides and then smear. After the squash, the two slides should be separated momentarily to let air in before smearing in order to produce a smooth smear. Methanol is the preferred fixative, and it is extremely important to put the slides immediately into the methanol without delay in order to avoid air dry artifacts. The authors turn hematoxylin-stained slides blue with tap water rather than ammonium water in order to preserve nuclear details and avoid washout of necrotic debris and macrophages. Routine hematoxylin and eosin stain is sufficient in most circumstances. Toluidine blue is a good adjunct in demonstrating the metachromatic mucoid substances in glioma and Romanowsky-type stains such as DiffQuick are helpful when lymphoma is suspected.

Most diagnostic procedures with the exception of cytogenetics can be performed on formalin fixed paraffin embedded sections. Collection of fresh and snap frozen tissue, however, is often required by research protocols. Immunohistochemistry and special stains (Table 6.2) remain the most frequently

Table 6.2 Common immunohistochemical markers and special stains

Immunohistochemistry	Properties and applications
Ki-67 and PHH3	*Summary*: Ki67 is a non-histone protein that is present in all phases of cell cycle except Go and the early G0-G1 transitional phase. Phosphohistone-H3 (PHH3) is a histone associated with condensed chromatin during mitosis *Application*: Ki67 is useful for estimation of overall proliferation and PHH3 is useful for highlighting mitotic figures [240]. The immunoreactivities are in the nuclei
Olig2	*Summary*: Olig1 and Olig2 are transcription factors that regulate oligodendroglial development [241, 242] *Application*: Olig2 has been shown to be widely expressed in gliomas that include both astrocytic and oligodendroglial tumors [182, 243–246]. Similar to other transcription factors, the immunoreactivities are in the nuclei
Glial fibrillary acidic protein (GFAP)	*Summary*: this is a class III intermediate filament of 55 kDa. GFAP is expressed in mature astrocytes. It may co-express with other intermediate such as vimentin *Application*: in gliomas, GFAP are often positive in tumors with glial differentiation. Oligodendroglioma also expression GFAP so it is not a useful marker in separating these two entities. GFAP is usually extensively expressed in ependymal tumors
Synaptophysin	*Summary*: Synaptophysin is an acidic, *N*-glycosylated integral membrane glycoprotein of 38–42 kDa that is expressed in the CNS *Application*: it is expressed in tumors with neuroendocrine differentiation including medulloblastomas and central neurocytomas. However, weak to moderate expressions have been described in gliomas including pilocytic astrocytomas [134] and oligodendrogliomas
NeuN	*Summary*: NeuN, for neuronal nuclei, is a neuronal nuclear antigen is expressed predominantly in the nuclei and some minor cytoplasmic expression and is a marker for mature neurons *Application*: it is a good tool for demonstration of mature neuronal phenotypes and to detected scattered neurons that are entrapped within an infiltrating glioma [247, 248]
Epithelial membrane antigen (EMA)	*Summary*: this is a group of high molecular mass molecules with a high carbohydrate content. They are widely expressed by many epithelial cells *Application*: EMA is expressed by meningiioma, ependymoma, and AT/RT. The expression, however, is not very consistent and therefore the absence of immunoreactivity does not rule out a meningioma or ependymoma
BAF47	*Summary*: this antibody is specific for the gene product of *hSNF5/INI1* (*SMARCB1*) gene *Application*: immunoreactivity can be detected in normal cells. In tumors of the central nervous system, this gene is mutated or deleted in AT/RT and therefore not expressed in these tumors (i.e., negative staining indicates positive result indicating deletion or mutation) [92, 93]
Special Stain	*Properties and applications*
Periodic acid Schiff (PAS) stain with diastase digestion	*Application*: this is useful in demonstration of eosinophilic granular bodies particularly when they are scant
Luxol fast blue	*Application*: Luxol fast blue can be combined with other stain for detection of demyelination. Luxol fast blue-PAS is a good combination as this stain demonstrate macrophages as well
Masson's trichrome	*Application*: this is a useful stain in separating collagenous/desmoplastic component from the glial component
Reticulin	*Application*: reticulin deposition is typically found around individual cells in schwannoma, pleomorphic xanthoastrocytomas, and desmoplastic infantile ganglioglioma/astrocytoma

used special studies followed by fluorescence in situ hybridization (FISH) and other molecular techniques.

Electron microscopy still has a minor role in the diagnosis of ependymal tumors, meningeal tumors, and a few other tumors. The use of molecular pathology has gained impressive momentum, and the details will be discussed with their relevant entities.

Non-neoplastic Tumor-Like Mimickers

The first important step in oncologic pathology is to rule out non-neoplastic mimickers. Detailed clinical and imaging studies are invaluable in recognizing these mimickers.

The bulk of these mimickers are related to inflammation with or without histiocytic infiltration, infection, and infarction. While a demyelinating process is a common tumor mimicker in adults in western countries, this is uncommon in the pediatric age group, particularly among boys. Other common tumor mimickers include abscess and local extension of infection from middle ear infection, tuberculosis in the form of tuberculoma, toxoplasmosis, and other parasites such as neurocysticercosis and echinococcosis, granulomatous inflammation other than tuberculosis, and infarction. The other entities that would lead to surgical intervention include vascular lesions, heterotopia, and ectopia such as hypothalamic hamartoma. Although radiation necrosis is a common mimicker of genuine neoplasm in adults, it is rather uncommon as a surgical specimen in pediatric patients.

Conversely, it should be noted that substantial histiocytic infiltration and inflammation can pose diagnostic challenges particularly in cases of germ cell tumors and lymphoma, although primary CNS lymphoma is rare in the pediatric group.

Tumors with Features of the Developing Central Nervous System

This is a family of tumors with morphological and molecular phenotypes recapitulating embryonal stages of the developing CNS. These tumors are highly cellular, highly aggressive tumors that occur most frequently, if not exclusively, in infants and children. Some may occur as congenital tumors. Specific genetic aberrations are common and often provide in-depth understanding in the biology.

In the WHO classification, there are three major groups: medulloblastoma and its variants including desmoplastic/nodular medulloblastoma, medulloblastoma with extensive nodularity, anaplastic medulloblastoma, large cell neuroblastoma; CNS primitive neuroectodermal tumor including CNS neuroblastoma, CNS ganglioneuroblastoma, medulloepithelioma, ependymoblastoma; and atypical teratoid/rhabdoid tumor (AT/RT).

Medulloblastoma and Its Variants

Definition: Medulloblastoma is a malignant, invasive embryonal tumor of the cerebellum.

Clinical features: Medulloblastoma is the most common malignant brain tumor of childhood. It occurs predominantly in children with a peak age at presentation of 7 years; it is the most frequent malignant tumor of the CNS in children with an estimated annual incidence of 5 per million children under 15 years of age. About 10 % appear in adults and occur almost exclusively in young adults between 20 and 40 years of age. There is no definitive sex predilection. While dissemination through the cerebrospinal fluid (CSF) is a rule, metastasis outside the CNS is uncommon and most frequent involves bone followed by lymph nodes [17].

Phenotypically, medulloblastoma recapitulates the embryonal CNS but morphologic features and phenotypic markers indicative of further differentiation such as glial, neuronal, photoreceptor, myogenic, and melanotic differentiation can be seen in some cases. While most cases are sporadic, medulloblastoma is associated with a short list of hereditary cancer syndrome (Tables 6.3 and 6.4). Variants of medulloblastoma include the two with improved prognosis, namely desmoplastic medulloblastoma and medulloblastoma with extensive nodularity, and the two variant with worse prognosis, namely anaplastic medulloblastoma and large cell medulloblastoma. Most medulloblastomas arise in the midline. Hemispheric tumors tend to arise in older patients (adolescents and young adults) many of these tumors are desmoplastic medulloblastomas [18] However, molecular advancements have revolutionized our understanding of these tumor well beyond their histopathology (see below). Rare cases of maturation of medulloblastoma after therapy have been reported [19].

Imaging findings: Over 75 % of medulloblastomas [18] occur at the vermis at the level of posterior vellum medullaris and protrude into the fourth ventricle. Although usually solid, a cystic component is not uncommon. The solid part is isodense or slightly hyperdense to the gray matter on CT. On MRI (Fig. 6.2), medulloblastomas are almost isointense to gray matter on T1-weighted images and hypointense on T2-weighted images likely due to their high cellularity. The potential association of the tumor with a cystic component, hemorrhage or calcification may result in a heterogeneous appearance. Contrast enhancement is variable and some cases have no enhancement at all. Because medulloblastoma has high cellularity it would be expected to have a relatively low ADC value but this observation is not universal [20]. Leptomeningeal dissemination presents as diffuse meningeal enhancement with or without enhancing nodules in the subarachnoid space of the brain or spinal cord [21]. Medulloblastoma encountered in older patients may originate in the cerebellar hemisphere and have a more heterogeneous appearance especially on MRI [22].

Table 6.3 Hereditary cancer syndromes associated with medulloblastoma

Syndrome	locus/gene	Features
Turcot syndrome (Type 2) [249]	*APC*, 5q21-q22	*Autosomal dominant Medulloblastoma tumor risk*: 20 %
Faconi anemia subtype D1 [250, 251]	*BRCA2*, 13q12.3	*Medulloblastoma tumor risk*: high
Nevoid basal cell carcinoma syndrome/Gorlin syndrome [252–255]	*PTCH*, 9q22.3	*Autosomal dominant Medulloblastoma tumor risk*: 4 %
Li-Fraumeni syndrome [256]	*TP53*, 17p13.1	*Autosomal dominant Medulloblastoma tumor risk*: 10 %
Rubinstein-Taybi syndrome[a] [257]	*CREBBP*, 16P13.3	*Medulloblastoma tumor risk*: rare
Coffin-Siris syndrome[a] [258, 259]	*ARID1A, AR1D1B, SMARCA4, SMARCB1, SMARCE1*	*Medulloblastoma tumor risk*: rare
Megalencephaly and perisylvian polymicrogyria with postaxial polydactyly and hydrocephalus syndrome [260]	*Unbalanced der(5)t(5;20) translocation*[b]	*Medulloblastoma tumor risk*: uncertain
DICER1 syndrome or Pleuropulmonary blastoma family tumor and dysplasia syndrome (PPB-FTDS) [261]	*DICER1*, 14q32.13	*Medulloblastoma tumor risk*: about 1 %

[a]These syndromes are rare, only three cases and eight cases are reported for Rubinstein-Taybi syndrome and Coffin-Siris syndrome respectively
[b]Based on the study of two cases

Classic medulloblastoma: Clinical manifestations are cerebellar symptoms and those resulted from increased intracranial pressure and hydrocephalus secondary to obstruction. These include truncal ataxia, gait disturbance, lethargy, headache, and morning vomiting.

Surgical specimens of medulloblastoma are typically composed of small pieces of pale, semitranslucent tissue with the consistency of sticky soft glue with no suggestion of necrosis. Disseminated translucent coating of the cerebellum (the so-called sugar coating) can be well appreciated in autopsy cases.

Cytologically, medulloblastoma is composed of hyperchromatic, small blue cells with a thin rim of cytoplasm, and slightly crumbled nuclei (Fig. 6.3) without prominent nucleoli. As stated previously, smears of internal granular layer should not be mistaken for medulloblastoma cells (Fig. 6.1a). Medulloblastoma cells are larger than internal granular cells and a comparison of size between different cells on the smear would help to avoid this pitfall (Fig. 6.1b). In smears with prominent nuclei and significant increase in amount of cytoplasm, the differential diagnoses of large cell/anaplastic medulloblastoma and AT/RT must be entertained. Histologically (Fig. 6.3a–c), classic medulloblastoma is a small blue cell tumor composed of carrot-shaped cells with hyperchromatic nuclei. Occasionally, Homer Wright rosettes and palisading ribbons of tumor cell nuclei reminiscent of a picket fence can be seen. Both necrosis and endothelial proliferation are uncommon, but small areas of pseudopalisading necrosis can occur. One of the salient features of the developing CNS is high rate of cell proliferation and apoptosis. These features are often, but not always, well reflected in medulloblastomas as they typically contain mitoses and apoptotic bodies, albeit, atypical mitosis are rather uncommon.

Superficial spread along the cerebellar surface and Virchow-Robin spaces should not be mistaken as persistent external granular layer. The age of the patient can be a useful hint. Invasion of the leptomeninges may trigger fibrotic reactive changes. These areas, when being examined out of context, particularly as frozen section, may suggest a sarcoma or entities other than medulloblastomas.

Large cell medulloblastoma and anaplastic medulloblastoma: Although large cell medulloblastoma and anaplastic medulloblastoma are different subtype in the WHO classification, they have significant overlapping histopathologic features. About 2–4 % of medulloblastomas are large cell medulloblastomas. Large cell medulloblastomas have anaplastic features including large, round, vesicular nuclei with prominent nucleoli, and nuclear wrapping is a common feature (Fig. 6.3d–f). Necrosis and apoptotic cells, often in the form of small clusters, are common. The prominent nucleoli can be efficiently identified on cytologic preparations. Although AT/RT also has large and prominent nucleoli, rhabdoid cells can be usually found to confirm the diagnosis.

Imaging findings: All types of medulloblastomas share similar signal characteristics and variable enhancement on conventional MRI. Anaplastic medulloblastomas have been found to have increased ADC values and rim enhancement attributed to central necrosis [23].

Desmoplastic/nodular medulloblastoma: This variant has an increased tendency to occur at a hemispheric location and typically in adolescent and young adults. Histologically (Fig. 6.4), the salient features are "pale islands" (or nodules) of reticulin free tumor with reduced cellularity, decreased nuclear-to-cytoplasmic ratio, negligible mitotic rate, and high apoptotic rate surrounded by a densely packed, highly proliferative, hyperchromatic tumor reminiscent of classic medulloblastoma that contains a dense reticulin network. These islands represent regions of more mature phenotype.

Table 6.4 Hereditary tumor syndrome involving tumor of the nervous system[a]

Syndrome	Pathology	Genetics	Study
Tuberous sclerosis	*Nervous system*: cortical hamartomas (tubers), subependymal hamartoma and subependymal giant cell tumor *Extraneural*: adenoma sebaceum and other manifestations of skin, retinal astrocytoma, renal angiolipoma, cardiac rhabdomyoma and other systemic manifestations	*Inheritance*: autosomal dominant *Prevalence*: between 1 in 5,000 and 100,000 Gene: *TSC1* gene (tuberin) on chromosome 9q34 and *TSC2* gene on chromosome 16p13.3.	van Slegtenhorst et al. [262]
Neurofibromatosis type 1 (NF1)	*Nervous system*: Neurofibromas and malignant peripheral nerve sheath tumor of the peripheral nerve, gliomas of the brain *Extraneural*: multiple café-au-lait spots, rhabdomyosarcoma, phaeochromocytoma, carcinoid tumor, juvenile chronic myeloid leukemia, bone lesions and other manifestations	*Inheritance*: autosomal dominant *Prevalence*: 1 in 3,000–4,000 of the general population *Gene*: *NF1* gene (neurofibromin) on chromosome 17q2	Pollack and Mulvihill [263]; Von Deimling et al. [264]
Neurofibromatosis type 2 (NF2)	*Nervous system*: bilateral vestibular schwannomas, peripheral schwannomas, meningiomas and meningioangiomatosis, ependymomas, astrocytomas, glial hamartoma, and cerebral calcifications *Extraneural*: posterior lens opacity	*Inheritance*: autosomal dominant *Prevalence*: 1 in 50,000 of the general population *Gene*: *NF2* gene (merlin) on chromosome 22q12	Pollack and Mulvihill [263]
Von Hippel–Lindau disease	*Nervous system*: haemangioblastoma of the retina and CNS *Extraneural*: renal cysts and renal cell carcinoma, pancreatic cysts, islet cell tumors, phaeochromocytoma, and other manifestations	*Inheritance*: autosomal dominant *Prevalence*: 1 in 36,000 to 1 in 45,500 of the general population *Gene*: *VHL* gene is located on chromosome 3p25.3	Maddock et al. [265]
Naevoid basal cell carcinoma syndrome (Gorlin syndrome)	*Nervous system*: Medulloblastoma *Extraneural*: multiple basal cell carcinoma and keratocyst of the jaw. Abnormal ribs and other skeletal abnormalities, epidermal cysts, ovarian cysts and other features	*Inheritance*: autosomal dominant *Incidence*: 1 in 57,000 of the general population *Gene*: human homologue of the *Drosophilia* segment polarity gene patched (*PTCH*) on chromosome 9q22.3	Hahn et al. (1996) [255]; Vorechovsky et al. [266]
Cowden disease	*Nervous system*: dysplastic gangliocytoma of the cerebellum (Lhermitte–Duclos disease). Other pathological changes include megalencephaly and heterotopic gray matter. Meningiomas and medulloblastomas have also been described *Extraneural*: verrucous skin changes, papules and fibromas of oral mucosa, multiple facial trichilemmomas, hamartomas polyps of the colon, thyroid tumor and breast cancer	*Inheritance*: Autosomal dominant *Gene*: *PTEN/MMAC1* gene on chromosome 10q23.	Sutphen et al. [267]; Robinson and Cohen [268]
Turcot syndrome (type 1)	*Nervous system*: usually glioblastoma *Extraneural*: Café-au-lait spots. Small number of large colorectal polyps and high incidence of colorectal carcinoma. Some patients are associated with hereditary non-polyposis colorectal carcinoma syndrome (HNPCC)	*Inheritance*: autosomal dominant *Gene*: several genes involved in mismatch repair including *hMLH1* at chromosome 3p21, *hMLH2* at 2p16, *hMSH3* at 5q11-q13, *hMSH6/GTBP* at 2p16, *hPMS1* at 2q32 and *hPMS2* at 7p22	Cavenee et al. [269]
Turcot syndrome (type 2)	*Nervous system*: usually medulloblastoma *Extraneural*: associated with familial adenomatous polyposis syndrome (FAP). Patient has innumerable adenomatous colorectal polyposis and high incidence of colorectal carcinoma	*Inheritance*: autosomal dominant *Gene*: *APC* gene on chromosome 5q21 that is associated with familial adenomatous polyposis syndrome (FAP)	Hamilton et al. [247], [249]; Cavenee et al. [269]
Cobbs syndrome (Cutaneous angiomatosis multiple cavernous angiomas)	*Nervous system*: multiple intracranial cavernous haemangiomas *Extraneural*: some patients also have haemangiomas in the skin and other organs	*Inheritance*: autosomal dominant transmission has been shown in many cases Gene: the gene has not been identified but appears to be present on chromosome 7q11, 7p, and 3q	Laberge-le Couteulx et al. [270]
Sturge-Weber syndrome (Encephalofacial angiomatosis or Encephalotrigerminal angiomatosis)	*Nervous system*: meningeal haemangioma and meningeal hypervascularity, calcification in the cortical layer under the hypervascular meninges *Extraneural*: choroid haemangioma, angiomatosis of the skin and mucosa of face and neck	*Inheritance and gene*: unknown	

(continued)

Table 6.4 (continued)

Syndrome	Pathology	Genetics	Study
Rhabdoid predisposition syndrome	*Nervous system*: a typical rhabdoid tumor, choroids plexus carcinoma *Extraneural*: renal and extra-renal malignant rhabdoid tumor	*Inheritance*: the pattern of inheritance has not been confirmed as the number of reported pedigrees are limited *Gene*: mutation or deletion of the *hSN5/INI1* gene on chromosome 22q11.2	Sevenet et al. [267]; Taylor et al. [271]
Retinoblastoma (RB) gene deletion syndrome	*Nervous system*: retinoblastoma in the retina with or without PNET in the pineal gland (pineoblastoma) *Extraneural*: increased incidence of second malignancy, multiple congenital abnormalities and mental retardation	*Inheritance*: autosomal dominant *Gene*: *RB1* gene on chromosome 13q14.2	Sopta et al. [272]; Pratt et al. [273]
Li–Fraumeni syndrome	*Nervous system*: astrocytic tumor, oligodendroglioma, medulloblastoma, supratentorial PNET, and choroid plexus tumor *Extraneural*: tumor in various organs including the breast, lung, stomach, colon, pancreas, skin and others	*Inheritance*: autosomal dominant *Gene*: *TP53* on chromosome 17p13 and checkpoint kinase 2 (*hCKh2*) gene on chromosome 22q12	Tachibana et al. [274]

[a]Please refer to Table 6.3 for hereditary tumor syndromes associated with medulloblastoma

Desmoplastic/nodular medulloblastoma carries a better prognosis. This diagnosis should be made when the tumor is predominantly or exclusively composed of this nodular pattern. Medulloblastoma with only focal nodular pattern should not be classified as desmoplastic/nodular medulloblastoma.

Imaging findings: Desmoplastic medulloblastoma often presents as a cerebellar hemisphere mass that is isointense to gray matter on T2-weighted images and demonstrates moderate enhancement. The mass may extend to the overlying meninges resulting in moderate meningeal enhancement [22, 24].

Medulloblastoma with extensive nodularity: These tumors were previously designated as "cerebellar neuroblastoma." They typically occur in infants and are associated with good prognosis. Histologically, it is characterized by an expanded lobular architecture with large separated by elongated reticulin-free zones of variable thickness. These areas contain streaming small cells resembling the cells of a central neurocytoma. Maturation into tumors dominated by ganglion cells has been reported [19].

Imaging findings: The tumor has been described as an extensively nodular, grape-like mass [21] These tumors most often are located off midline, reveal isointense signal on T2W sequences and enhance on post-contrast imaging [25].

Melanotic and myogenic differentiation: Medulloblastomas mimic embryonal tissues in being able to differentiate along different phenotypes. Aside from glial and neuronal (including photoreceptors) features, occasional medulloblastomas have myogenic differentiation (previously termed medullomyoblastoma) and others have melanotic differentiation (previously melanocytic medulloblastoma). The former is composed of primitive neuroectodermal cells with rhabdomyoblastic cells, and the latter is characterized by primitive neuroectodermal cells with intracytoplasmic melanin. A case of medulloblastoma with melanotic and myogenic features has been reported [26]. These cases are rare and no specific imaging findings have been published.

Molecular pathology of medulloblastoma: A consortium of genetic abnormalities is associated with medulloblastoma. A multiparameter approach based on histology subtype, metastatic status, and genetic profile has recognized that medulloblastoma is composed of four distinct molecular groups with different risks: *WNT*/Wingless group, Sonic Hedgehog group, Group 3, and Group 4 [27–31], In general, the prognosis of group 3 and 4 is less favorable. A fifth group that can be designated as "not otherwise specified" may be included for rare tumors that cannot be assigned to a group in the 4-tier classification. Among the *WNT*/Wingless and Sonic Hedgehog groups, tumors with different features can be further separated into different risk groups [27, 32].

Immunohistochemistry and electron microscopy: Medulloblastoma and its variants are at least focally, if not diffusely, positive for synaptophysin. It is also positive for class III β-tubulin or microtubule-associated protein 2 [33, 34]. Positive immunoreactivity is often intense in Homer Wright rosettes and pale islands of desmoplastic/nodular medulloblastomas. Occasional immunoreactivity for neurofilament proteins, markers specific for photoreceptors such as S-antigen, and interphotoreceptor retinoid-binding protein can be demonstrated [33–35]. GFAP-positive cells may represent reactive cells, and possible focal tumor cell staining may be difficult to ascertain. In one study, about 10 % of the GFAP positive cells were found to be genuinely neoplastic [36]. Medulloblastomas has high Ki67 labeling index and apoptotic index among tumors of the CNS [37, 38]. The Ki67 labeling index can easily exceed 30 % but areas with neuronal development such as the pale islands have much lower labeling. Mutation of *CTNNB1*, an important gene in the *WNT* pathway, is associated with nuclear accumulation of β-catenin [36] that can be demonstrated by immunohistochemistry and, as per one study, is present in about 10 % of medulloblastomas [39].

Fig. 6.2 MR-medulloblastoma. (**a**) Axial FSE T2W MR image shows a mass expanding and completely obliterating the fourth ventricle. The intermediate hyperintense signal reflects the high cellularity of medulloblastoma. Peritumoral edema is also evident. (**b**) Axial post-contrast, T1W MR image demonstrates heterogenous, predominantly minimal tumor enhancement. (**c**, **d**) Sagittal FSE T2W MR images demonstrate drop metastases (*arrows*) in the form of nodules (3-year-old male)

Ultrastructually, tumor cells may contain neurosecretory granules (dense core granules), synapses, and Intermediate filaments but no specific diagnostic structures [40].

Differential diagnoses: Ependymoma, AT/RT, medulloepithelioma, embryonal tumor with abundant neuropil and true rosettes (ETANTR), and metastatic small blue cell tumors can histologically mimic medulloblastomas particularly on small specimens for intraoperative consultation. Cytologically, ependymoma nuclei are more monotonous, round, and do not have the crumbled appearance. Histologically, perivascular rosettes and ependymal canals, when present, are good diagnostic clue. Immunohistochemistry for GFAP is often diffusely positive in ependymoma but only patchy or in the form of reactive astrocytes in medulloblastoma. Ependymoma can be positive for epithelial membrane antigen (EMA), but medulloblastoma is typically negative. A substantial number of AT/RT has a small cell component resembling medulloblastoma but careful search particularly on the cytologic preparation at intraoperative consultation almost always identify rhabdoid cells. Immunohistochemistry for BAF47 is negative in AT/RT but positive in most other tumors including medulloblastoma.

Prognostic indicators: The prognosis of medulloblastoma and its variants in children is dependent on multiple factors including

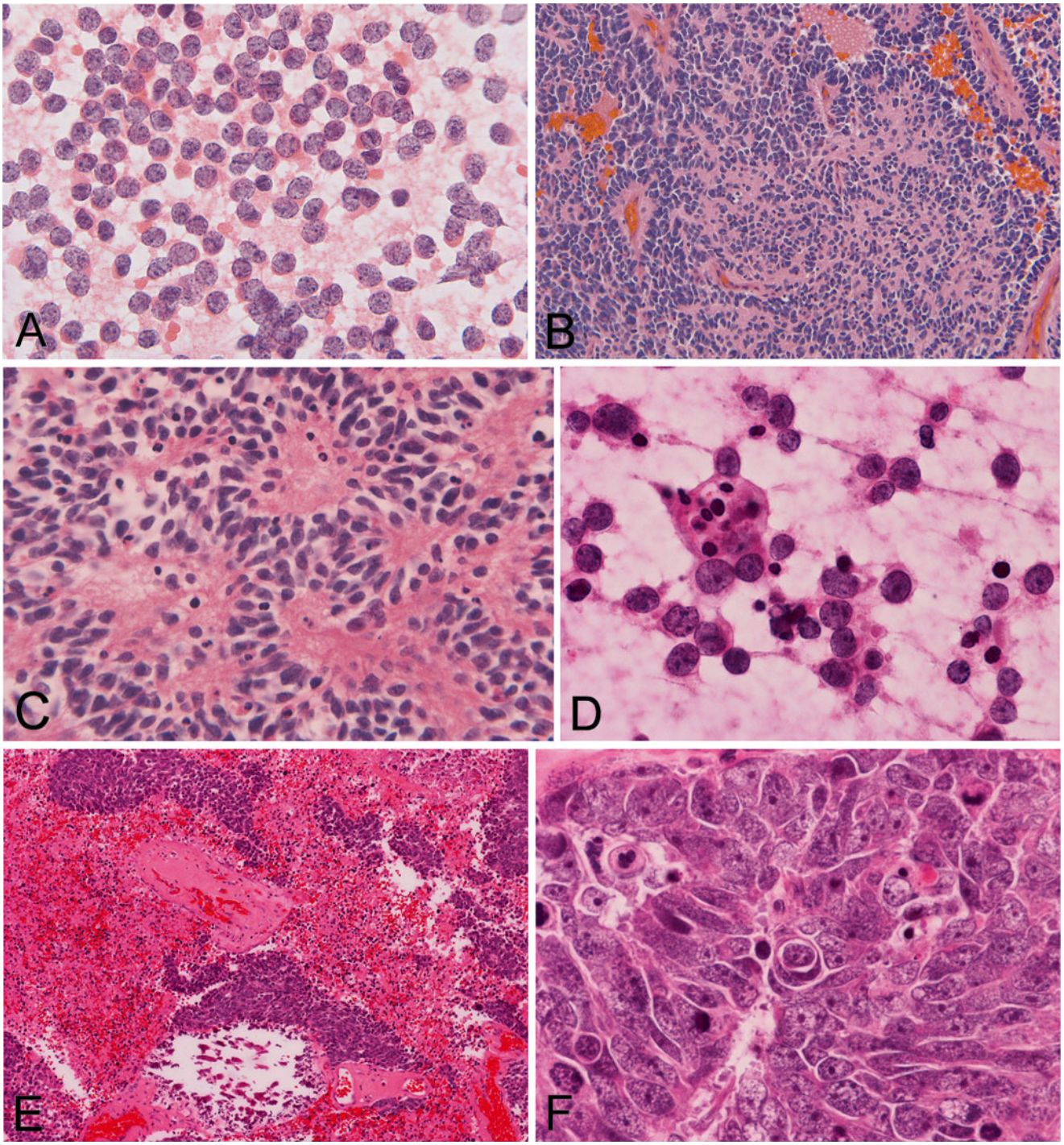

Fig. 6.3 Medulloblastoma and large cell medulloblastoma: (**a**–**c**) are taken from a medulloblastoma. (**a**) On cytologic preparations, the nuclei are hyperchromatic and slightly crumbled. (**b**) Histologically, areas with small amount of neuropils are usually present. (**c**) Homer Wright rosette as illustrated here is not always present. (**d**–**f**) are taken from a large cell medulloblastoma. (**d**) The nucleoli are distinct and apoptotic bodies are present. (**e**) Extensive necrosis is a common feature. (**f**) The nuclei are large and pleomorphic. Nucleoli are distinct and nuclear warping is a typical feature. Mitotic figures and apoptotic bodies are common

age, completeness of surgical resection, and metastatic status at presentation. The overall 5-year survival rate is about 60–80 % [28, 41]. Histologic correlation with clinical behavior is not always accurate. The recently proposed stratification into four groups as discussed above seems to be a good way for prognostic purposes. High expression of *hTERT* [42], high expression of *ERBB-2* [43], high *MYC* mRNA expression, and low *TrkC* mRNA expression [44, 45] are associated with poor clinical outcome. In general, better prognosis is noted in tumors associated with the *WNT* pathway.

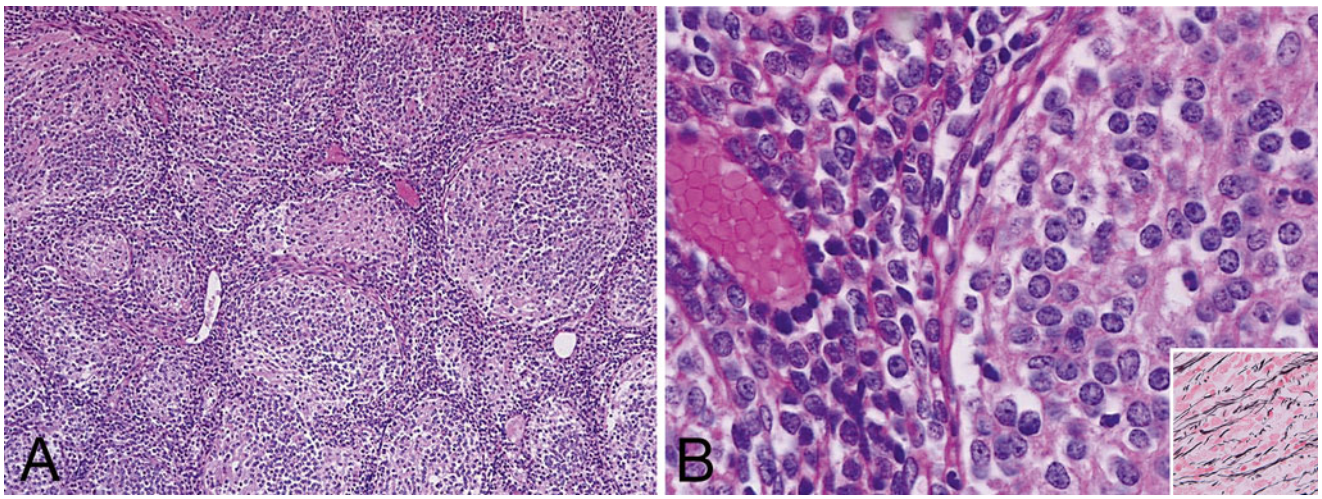

Fig. 6.4 Desmoplastic medulloblastoma: (**a**) The salient features are "pale islands" surrounded by densely packed hyperchromatic cells. (**b**) The pale nodules have lower nuclear cytoplasmic ratio than the surrounding densely packed areas. Reticulin substances could be demonstrated in the dense packed areas (Inset)

Primitive Neuroectodermal Tumor (PNET)

This is a collection of tumors characterized by undifferentiated or poorly differentiated neuroepithelial cells resembling the embryonal neuroectoderm (neuroepithelium) that occurs outside the posterior fossa. Histologically, some of them are indistinguishable from medulloblastoma. Morphologic differentiation along neuronal, glial, and ependymal lineage can occur.

Medulloepithelioma

Definition: Medulloepithelioma of the CNS [46, 47] is a rare and highly aggressive tumor that phenotypically recapitulates a very early stage, the neurotube stage, of the developing nervous system. Please refer to the discussion of ETANTR for the genetic relationship between medulloepithelioma, ependymoblastoma, and ETANTR.

Clinical features: Medulloepithelioma occurs almost exclusively in infancy and early childhood with half of them occurring before 2 years of age [47]. Some may occur as congenital tumors. Medulloepithelioma has a sinister reputation of dissemination through the neuroaxis and therefore initial treatment always includes irradiation of the entire neural axis. Dissemination through the cerebral spinal fluid (CSF) is a grave sign with median survival of 10 months [46, 47]. Over half of these cases arise in the lateral ventricles, many also arise in the posterior fossa and rare examples can be found in uncommon locations such as the cauda equine [47] and ciliary body [48]. Some cases of medulloepitheliomas arising in ciliary bodies have been associated with pleuropulmonary blastoma [48]. Although the CNS is a favored site, the so-called peripheral medulloepitheliomas have been described outside the CNS [49, 50]. In addition, medulloepithelioma components can also be found in immature teratomas arising in the ovaries and testicles [51, 52]. The prognosis of teratomas with medulloepithelioma component is far more favorable than medulloblastomas occurring in the central nervous system [51, 52].

Imaging findings: The tumor is usually large at the time of presentation. The features on CT and MRI are variable. On MRI these tumors are usually well circumscribed, hypointense or isointense on T1, hyperintense on T2, and non-enhancing at presentation [47, 53]. Enhancement occurs with tumor progression. The tumor may include cysts and calcifications which contribute to the variability of the mass on imaging.

Histopathology: The histopathologic picture is highly distinctive. The tumor is composed of tubular or papillary structures formed by mitotically active, hyperchromatic, pleomorphic, epithelial cells supported by basement membrane material (Fig. 6.5). The tumor cells have very high nuclear to cytoplasmic ratio. Other areas are composed of sheets of primitive cells with no specific pattern formation. Some tumors may differentiate along neuronal, astrocytic, ependymal, oligodendroglial and, on rare occasions, mesenchymal lineage [54, 55]. Rare cases can be pigmented (contain melanin pigmentation) [56].

Extensive primitive lateral cell junctions (zonulae adherents) and basal lamina, both reflecting the epithelial phenotype of the neuroepithelium, are demonstrated at the ultrastructural level [57].

Molecular pathology and genetics: Due to the rarity of these cases, the understanding on genetic changes is limited. Amplification of *hTERT* gene has been identified in this rare tumor [42]. Amplifications at 19q13.42 involving the *C19MC* cluster, a feature shared by ependymoblastoma and ETANTR has been demonstrated [58] and serve as a useful diagnostic tool.

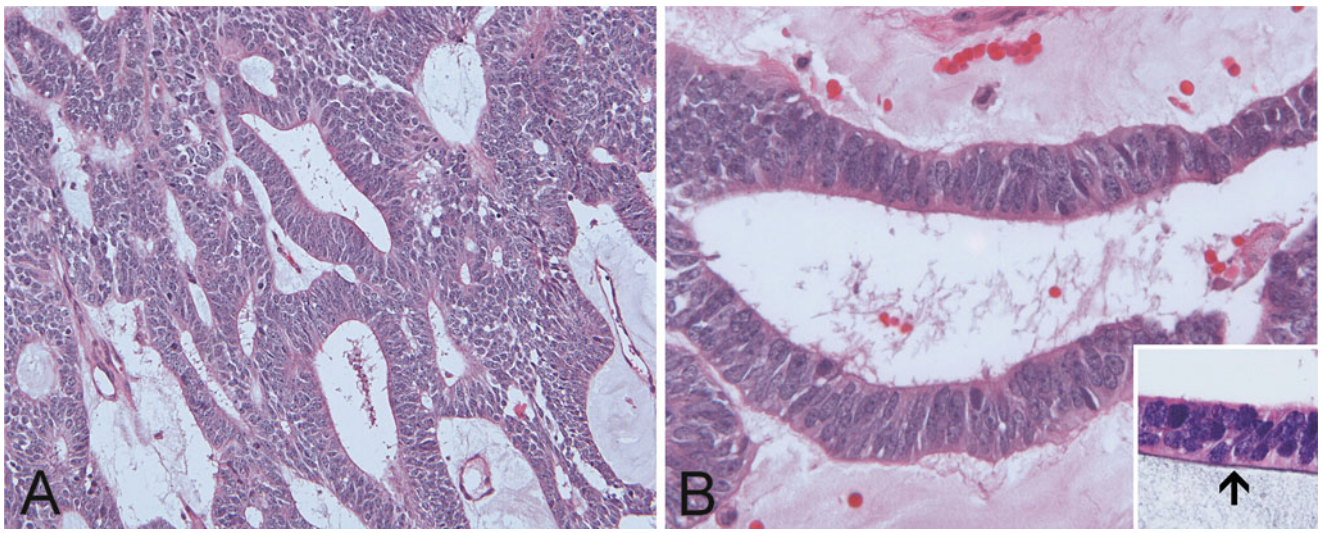

Fig. 6.5 Medulloepithelioma: (**a**) In contrast to medulloblastoma, the tumor cells have an epithelial growth pattern and cytology. (**b**) Stratified epithelial cells with a basement membrane on one side can be demonstrated by Jones stain (inset)

Electron microscopy and immunohistochemistry: On immunohistochemistry, medulloepithelioma is positive for nestin, vimentin, two intermediate filaments that are expressed in the primitive neuroectoderm. These tumors are also positive for synaptophysin, neurofilament, glial fibrillary acidic protein, and microtubule associated proteins, markers that are found in neural tissue [59, 60]. Medulloepithelioepitheliomas also express cytokeratin and EMA, which reflects the epithelial phenotype of the primitive neuroectoderm [59]. Immunohistochemistry shows diffuse immunoreactivity for LIN28A in these tumors [61].

Differential diagnosis: The histologic pattern of medulloepithelioma is very distinct and allows separation from medulloblastoma and primitive neuroectodermal tumors easily even though these tumors share a very similar, if not identical, immunohistochemical profile.

Supratentorial Primitive Neuroectodermal Tumor (PNET)

Definition: This is a collection of poorly differentiated or undifferentiated neuroepithelial tumors with morphologic resemblance to medulloblastoma. These tumors have the capacity to differentiate. Cerebral neuroblastomas and ganglioneuroblastomas refer to these tumors with only neuronal or ganglionic differentiation, respectively.

Clinical features: The majority of these tumors occur in children, adolescent, and young adults with a mean age of 5.5 years. The cerebrum is the most common site but they may occur in the suprasellar region and spinal cord. Clinical manifestation ranges from seizure to visual and endocrine problems in cases with suprasellar involvement.

Imaging findings: The tumor usually presents as a sizable, heterogeneous mass with sharp, irregular margins. The heterogeneity is the result of the presence of cysts due to tumor necrosis, or hemorrhage. The solid component appears iso-to hypointense compared to gray matter on T1- and T2-weighted MR images and demonstrates variable enhancement. The surrounding edema is insignificant for the size of the mass. Leptomeningeal spread and dissemination through cerebral spinal fluid manifesting as leptomeningeal enhancement is common [62].

Macroscopic pathology and histopathology: The tumors are soft and well demarcated. Hemorrhages and cysts may be present. Histologically, the classic picture is that of a small blue cell tumor with cytologic features reminiscent of a medulloblastoma, but the cells may be larger than classic medulloblastomas. Tumor cells may arrange in parallel streams, palisade, and in single files. There is a fibrillary cytoplasmic background and Homer-Wright rosettes are often found. Morphologic evidence of neuronal differentiation may be found in neuroblastomas and dominate the histologic picture in ganglioneuroblastoma. Rich vascular network may be present. Calcifications are common. This combination makes heterogeneity of morphology in supratentorial PNETs a rule.

Immunohistochemistry and electron microscopy: The immunohistochemical profile is similar to that of medulloblastoma and these tumor express synaptophysin, class III ß-tubulin, neurofilament proteins, S100, and Leu-7 (CD56). GFAP may occasionally be detected in the small tumor cells [63, 64]. No specific findings of diagnostic value are demonstrated by electron microscopy.

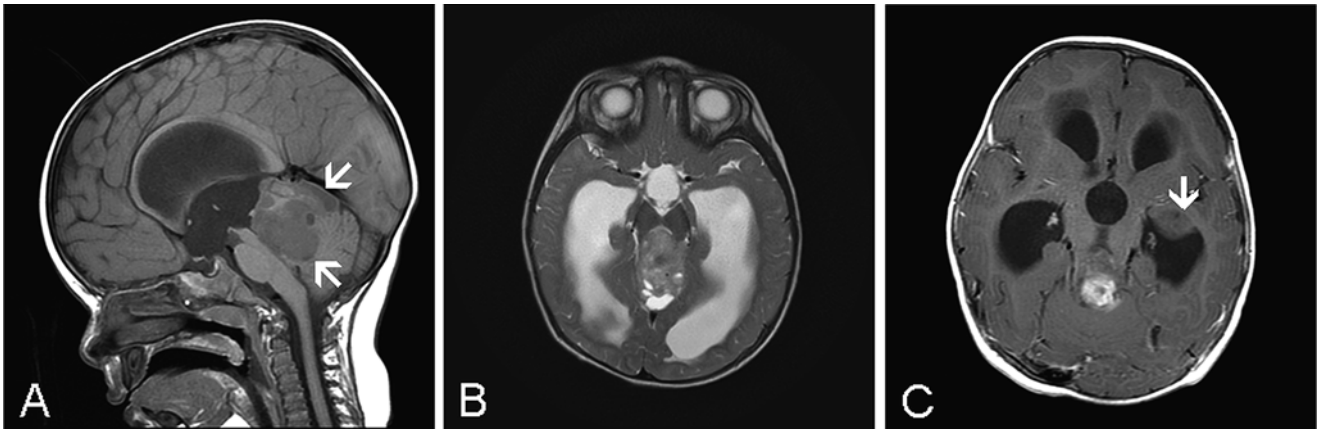

Fig. 6.6 MR-AT/RT. (**a**) Sagittal T1W MR image demonstrates a midline, heterogeneous mass invading the vermis (*arrows*). The mass is compressing the aqueduct and causes hydrocephalus. (**b**) Axial FSE-T2W MR image demonstrates mostly intermediate hyperintensity. (**c**) Axial T1W post-contrast MR image shows that only part of the tumor enhances. A non-enhancing lesion in the lateral ventricle (*arrow*) is likely the result of intraventricular seeding (13 month-old male)

Molecular pathology and cytogenetics: In contrast to medulloblastoma, isochromosome 17 has only been rarely reported. The genetic profile of supratentorial PNET and medulloblastoma is also different [65, 66]. The genetic mechanisms on tumorigenesis between medulloblastoma and supratentorial PNET is likely to be different.

Differential diagnosis: The supratentorial location and heterogeneous histopathologic picture open this entity to a long list of differential diagnoses including ependymoma, central neurocytoma, and oligodendroglioma.

Ependymoblastoma

Definition: This is an extremely rare, malignant, embryonal tumor featured by distinctive multilayered rosettes. Please refer to the discussion of ETANTR for its relationship with ETANTR and medulloepithelioma.

Overview: These tumors are seen predominantly in neonates and young children and often occur as large, supratentorial tumors that are close to the ventricles. Neither clinical manifestations nor radiographic features are specific. The incidence is uncertain due to its rarity and congenital examples have been described [67].

Macroscopic pathology and histopathology: These tumors are typically well circumscribed but leptomeningeal invasion and widespread CSF dissemination are common. Histologically, the tumor is featured by highly cellular, densely packed, primitive appearing small blue cells harboring occasional ependymal rosettes and tubules. However, it lacks the high grade pleomorphism that would otherwise qualify these tumors as anaplastic ependymomas. Endothelial proliferations are lacking. Ultrastructural features of ependymal differentiation including apical surfaces bearing cilia and microvilli projecting into a lumen, interconnected adjacent cells by zonulae adherents, and basal lamina-lined labyrinth have been demonstrated [68, 69]. Immunohistochemically, these tumors are positive for S100, vimentin, and GFAP [69–71]. Amplifications at 19q13.42 involving the *C19MC* cluster [58] and immunoreactivity for LIN28A [61], two features shared by ependymoblastoma and ETANTR, has been demonstrated and serve as a useful diagnostic tool.

Imaging findings: At present there no specific features described that would reliably distinguish ependymoblastoma from PNET.

Atypical Teratoid/Rhabdoid Tumor (AT/RT)

Definition: This is a highly malignant tumor that occurs predominantly in infants and young children, featured by neoplastic rhabdoid cells without and with non-rhabdoid elements, most often primitive neuroectodermal neoplastic component, and typically associated with inactivation (deletion or mutation) of *hSNF5/SMARCB1/INI1*.

Clinical features: Most tumors occur in children under 6 years of age with a male predominance. AT/RTs comprise about 1–2 % of pediatric brain tumors [72] but are estimated to represent about 10 % of tumors in infants [73]. Rare adult cases have been reported [74–78]. AT/RTs are slightly more common in supratentorial than infratentorial locations. Depending on the location of the tumor and the age of the patient, the clinical presentations can be variable and include nonspecific symptoms (e.g. lethargy, vomiting, headache, failure to thrive) and/or to focal manifestations (e.g. sixth and seventh cranial nerve palsy).

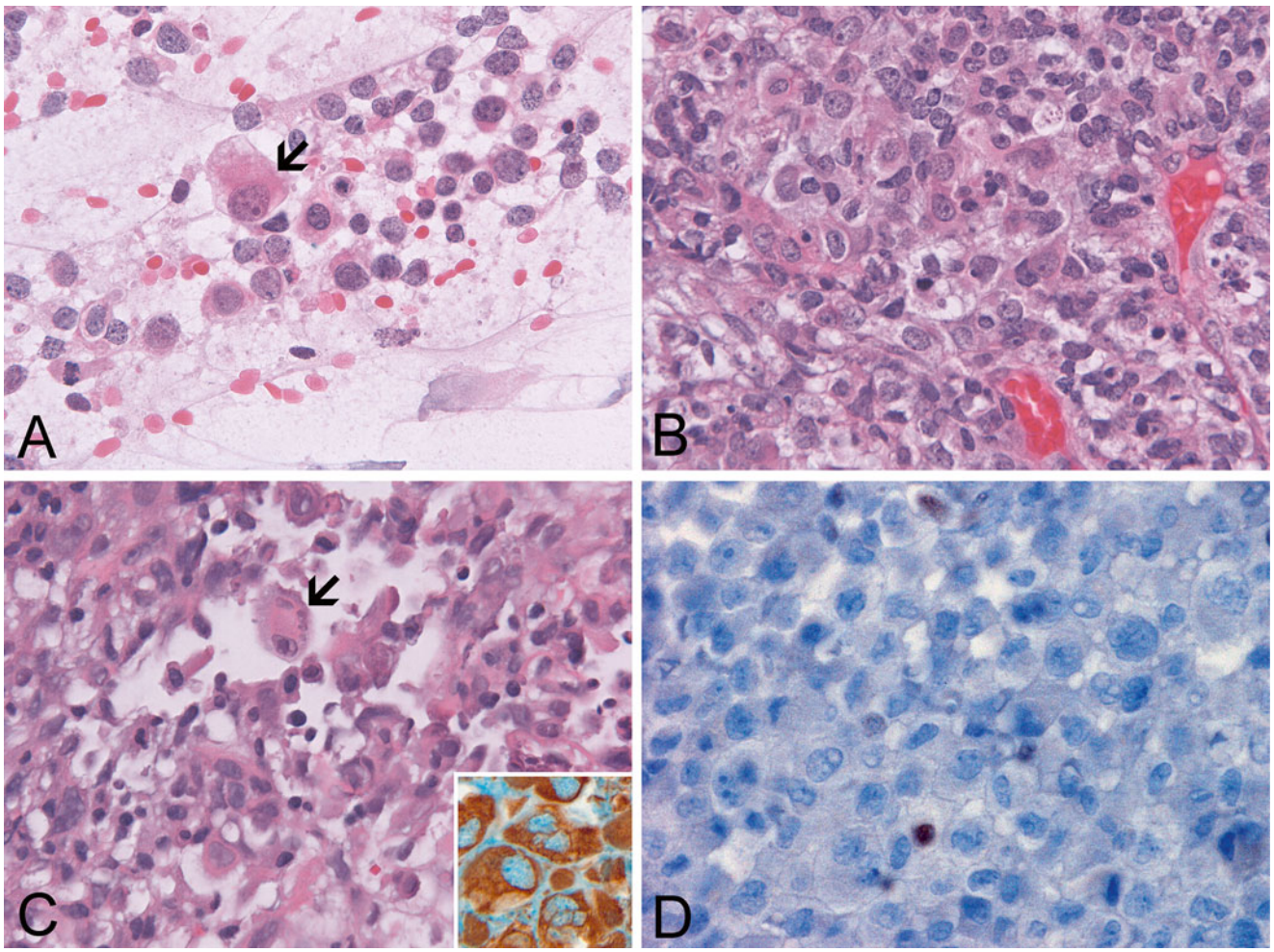

Fig. 6.7 Atypical teratoid rhabdoid tumor: (**a**) A cytologic preparation with a large rhabdoid cells containing a cytoplasmic inclusion-like body (*arrow*). A range of rhabdoid changes can be seen in the rest of the cells. (**b**) and (**c**) are taken from the same tumor but different areas. Note that the rhaboid changes (arrow) are more common in (**c**). The rhabdoid cells have strong cytoplasmic immunoreactivity for vimentin (inset in (**c**)). (**d**) AT/RT is non-immunoreactive for BAF47 (INI1). Occasional positive cells, most likely entrapped non-neoplastic cells, can be found, which serves as an internal positive control

Imaging findings: AT/RT usually present as a large, lobulated, heterogeneous mass sharing many similarities to supratentorial PNET although the solid component may be iso- to slightly hyperintense on T2-weighted sequences (Fig. 6.6). Cystic necrosis is common. Enhancement of the solid component is usually avid albeit often inhomogeneous [79]. The tumor can arise in the intratentorial as well as supratentorial compartment. When infratentorial, the tumor may involve the cerebellopontine angle [80]. Cerebrospinal dissemination is common and can be detected with post-contrast MRI manifested as enhancement along the leptomeninges and/or drop metastasis.

Macroscopic pathology and histopathology: Typically, AT/RTs are large, well-demarcated, necrotic and hemorrhagic. Fragments that are submitted as surgical specimens are soft and have a consistency similar to that of medulloblastoma.

Microscopically, AT/RTs are heterogeneous and the amount of rhabdoid cells can range from abundant to scant [81]. Tumors with *hSNF5/SMARCB1/INI1* inactivation but no rhabdoid cells have been described [82, 83]. The salient feature is large neoplastic cells with abundant cytoplasm that displaces the nuclei to an eccentric location. Commonly, a round inclusion-like amphopilic to slightly eosinophilic round body will occupy the bulk of the cytoplasm. Artifactual cytoplasmic vacuoles are common. Nuclei are large and have vesicular chromatin with prominent eosinophilic nucleoli. Multinucleated tumor cells are not uncommon. During intraoperative consultation, cytologic evaluation effectively identifies rhabdoid cells (Fig. 6.7a).

The classic rhabdoid changes can range from subtle to obvious and vary in different tumors and different parts of the same tumor. Histologically, rhabdoid cells do not exhibit a particular growth pattern; instead, the tumor cells are often jumbled up and give a picture reminiscent of a jigsaw puzzle (Fig. 6.7b–c).

The presence of non-rhabdoid elements, most frequently small cell component reminiscent of medulloblastomas and supratentorial PNETs are often present. These components may dominate the histologic picture, which makes identification of rhabdoid cells difficult. Mesenchymal differentiation is less common and epithelial differentiation is rare. When the epithelial component represents the dominant component, the diagnosis of choroid plexus carcinoma must be entertained.

Molecular pathology: Deletion of chromosome 22q was the first genetic aberrations identified [84, 85] and *hSNF5/SMARCB1/INI1*, a chromatin remodeling complex which functions as a tumor suppressor gene, was later identified as the critical gene [86]. While homozygous or heterozygous deletion is demonstrated in most AT/RTs, point mutations without structural abnormality of chromosome 22 can be demonstrated in a number of tumors. Fluorescent in situ hybridization (FISH) is an efficient way to demonstrate these deletions. Germline mutations have been well documented [87] and sequencing may be required to detect them. Patients with familial AT/RTs are more likely to have extensive disease and more likely to die of their disease than patients with sporadic AT/RTs [88]. Other than rare exceptions [89], deletion and mutation of *hSNF5/SMARCB1/INI1* are typically absent in adult composite rhabdoid tumors [90]. It should be noted that *hSNF5/SMARCB1/INI1*-deficient tumors do not always have rhabdoid histology [83], while primitive neuroectodermal tumor with *hSNF5/SMARCB1/INI1* with no rhabdoid features also behave aggressively [82].

Immunohistochemistry and electron microscopy: The protein product of *hSNF5/SMARCB1/INI1* is demonstrated by immunohistochemistry for BAF47, a 47 kDa BRG1-associated factor (BAF) as nuclear immunoreactivity [91]. This protein is present in practically all normal tissue but tumor cells with deleted or mutated *hSNF5/SMARCB1/INI1* are negative (Fig. 6.7d). Initially, this lack of immunoreactivity was demonstrated in AT/RT and other primary rhabdoid tumors of infancy and childhood occurring outside the CNS [92–95] but not composite rhabdoid tumors in adult [90]. Subsequently, a variety of *INI1*-deficient tumors other than primary childhood rhabdoid tumors characterized by negative BAF47 immunoreactivity have been demonstrated [96]. These tumors include medullary carcinoma of the kidney, epithelioid sarcoma, epithelioid malignant peripheral nerve sheath tumor, myoepithelial carcinoma, extraskeletal myxoid chondrosarcoma [96], and pediatric undifferentiated soft tissue sarcomas that lacks rhabdoid features [97] and meningiomas [98, 99]. Rare cases of AT/RT with intact *hSNF5/SMARCB1/INI1* and mRNA but no protein expression [100] and retained protein expression with nonsense mutation of *hSNF5/SMARCB1/INI1* have also been described. Under appropriate clinical and histopathologic circumference, a lack of immunoreactivity for BAF47 still offers a firm confirmation of AT/RT and other primary rhabdoid tumor of childhood and remains an important tool in the correct diagnosis of AT/RT in the CNS [81].

On immunohistochemistry, AT/RTs are characteristically immunoreactive for EMA and vimentin. The cytoplasmic inclusion-like bodies are composed of whorls of bundles of intermediate filaments [85, 101]. Strong immunoreactivity for vimentin is seen in practically every rhabdoid cells (Fig. 6.7c inset). Many AT/RTs are also immunoreactive for smooth muscle actin, GFAP, and cytokeratin. Neurofilament, synaptophysin, and chromogranin are less likely to be positive and most cases are negative for desmin [85, 102]. Markers for germ cell tumors (placental alkaline phosphatase, α-fetoprotein, and β-human chorionic gonadotropin) are negative [85, 102]. Patchy staining for S100 and rare positive cells for HMB-45 have been described [102]. Ependymal differentiation has been recently documented in one case [103].

Differential diagnosis: The common mimickers of AT/RT include large cell/anaplastic medulloblastoma, anaplastic ependymomas, and choroid plexus carcinoma. Identification of rhabdoid cells is key to the diagnosis. In histologically challenging cases, immunohistochemistry for BAF47 or molecular studies on *hSNF5/SMARCB1/INI1* should be performed [81]. Primary rhabdomyosarcoma is a rare entity in the CNS, and such tumors are positive for desmin and other myogenic markers such as myogenin and have intact *hSNF5/SMARCB1/INI1* (positive nuclear immunoreactivity for BAF47 on immunohistochemistry).

Miscellaneous Tumors with Morphologic Features of the Primitive Neuroectoderm

Tumor with primitive neuroectoderm is a heterogeneous group of tumor. The following entities are not, or not yet, included in the current WHO classification.

Embryonal Tumor with Abundant Neuropil and True Rosettes (ETANTR) and Embryonal Tumor with Multilayered Rosettes (ETMR)

Embryonal tumor with abundant neuropil and true rosettes (ETANTR), also known as neuroblastic brain tumor containing abundant neuropil and true rosettes and embryonal tumor with abundant neuropils and ependymoblastic rosettes, is a newly recognized entity [104]. This rare tumor occurs mostly in infants and childrens and is more common in girls than boys. Most often, it is a supratentorial hemispheric mass that is well demarcated on imaging studies. The prognosis is poor. This tumor is characterized by a distinct microscopic picture of true ependymoblastic rosette formation in a background of neuropil. The rosettes are formed by circumferentially arranged pseudo-stratified embryonal cells around a central

lumen with limiting membrane. Homer Wright rosettes and perivascular pseudorosettes can be present. Mitosis and apoptosis are frequent [104]. The morphologic features overlap with medulloepithelioma, ependymoblastoma, medulloblastoma, and PNETs. The rich neuropil background distinguishes ETANTR from these tumors. Neurocytic differentiation [105], rhabdomyoblastic and melanotic differentiation [106] as well as rare sarcomatous-like areas have been described. Amplification in chromosome 19q12.42 has been documented in a few cases. The undifferentiated cells are negative for synaptophysin and neurofilaments but the neuropil is strongly positive. Immunohistochemistry for GFAP essentially show a reactive astrocyte pattern [104].

Recent genetic studies, however, show that medulloepithelioma, ETANTR, and ependymoblastoma share similar molecular features and probably comprise the spectrum of a single clinicopathological entity [58]. These entities also share similar overall poor prognosis [58]. An umbrella term of embryonal tumor with multilayered rosettes (ETMR) has been proposed for these tumors [107].

Imaging findings: Limited literature regarding the imaging features this tumor describe T1 hypointensity, T2 iso to hyperintensity and heterogeneous enhancement [108]. The tumor, therefore, shares very similar features with PNET and AT/RT.

Tumors with Features of Glial and Neuronal Tissue

Glial neoplasm comprises the bulk of this group in both adult and pediatric populations. However, tumors with glial-neuronal differentiation such as ganglioglioma and dysembryoplastic neuroepithelial tumors are far more common in the pediatric population. In addition, several molecular alterations that are useful in adult tumors—deletion of chromosome 1p and 19q, mutations of isocitrate dehydrogenase 1 and 2 gene (*IDH 1, IDH 2*), and epigenetic silencing of the *MGMT* (O6-methylguanine–DNA methyltransferase) gene—are uncommon to rare in pediatric gliomas. In contrast, V600E mutation of *BRAF* has been shown to have high mutation frequency in pleomorphic xanthoastrocytoma, gangliogliomas and extra-cerebellar pilocytic astrocytomas and is a diagnostic adjunct of these tumors that are often seen in pediatric patients [109].

Astrocytic and Oligodendroglial Tumors

Although the full spectrum of astrocytic, oligodendroglial, and mixed oligoastrocytic tumors can be seen in pediatric patients, the incidence is different from that of adults. In general, astrocytic tumors and ependymomas are common in children but oligodendrogliomas are rare [5].

Pilocytic Astrocytoma and Pilomyxoid Astrocytoma Definition

Pilocytic astrocytoma is a WHO grade I tumor characterized by a well-circumscribed, biphasic astrocytic tumor with densely packed fibrillary areas and loosely packed area with spongy and/or microcystic areas accompanied by Rosenthal fibers and eosinophilic granular bodies/hyaline droplets. Pilomyxoid astrocytoma is closely related to pilocytic astrocytoma and is currently regarded as a subtype of pilocytic astrocytoma. This is a WHO grade II tumor featured by prominent mucoid matrix and angiocentric arrangement of tumor cells typically without Rosenthal fibers or eosinophilic granular bodies/hyaline droplets.

Pilocytic Astrocytoma

Clinical features: Pilocytic astrocytoma is a clinically indolent tumor with excellent prognosis that occurs predominantly in children and, less commonly, in young adults.

It is the most common pediatric glial tumor and constitutes 18.2 % of all brain tumors and 11.2 % of all spinal tumors [5]. The incidence exceeds the combined incidence of diffuse astrocytoma, anaplastic astrocytoma, and glioblastoma in pediatric patients. Over 75 % of patients are under the age of 20 and the peak incidence is between 8 and 13 years. They tend to occur along the midline with the cerebellum as the most common site. Other primary sites include the optic nerve-chiasma-hypothalamus axis, thalamus and basal ganglia, cerebral hemispheres, brainstem. Pilocytic astrocytoma represents 11 % of the tumors arising in spinal cord of children [5] and its incidence is only second to ependymomas. About 15 % of patient with type 1 neurofibromatosis (NF1) develop pilocytic astrocytoma with optic nerve as the preferred site. About 45 % of gliomas associated with NF1 are pilocytic astrocytomas [110]. Malignant transformation is extremely rare and changes over time are typically regressive in nature [111–113].

Seizure in cerebellar tumors is uncommon. In contrast, cerebellar tumors cause clumsiness, worsening headache, nausea, vomiting, and manifestations of hydrocephalus are common. Visual defects and hypothalamic dysfunctions are often present tumors arising in the optic nerve-chiasma-hypothalamic axis which are often associated with NF1 [4].

Imaging findings: Cerebellar pilocytic astrocytoma is typically a well-circumscribed mass with rather homogenous enhancement when solid. A cyst with an enhancing nodule formation is common [114, 115] and an important finding that distinguishes pilocytic astrocytoma from other glial tumors particularly those occurring outside the cerebellum (Fig. 6.8). In contrast to astrocytomas that diffusely enlarge the pons, pilocytic astrocytomas of the brainstem are usually exophytic, enhance, and contain cysts [116].

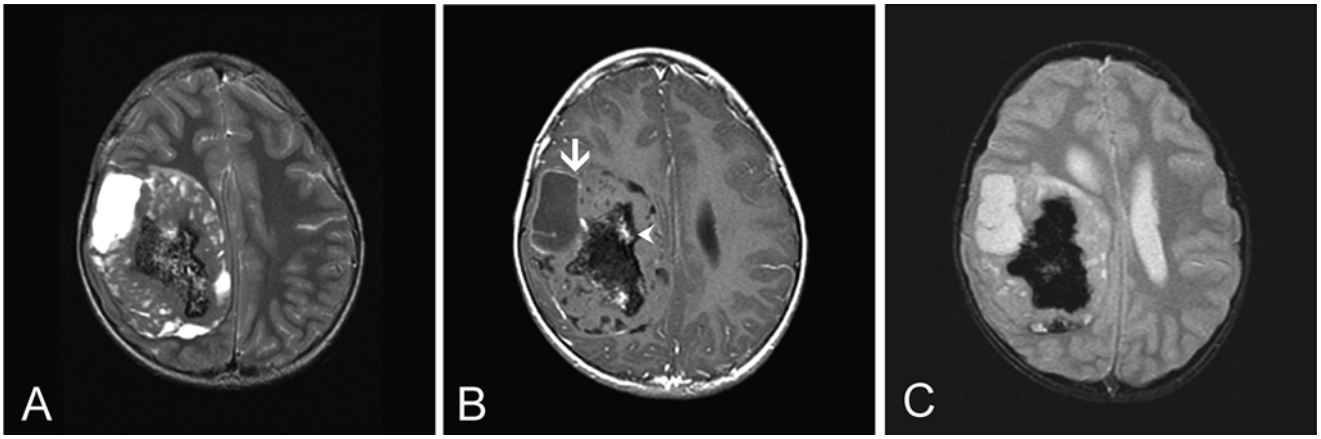

Fig. 6.8 MR-pilocytic astrocytoma. (**a**) Axial FSE-T2W MR image demonstrates a large, well-circumscribed mass with mixed cystic and solid component. Mild midline shift is also present. (**b**) Axial T1W post-contrast MR image shows rim enhancement of the cystic component (*arrow*). Patchy enhancement is also present in the solid component (*arrowhead*). (**c**) Axial gradient recalled echo (GRE) MR image reveals susceptibility artifact suggestive of blood byproducts (10-year old male). Note that the tumor illustrated here arises from an uncommon location for pilocytic astrocytoma

Macroscopic pathology and histopathology: Pilocytic astrocytoma is typically well circumscribed and often associated with intra- or paratumoral cysts. The long, hair-like cytoplasmic processes (pilo-) and slightly elongated, bland nuclei, and mucoid materials are well appreciated in cytologic preparations (Fig. 6.9a). The cytoplasmic processes tend to form a mesh on the smeared/squashed preparations. The histologic picture of pilocytic astrocytoma characteristically varies in different parts of the tumor (Fig. 6.9b–f). Alternating densely packed fibrillary and loosely packed areas featured by spongy, microcystic areas are histologic signatures. The densely packed area contains bipolar cells with elongated, coarse cytoplasmic processes. Rosenthal fibers are eosinophilic, hyalinized elongated intracytoplasmic curvy structures common in these dense areas (Fig. 6.9c). The loosely packed areas often contain microcyst in a mucoid background. Eosinophilic granular bodies (Fig. 6.9f) and hyaline droplets are important diagnostic features of pilocytic astrocytomas and are typically found in loosely packed areas. The density of eosinophilic granular bodies can be quite variable. They can be demonstrated with PAS stain with diastase pretreatment. Areas with perinuclear halo reminiscent of oligodendrogliomas are not uncommon. Focal calcifications may be present.

Pilocytic astrocytoma is richly vascularized. Perivascular chronic inflammatory cell infiltration is common. Hyalinized glomeruloids of blood vessels are characteristic of pilocytic astrocytoma (Fig. 6.9e). These blood vessels contain fenestrations and vesicles in the endothelial cells [117]. Endothelial proliferation similar to those seen in glioblastoma can be present in pilocytic astrocytoma but, in contrast to glioblastomas, maturation is often present and a spectrum of blood vessels ranging from plump endothelial cells to vessels with hyalinized vessel wall and thin endothelial cells would be seen. These features probably contribute to contrast enhancement on imaging studies.

Pilocytic astrocytomas involving optic nerve often invade into the subarachnoid space to form a collar-like structure around the optic nerve that has been enlarged by tumor (Fig. 6.10).

Rare mitosis, hyperchromatic nuclei, increased pleomorphism, and infarct-like necrosis, are compatible with the diagnosis of pilocytic astrocytoma. Increased cellularity, nuclear atypia, and occasional mitoses are not indications of malignancy [113]. In long standing cases, degenerative atypia featured by enlarged and hyperchromatic nuclei with smudgy chromatin and nuclear pseudoinclusions. Occasionally, an infiltrative growth pattern can be seen at the periphery of the tumor. Although pilocytic astrocytomas frequently invade the leptomeninges, subarachnoid dissemination is rare and survival rate of these cases are comparable to those without dissemination [118].

Anaplastic (malignant) pilocytic astrocytoma refers to pilocytic astrocytomas with multiple mitoses, endothelial proliferation, and palisading necrosis. It is not uncommon that these are recurrent tumor after radiation [112, 113].

Pilomyxoid Astrocytoma

Clinical features: This is a WHO grade II tumor [119, 120]. This uncommon tumor occurs predominantly in children with a median age of 10 months but rare cases have been reported in adolescents [121, 122] and adults. In contrast to pilocytic astrocytoma, the suprasellar and hypothalamic/chiasmatic region is the preferred location and tumors may occur in other part of the brain and spinal cord. Clinical symptoms are related to the location of the tumor with visual and hypothalamic/pituitary symptoms as major manifestations. Dissemination through CSF may occur. Progression of a rare case of pilomyxoid astrocytoma in the spinal cord to glioblastoma has been reported [123, 124].

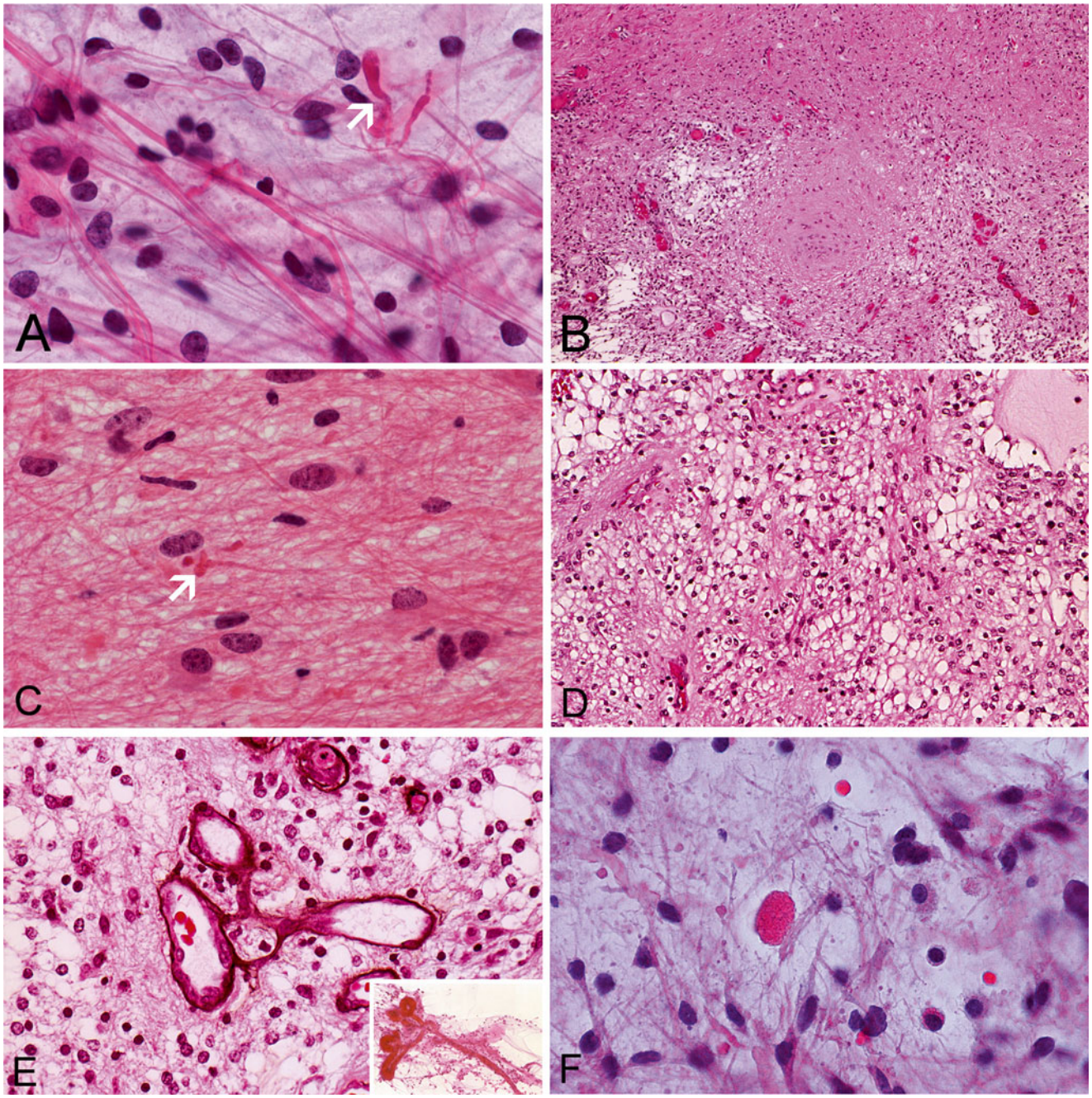

Fig. 6.9 Pilocytic astrocytoma: (**a**) Squash preparation shows bipolar tumor cells with long, coarse, hair-like process and occasional Rosenthal fiber (*arrow*) in a mucoid background. The nuclei are small, monotonous, and lack pleomorphism. (**b**) The alternating densely packed, loosely packed pattern is shown in this image. (**c**) Rosenthal fibers, elongated cytoplasmic processes and bland nuclei are shown in densely packed area. (**d**) Areas with perinuclear halo mimicking oligodendroglioma can be found. (**e**) Complex glomeruloid blood vessels are common in pilocytic astrocytoma. The outline is well illustrated by Jones stain here. This type of glomeruloid vessels can appear as a multi-headed, club shape structure on cytologic preparation (inset in (**e**)). (**f**) Eosinophilic granular bodies are often found in loosely packed areas

Imaging findings: Pilomyxoid astrocytomas are well-circumscribed tumors, hypointense on T1-weighted imaging, and hyperintense on T2-weighted imaging reflecting the mucoid component (Fig. 6.11). In contrast to pilocytic astrocytoma, pilomyxoid astrocytoma tends to occur as a solid suprasellar mass with enhancing and non-enhancing areas and occasional leptomeningeal dissemination [125].

Macroscopic pathology and histopathology: Surgical specimens typically appear gelatinous. Histologically, this tumor is composed of a mucoid, hypocellular mucoid neoplastic growth in a "cobweb" pattern punctuated by perivascular palisading arrangement of tumor cells around blood vessels reminiscent of ependymomas (Fig. 6.12). In contrast to pilocytic astrocytoma, pilomyxoid astrocytomas do not have

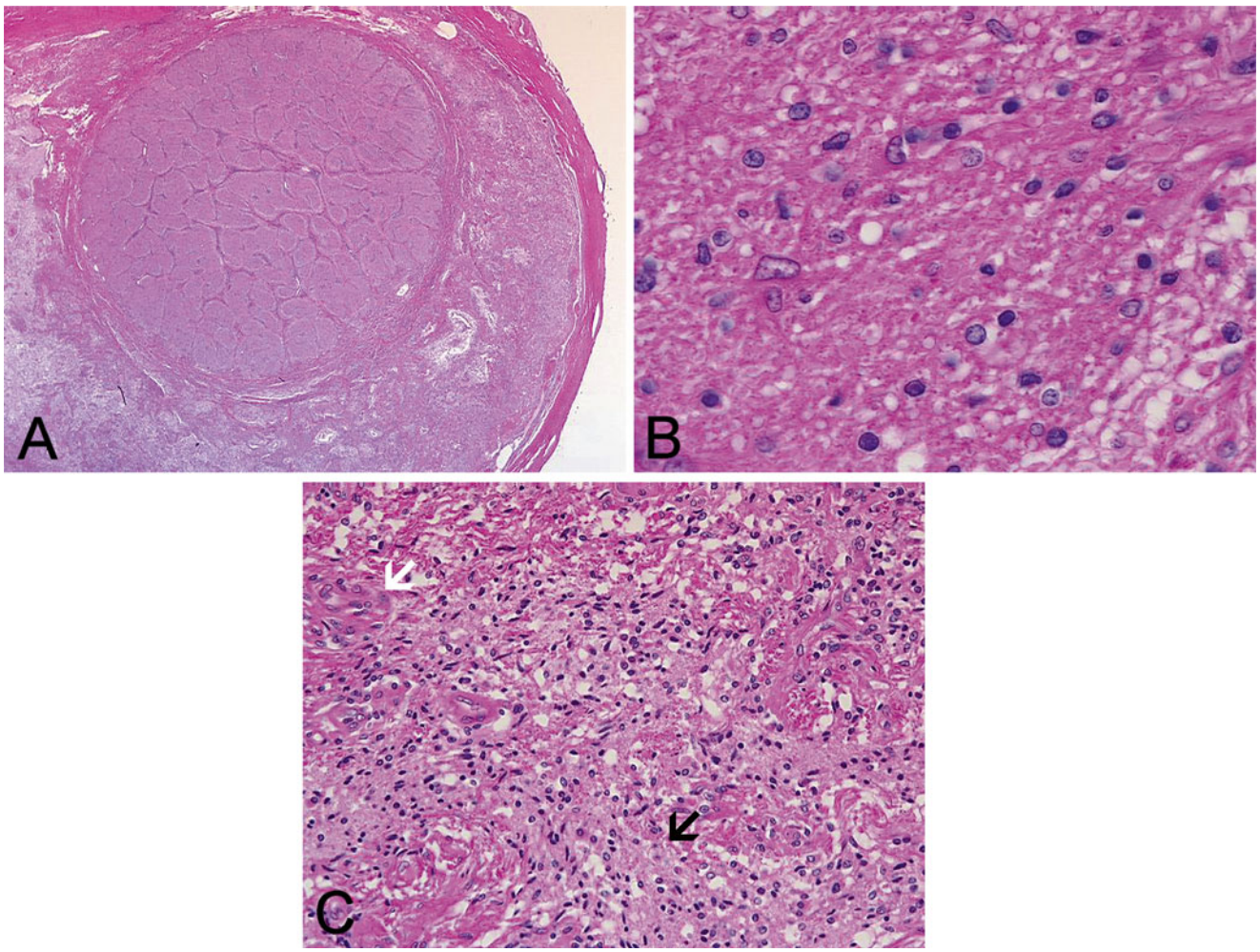

Fig. 6.10 Optic nerve glioma: (**a**) The optic nerve is infiltrated and expanded by an astrocytoma. Note that the fibrous septa within the optic nerve are preserved but the subarachnoid space around the optic nerve is expanded by the tumor. (**b**) The tumor has low grade nuclei. (**c**) The expanded subarachnoid space is composed of a mixture of tumor (*black arrow*) and reactive meningothelial cells (*white arrow*) which appears slightly more eosinophilic

biphasic growth pattern and lack Rosenthal fibers, eosinophilic granular bodies, or calcifications [119]. The neoplastic cells are monotonous, small spindle cells with bland nuclei and the cells palisading around blood vessels have similar morphology. The mucoid background is positive for Alcian blue. Features worrisome of poor prognosis such as necrosis, mitoses, and vascular proliferation are not uncommon in pilomyxoid astrocytoma [119, 126].

Pilocytic-Pilomyxoid Spectrum

Pilocytic astrocytoma and pilomyxoid astrocytoma have significant overlap in clinical and radiographic features, histologic features [126], and genetic aberrations [127]. Tumors with intermediate features are typically found in older patients, and cases of "maturation" of pilomyxoid astrocytoma into pilocytic astrocytoma [126] have been documented. Pilocytic astrocytoma and pilomyxoid astrocytoma are probably related entities along a common spectrum, and the pure form represents the two extremes of this spectrum.

Differential diagnosis: It is important to distinguish classic WHO grade I pilocytic astrocytoma from WHO grade II pilomyxoid astrocytoma, diffuse astrocytoma and oligodendroglioma, and ependymoma. The palisading perivascular arrangement in pilomyxoid astrocytoma can suggest ependymoma particularly when the specimen is small and the mucoid, hypocellular background can suggest dysembryoplastic neuroepithelial tumor (DNET). The clear cell component may suggest oligodendroglioma but pilocytic astrocytoma is typically heterogeneous in histopathology, and areas with typical morphology are generally found. Eosinophilic granular bodies are a useful feature in recognition of pilocytic astrocytomas.

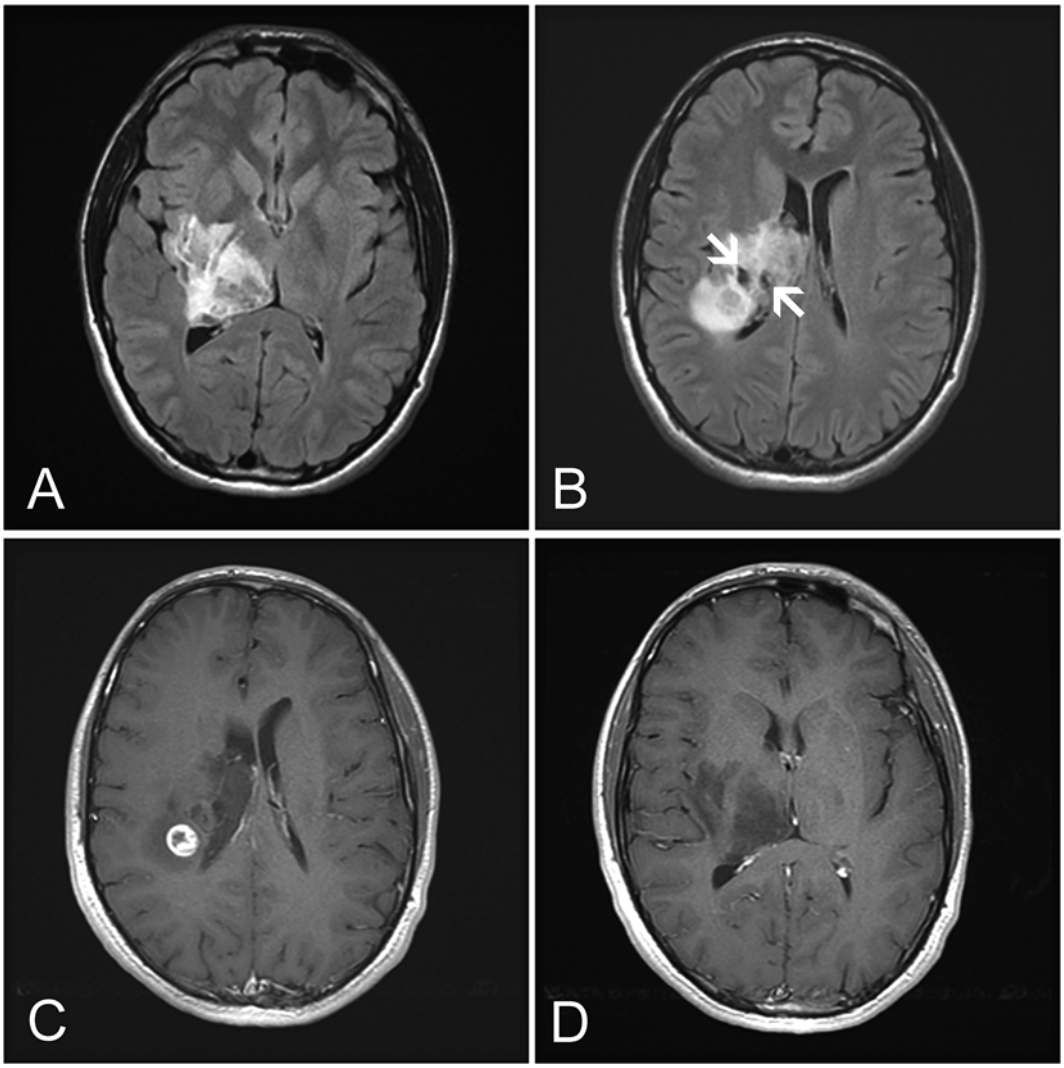

Fig. 6.11 MR-pilomyxoid astrocytoma**.** (**a**) Axial FLAIR MR images show (**a**) an infiltrating tumor involving the basal ganglia and thalamus. (**b**) A cystic component is present (*arrows*) and there is extension into the corona radiata. Axial T1W post-contrast enhanced MR images show (**c**) nodular enhancement in some areas while (**d**) enhancement is not found in other areas (adolescent male)

Immunohistochemistry and Molecular Pathology of Pilocytic-Pilomyxoid Spectrum

Immunohistochemistry: The immunohistochemical profile of pilomyxoid and pilocytic astrocytomas are very similar. The astrocytic cells are reactive for GFAP, Olig2, and S100 [128]. Rosenthal fibers are composed of α B-crystallin [129] and are often, but not always, negative for GFAP. Eosinophilic granular bodies are immunoreactive for α-1-antichymotrypsin and α-1-antitrypsin [130]. The Ki67 labeling index is usually under 1 % for most pilocytic astrocytoma [131], but a Ki67 labeling index of up to 18 % [132] has been reported. The range of Ki67 labeling varies from <1 % to 10 % in one small study [128]. Immunohistochemistry for synaptophysin varying from weak to strong has been documented in slightly less than half of the cases in a large study [133].

Cytogenetics and molecular pathology: Patients affected by neurofibromatosis 1 (NF1) has a high tendency to develop bilateral pilocytic astrocytoma in the optic nerve [134]. Mutation of *TP53* is usually absent in pilocytic astrocytoma [132]. No diagnostic ultrastructural features specific for pilomyxoid astrocytoma have been described [135]. BRAFKIAA1549 fusion can occur in up to 80 % of pilocytic astrocytoma [136–138] but are uncommon in other WHO grade II pediatric astrocytomas and oligodendrogliomas. The fusion gene may act as an adjunct in separating pilocytic astrocytoma from other WHO grade II pediatric astrocytomas and oligodendrogliomas. Tumors with fusion genes occur more commonly in the posterior fossa [133, 139] and behave less aggressively [138]. Point mutation leading to *BRAF* V600E substitution is less common (about 9 % of pilocytic astrocytomas) [109]

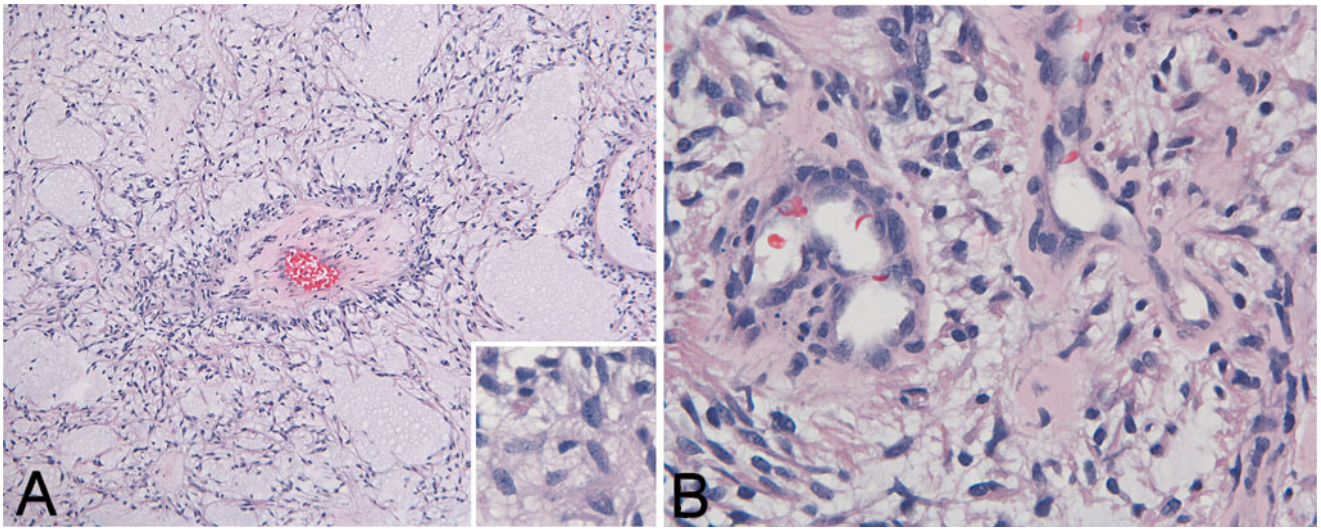

Fig. 6.12 Pilomyxoid astrocytoma: (**a**) Angiocentric arrangement of tumor cells scattered within a background with diffuse mucoid changes are the salient features. The tumor cells lack high grade pleomorphic changes (inset). (**b**) Endothelial proliferation is not uncommon in pilomyxoid astrocytomas (Images are courtesy of Dr. Gregory Fuller)

and often occurs in tumor outside the posterior fossa. Heterozygous PTEN/10q and homozygous p16 deletions have been demonstrated in 32 and 20 % of anaplastic pilocytic astrocytoma, respectively, but not in classic pilocytic astrocytoma or recurrent pilocytic astrocytoma [139]. Mutation of *IDH1* and *IDH2* [140] and other genetics changes in diffuse astrocytomas are uncommon in pilocytic astrocytomas [139].

Diffuse Astrocytoma, Anaplastic Astrocytoma, and Glioblastoma

Diffuse Astrocytoma and Anaplastic Astrocytoma

Definition: Diffuse astrocytoma, WHO grade II, is a slow growing tumor containing cells with features of highly differentiated astrocytes. Anaplastic astrocytoma, WHO grade III, is the aggressive form of astrocytoma.

Clinical features: Both tumors tend to occur in white matter area and are most common in supratentorial locations. Diffuse astrocytomas occur most commonly in young adults with some of the cases seen in adolescent and children. These tumors have an intrinsic tendency to progress to anaplastic astrocytoma or glioblastoma. Anaplastic astrocytoma is a tumor of adults and is far less common in pediatric patients.

The incidence of diffuse astrocytoma and anaplastic astrocytoma in pediatric brain is 6.2 % and 4.4 %, respectively, and that in the spinal cord is 9.5 % and 3.4 %, respectively [5]. In contrast to pilocytic astrocytomas, diffuse astrocytomas and anaplastic astrocytomas occur more frequently in the cerebral hemispheres with new onset seizure frequently seen. Other manifestations are resulted from increased intracranial pressure such as headache, nausea, vomiting, personality change, speech difficulties, and other nonspecific symptoms. Locations of the tumors dictate the nature of focal neurologic signs and symptoms.

Imaging findings: Diffuse astrocytoma appears as an ill-defined, homogeneous, non-enhancing mass that is hypointense on T1-weighted sequences and hyperintense on T2-weighted sequences. The tumor grows along the white matter tracts in the hemispheres or the infratentorial brain and may cross the corpus callosum or progress along the long tracts in the cerebral peduncles. Anaplastic astrocytoma is iso- to hypointense on T1-weighted sequences with a variable hypo- to hyperintense appearance on T2-weighted sequences. These tumors may be associated with substantial edema that is best demonstrated by FLAIR images.

Macroscopic pathology and histopathology: Gross pathology of these tumors is best appreciated, unfortunately, in untreated autopsy cases, a rare case scenario currently. In surgical specimens, tumors typically consist of small fragments or lumps of gray, tan soft tissue. Lower grade tumors tend to be more mucoid and thus have a gel-like consistency.

The histopathologic changes of classic diffuse astrocytoma and anaplastic astrocytoma are similar to those arising in adults. Diffuse astrocytomas of WHO grade II are featured by infiltrating low-grade neoplastic astrocytes (Fig. 6.13). A variable amount of mucoid background is present (Fig. 6.14). Pediatric cases often tend to be fibrillary, but gemistocytic and protoplasmic patterns can also be encountered. Mucoid substance is common in the background and it can vary from little to intermediate (Fig. 6.14a, b) to substantial and accompanied by microcyst formation.

Although anaplastic astrocytoma (WHO grade III) has many features similar to diffuse astrocytoma, these tumors have increased cellularity, distinct nuclear atypia and mitotic figures. However, by definition no endothelial proliferation or necrosis should be present.

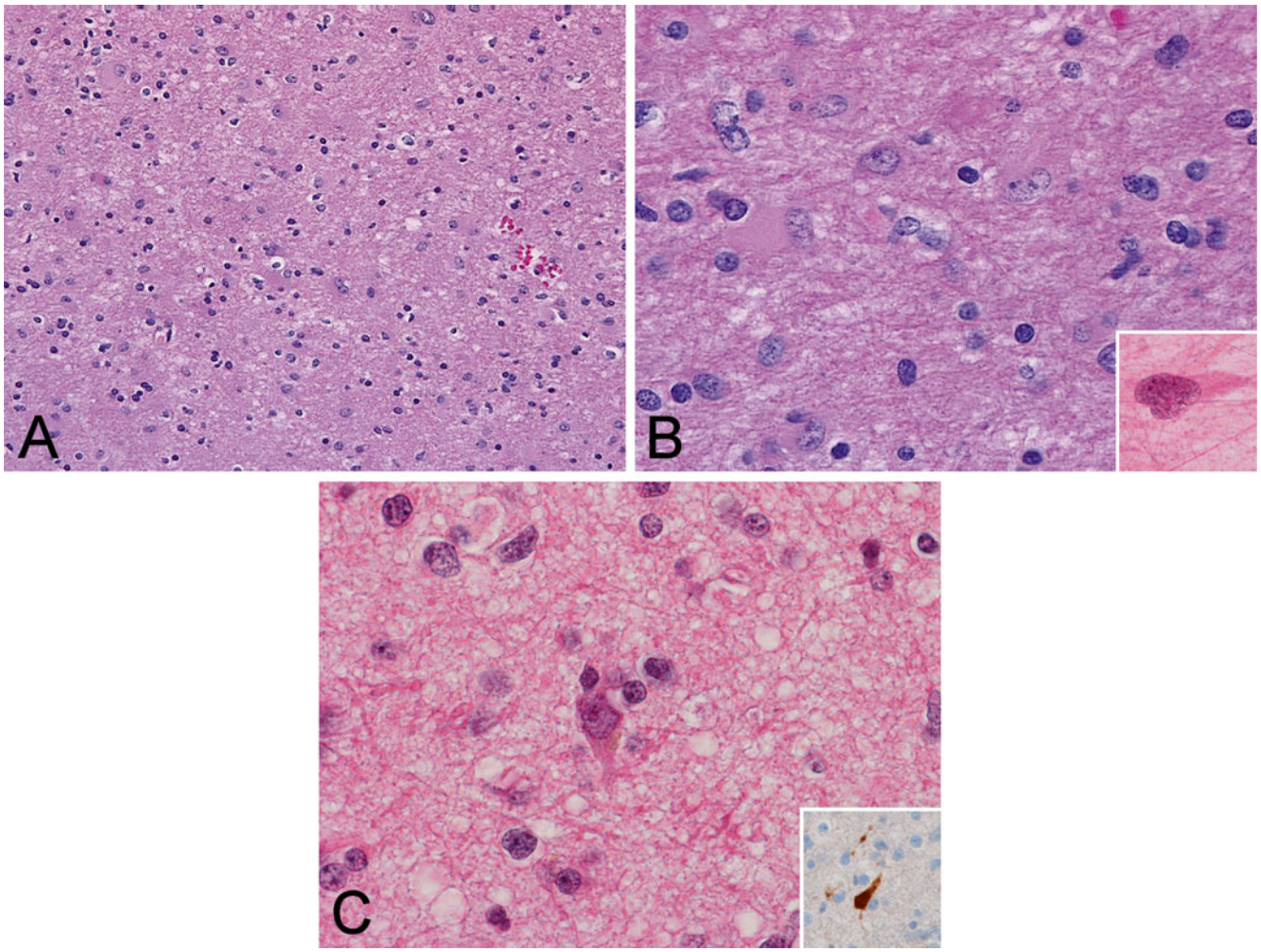

Fig. 6.13 Astrocytoma: (**a**) The cellularity is only mildly increased. (**b**) Note that the neoplastic astrocytes have enlarged nuclei as compared to the normal astrocytes in the same field. Enlarged nucleoli are not common features (inset is cytologic preparation). (**c**) Entrapped neurons are common and easily demonstrated by immunohistochemistry for neurofilament proteins (inset)

While the number of mitoses is an important criterion of malignancy, one or two mitotic figures in a large (resection) specimen unaccompanied by other features indicative of malignancy is not sufficient for a diagnosis of anaplastic astrocytoma. On the other hand, even one mitotic figure in a small stereotactic biopsy should raise the concern of an anaplastic astrocytoma.

Glioblastoma

Definition: Glioblastoma is a WHO grade IV tumor predominantly with astrocytic differentiation and histologically characterized by high-grade histology, endothelial proliferation and/or necrosis.

Clinical features: Although glioblastoma is the most common malignant brain tumor in adults, its incidence is far less common in the pediatric age group. Pediatric glioblastomas comprises about one-tenth of all glioblastoma. It may appear as a second tumor due to prior radiation treatment for other malignancies such as acute leukemia. The clinical manifestations are similar to those of diffuse astrocytoma and anaplastic astrocytoma but the clinical history is usually shorter. Rare congenital glioblastomas can occur [8]. Secondary glioblastoma (arising from a preexisting low-grade glioma) is extremely rare in children.

Imaging findings: Glioblastoma often presents as a heterogeneous mass with areas of cystic necrosis and hemorrhage. The solid component may be hypo- to isointense on T1-weighted sequences and moderately to significantly hyperintense on T2-weighted sequences. Surrounding edema is usually significantly. The enhancement is usually avid but inhomogeneous, or the so-called dirty looking and the tumor may extend to the leptomeninges resulting in leptomeningeal spread and drop metastasis (Fig. 6.15).

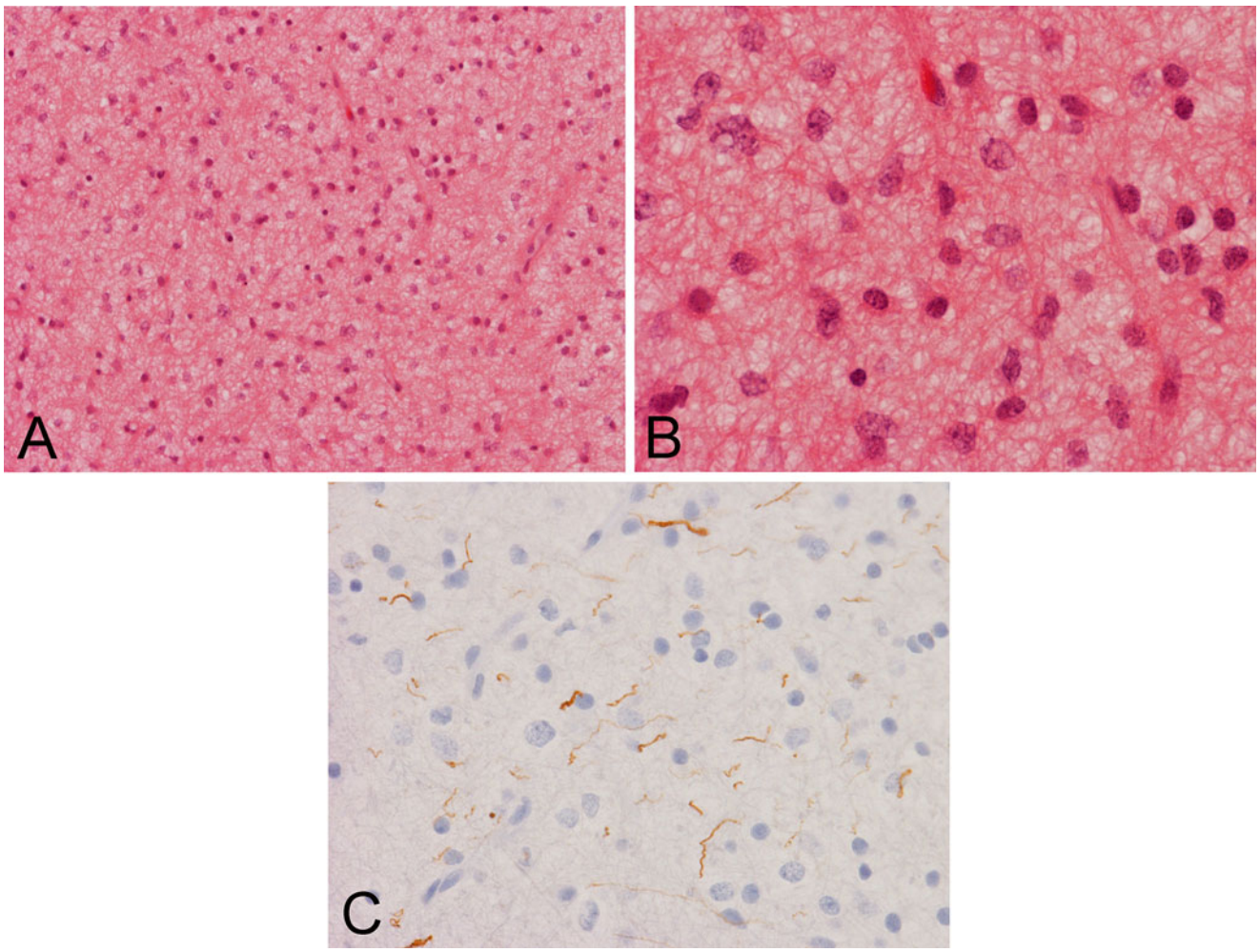

Fig. 6.14 Astrocytoma, brainstem: (**a**) and (**b**)**,** In contrast to Fig. 6.12, this tumor is composed exclusively of neoplastic astrocytes with processes that form a mesh work with mucoid fluid in the background. (**c**) The infiltrative nature is best testified by the entrapped axons as demonstrated by immunohistochemistry for neurofilament proteins

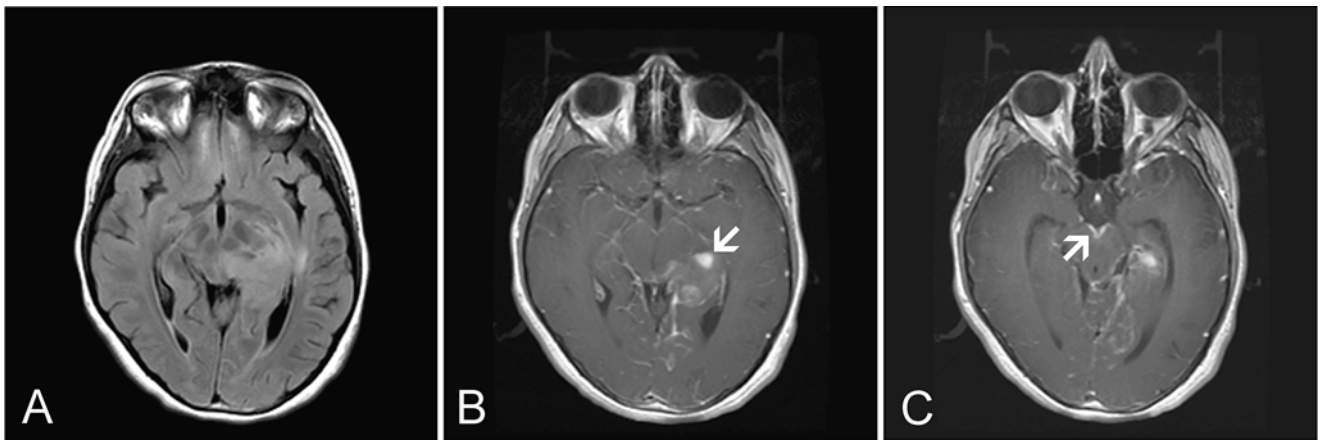

Fig. 6.15 MR-glioblastoma with CSF seeding**.** (**a**) Axial FLAIR MR image demonstrates an infiltrative, poorly defined mass involving the thalamus and temporal lobe. (**b**) Axial post-contrast enhanced T1W MR image shows inhomogeneous enhancement of the tumor. (**c**) Leptomeningeal enhancement consistent with tumor seeding (*arrow*)

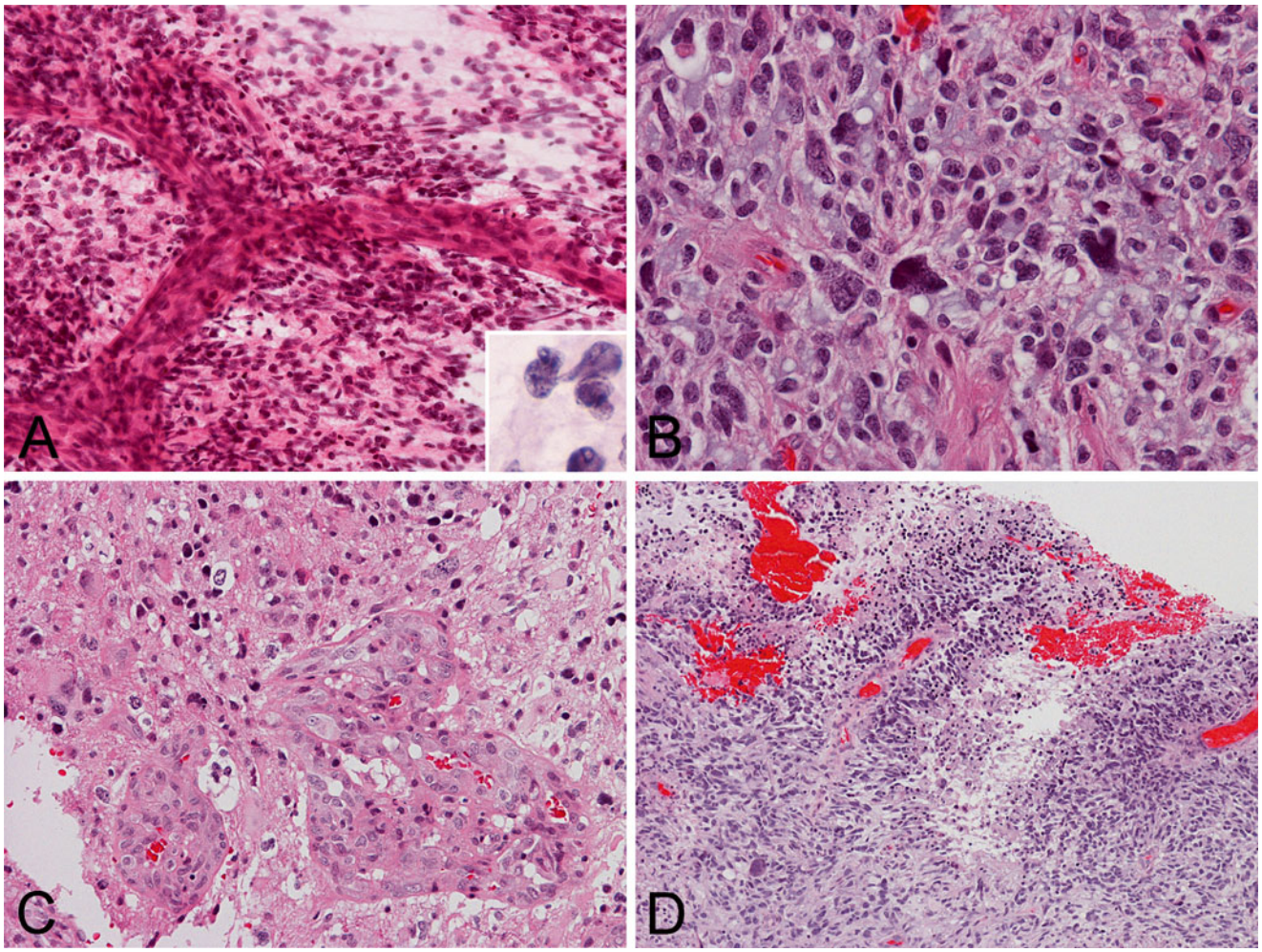

Fig. 6.16 Glioblastoma: (**a**) Tumor cells are large and atypical. Note the blood vessels with endothelial proliferation giving a tree-trunk like appearance on cytologic preparations. High grade nuclear features are shown in the inset. (**b**) Tumor cells are large and, bizarre cells can be present. (**c**) Endothelial prolilferation and (**d**) pseudopalisading necrosis are diagnostic features

Macroscopic pathology and histopathology: Glioblastoma typically arises in cerebral hemispheres and may present as a large mass. It is one of the few tumors that infiltrate across the midline through the corpus callosum to form the so-called butterfly tumor. Glioblastoma is usually poorly delineated, but genuinely multifocal tumors are rare. The size of surgical specimens varies, and gross areas of opacity corresponding to necrotic tumor generally offer a clue to the diagnosis.

In cytologic preparation, glioblastoma shares characteristics of other glial tumors with neoplastic cells having signature long cytoplasmic processes. In general, glioblastomas do not smear out as evenly as diffuse astrocytoma, and the preparation typically appears clumpy (Fig. 6.16). Tumor cell nuclei may range from medium size to large and anaplastic. Tumor cells often contain less cytoplasm than lower grade gliomas. The combination of these features may suggest other high grade tumors such as atypical teratoid/rhabdoid tumors in pediatric patients. Vessels with endothelial proliferation typically appear as thick tree-trunk-like structures with clubbing ends. The amount of necrosis can be significant, and small biopsy specimens may not contain viable tissue.

On histologic sections, the tumor is composed of neoplastic glial cells with nuclear features similar to those seen in cytologic preparations. Endothelial proliferation and/or necrosis are hallmarks of glioblastoma. Glioblastoma is notorious for having multiple tissue patterns such as glandular, ribbon-like epithelial structures suggestive of an epithelial tumor, lipid rich epithelioid cells [141], granular cells, gemistocytic cells, small cell, multinucleated giant cells, and oligodendroglioma components.

Immunohistochemistry and Molecular Pathology of Astrocytoma, Anaplastic Astrocytoma, and Glioblastoma

Astrocytoma, anaplastic astrocytomas, and glioblastomas share many common phenotypic features. These tumors are positive of GFAP and olig2. Molecular aberrations that are often found in glioblastoma include loss of heterozygosity of chromosome 10q, amplification of *EGFR*, $p16^{INK4a}$ deletion, *PTEN,* and p53 mutations. In contrast to glioblastomas of adults, *TP53* is rarely mutated in pediatric cases. Mutations of *IDH1* and *IDH2* are uncommon in pediatric cases.

Differential Diagnosis of Astrocytoma, Anaplastic Astrocytoma, and Glioblastoma

Highly cellular glioblastomas may closely mimic medulloblastoma particularly when the expression of synaptophysin is patchy. Molecular features such as EGFR amplification, loss of heterozygosity of chromosome 10q in glioblastoma, isochromosome 17 and *c-Myc* ampliation are helpful adjuncts. Comprehensive analysis of the genetic profile can also help to resolve this diagnostic dilemma [32].

Glioblastoma can mimic AT/RT, but immunohistochemistry for BAF47 and FISH for the loss of chromosome 22q generally resolve this situation. In addition, EMA is frequently expressed in AT/RT but not glioblastoma.

Pleomorphic xanthoastrocytoma contains bizarre, enlarged, and lipidized cells. Its differentiation from glioblastoma will be discussed in the section on pleomorphic xanthoastrocytoma. *BRAF* mutation is seen in slightly more than half of all cases of pleomorphic xanthoastrocytoma and is a good diagnostic help [109].

Oligodendroglioma and Anaplastic Oligodendroglioma

Definition: Oligodendroglioma (WHO grade II) and anaplastic oligodendroglioma (WHO grade III) are composed of neoplastic cells morphologically resembling oligodendroglia.

Clinical features: Both are rare in the pediatric age group. Oligodendrogliomas of WHO grade II or III occur predominantly in adults. Uncommon cases can be seen in the second decade but they are almost nonexistent during infancy and childhood. Clinical presentation is similar to other hemispheric brain tumors and is generally nonspecific.

Macroscopic pathology and histopathology: The frontal lobe is the most common site in adults and tumor arises from the cortex and white matter. Histologically, oligodendroglioma is characterized by solid sheets of tumor cells with perinuclear halo giving the so-called fried-egg cytology and a network of delicate blood vessels embedded in between. Calcifications are common. Anaplastic oligodendrogliomas have features of aggressive tumors including increased cellularity, pleomorphism, and mitotic activity, microvascular proliferation and necrosis. The tumor cells also tend to have amphophilic or eosinophilic cytoplasm rather than clear cytoplasm. In contrast to adult cases, mutations of *IDH 1* and *IDH 2*, deletion of 1p and 19q are uncommon in pediatric cases [142, 143].

Oligoastrocytoma and Anaplastic Oligoastrocytoma

Oligoastrocytoma (WHO grade II) and anaplastic oligodendroglioma (WHO grade III) are tumors composed of a mixture of both neoplastic oligodendroglial cells and astrocytic cells. Similar to oligodendroglioma, they are rare in the pediatric age group.

Pleomorphic Xanthoastrocytoma

Definition: Pleomorphic xanthoastrocytoma (PXA) (WHO grade II) is a tumor of relatively favorable prognosis and occur most frequently in children and young adult. Histologically these tumors are characterized by large, lipidized, pleomorphic cells.

Clinical features: PXA is uncommon and accounts for less than 1 % of all gliomas. The symptoms usually reflect the location of the tumor. Since PXA typically occurs in a superficial location, seizure is a commonly associated symptom.

Imaging findings: This tumor is slow growing and is usually not associated with substantial peritumoral edema. Typically tumors present as a well-circumscribed mass involving the surface of the cerebral hemispheres, particularly the temporal lobes. It can vary from a solid to cystic tumor with a mural nodule. On MRI, these tumors usually demonstrate hypointense or mixed-signal intensity on T1-weighted images and hyperintense or mixed signals on T2-weighted images. The solid areas of the tumor, including mural nodules, enhance after administration of contrast agent [144].

Macroscopic pathology and histopathology: PXA is typically superficial tumor attached to the leptomeninges with or without a cyst formation associated with a mural module. The histologic signature of PXA is the large, pleomorphic, lipidized cells with eccentrically located, bizarre, and often multinucleated nuclei. The cytoplasm of these tumor cells demonstrates a characteristic fine bubbly, lipidized xanthomatous cytoplasm. The histopathology of PXA is often heterogeneous. Areas composed predominantly of spindle to epithelioid cells without large pleomorphic cells can pose a diagnostic challenge (Fig. 6.17). Xanthomatous changes in these cells are usually subtle. Eosinophilic granular bodies are often present. Occasional association with cortical dysplasia has also been described [145, 146].

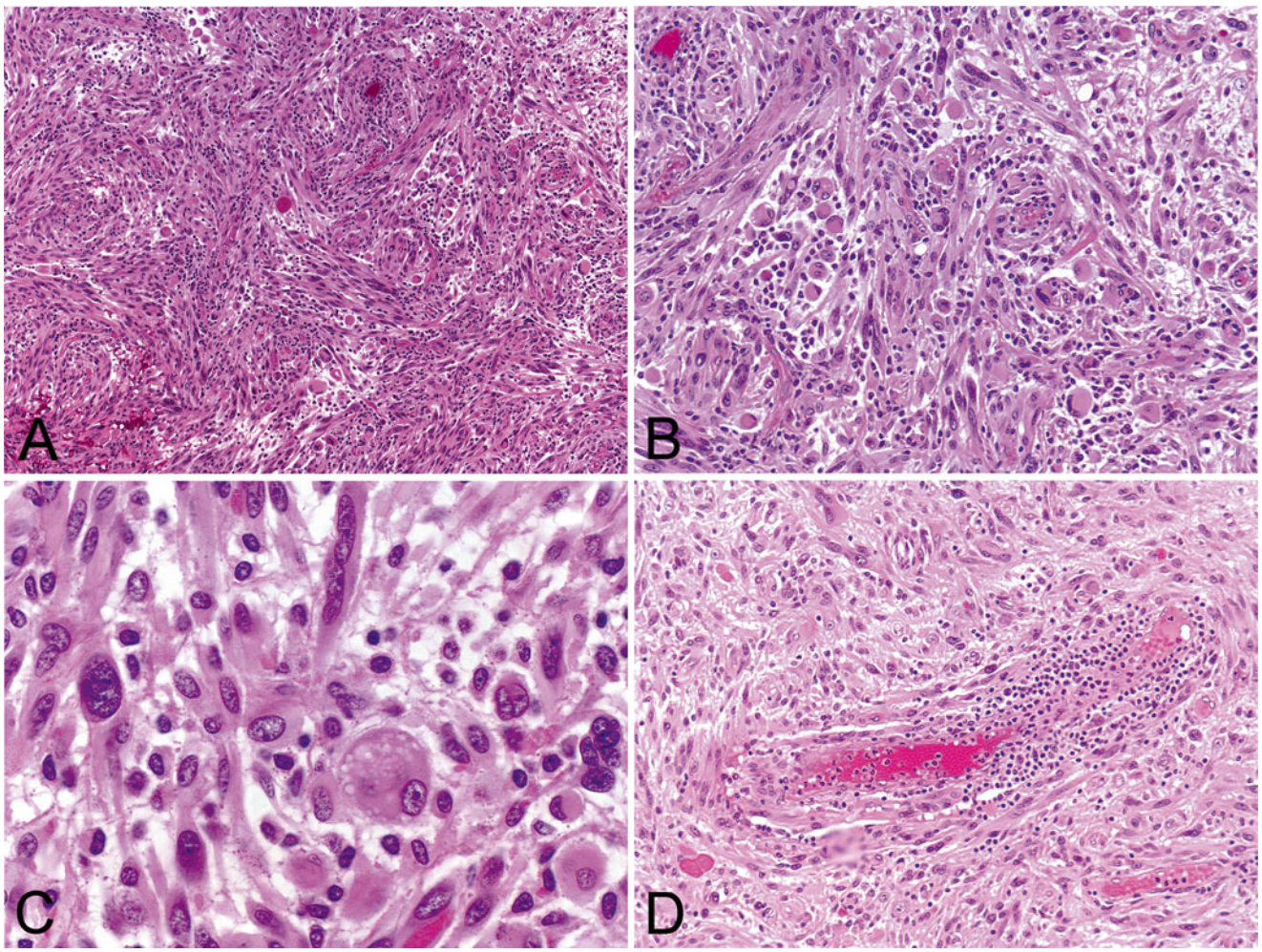

Fig. 6.17 Pleomorphic xanthoastrocytoma. (**a**, **b**) Pleomorphic xanthoastrocytoma often contains an intermixed pattern of spindle cells and large, lipidized, pleomorphic cells. The spindle cell component can be overwhelming and constitute a diagnostic challenge. (**c**) The large, pleomorphic cells often have eccentrically located nuclei and lipidized cytoplasm. (**d**) Perivascular lymphocytic infiltration is common

Despite the presence of pleomorphic cells, neither necrosis nor mitoses are features of PXA. Their presence should raise a strong suspicion of more aggressive behavior. WHO recommends the use of the term "pleomorphic xanthoastrocytoma with anaplastic features" in PXA with five or more mitoses per ten high-powered fields and/or necrosis [147, 148].

Eosinophilic granular bodies are important diagnostic features and their search is well facilitated by PAS stain with diastase pretreatment. Deposition of reticulin fibers around individual tumor cells is another diagnostic feature which reflects the possible origin of PXA from subpial glial cells. While markers for glial differentiation are typically positive in PXA, immuno reactivities for neuronal markers such as neurofilament, synaptophysin can be demonstrated in a small subset of PXA [147]. These findings suggest biphenotypic differentiation in some PXA, a finding that is confirmed by ultrastructural studies [147, 149] and p53. The latter does not appear to have prognostic value [150].

Molecular genetics: The recent demonstration of mutation of *BRAF* mutations [109, 151] in PXA represents an important adjunct of diagnosis as well as a predictive marker for potential target therapy. Like other pediatric tumors, mutation of isocitrate dehydrogenase 1 and 2 genes (*IDH1, IDH2*) is uncommon in PXA [151].

Prognostic features: The overall 5- and 10-year survival rate is about 72 and 61 %, respectively. About 20 % of PXS will progress to higher grade tumor [147].

Gliomatosis Cerebri

Gliomatosis cerebri (WHO grade III) is an uncommon, extensively infiltrative diffuse glioma. As the extent of involvement comprises part of the WHO diagnostic criteria, correlation of pathologic changes with neuroimaging studies is mandatory. Gliomatosis cerebri is most common in the fifth and sixth decade but it can be seen in all age groups. It can be seen in

adolescents and young adults but it is rare. Due to the variable and extensive involvement, the clinical manifestation has a broad spectrum including seizures, headache, cranial nerve dysfunction, dementia, lethargy, and others.

Gliomatosis cerebri is characterized by diffuse infiltration without enlargement of the involved areas. It should involve at least three cerebral lobes. Involvement across midline and deep gray matter with extension to the brainstem are common. Grossly, the involved area is usually enlarged and firm. Histologically, astrocytic phenotype is most common and the extent of infiltration is variable among different areas. The classic histology is that of infiltrating small glial cells with elongated, fusiform nuclei. Nuclear atypia is common but mitotic figures are not abundant. In stereotactic biopsies obtained from an area with low density of infiltrating tumor cells, recognition of the scattered atypical cells can be challenging but important for a correct diagnosis. Immunohistochemistry for GFAP and S100 in tumor cells is variable. Ki67 labeling can vary from less than 1 % to about 30 %. Immunohistochemistry for Ki67 is a helpful adjunct in identifying infiltrating atypical cells particularly those with subtle changes.

Imaging findings: Gliomatosis cerebri is a diffuse process involving central and peripheral structures in more than one cerebral lobe. Expansion of the involved brain structures may be seen with preservation of the brain architecture. The tumor reveals hypo- to isointense signal on T1-weighted sequences, increased signal intensity on T2-weighted sequences and, very rarely, scant enhancement. Perfusion MR imaging is a useful adjunct [152].

Leptomeningeal Neurogliomatosis

This is a rare [153, 154] disseminated glial or glial-neuronal lesion that is found predominantly in children and adolescents. This lesion has also been known as leptomeningeal oligodendrogliomatois. However, since some of these cells are immunoreactive for neuronal markers the term leptomeningeal neurogliomatosis has been adopted. In at least 1 study, the tumors showed period of stability but about one fifth of the cases had anaplastic progression. Radiographically, they appear as leptomeningeal enhancement within the spinal cord/brain along the subpial surface with cystic or nodular lesion. Histologically (Fig. 6.18), the tumor is composed of infiltrating oligodendroglioma-like cells with low mitotic rate in a desmoplastic to myoid background. The cellularity can vary from high to low. These tumors may have ganglion/ganglioid cells and intraparenchymal component. The tumor cells are positive for olig2, S100, GFAP, and synaptophysin and negative for NeuN, EMA. There is no *IDH1* mutation as detected by immunohistochemistry for R132H mutation. Co-deletion of chromosome deletion of chromosome 1p, and 19q have been demonstrated in only a minor subset of cases [154, 155]. Histologically, this is a challenging diagnosis and one of the differential diagnoses is chronic meningitis [156].

Mixed-Glial Neuronal and Neuronal Tumors

Tumors with mixed-glial neuronal and neuronal tumor comprise a family of neoplasms with a high incidence in pediatric patients and young adults. Mixed glial-neuronal tumors have a broad array of histologic feature but are essentially variation on the same theme in which recognition of neoplastic glial and neuronal components is the key to the diagnosis.

Ganglioglioma and Gangliocytoma

Definition: Ganglioglioma contains neoplastic glial cells and neuronal (ganglionic) cells while gangliocytoma contains only neoplastic neuronal cells. While gangliocytoma and most ganglioglioma are of WHO grade I, anaplastic ganglioglioma (WHO grade III) has anaplastic features in their glial component.

Clinical features: Gangliogliomas are uncommon but not rare tumors. Although gangliogliomas can occur in any age, the majority arise in children and young adults. While they can be found anywhere in the CNS including the optic nerve, the majority occur in the temporal lobe. For those that occurred in the cerebral hemispheres, seizure is the most common presentation. Less common symptoms include headaches, vomiting, ataxia, and others.

Imaging findings: Ganglioglioma is typically a well-circumscribed mass without excessive edema in surrounding tissue or mass effect (Fig. 6.19). It can be cystic and contain a mural nodule. It appears hypointense on T1-weighed images, hyperintense on T2-weighted images, and enhances. Foci of calcification are common. Due to their slow growth rate, superficially located tumors may have scalloping effects on the calvarium [157].

Macroscopic pathology and histopathology: Grossly, ganglioglioma can be rather rubbery and particularly unamenable to adequate cytologic preparation. Histologically, the histopathology is heterogeneous. The spectrum varies from a predominantly neuronal tumor (gangliocytoma) to a ganglioglioma with predominantly glial component mimicking a glioma. The distribution of neoplastic neuronal and glial component varies considerably [158, 159]. A thorough examination is often required to recognize both neoplastic glial and neuronal components. The distribution of ganglionic cells is typically uneven and clustering is the rule. Cytologically, ganglionic cells resemble normal neurons, or large ganglionic cells with bizarre shape, abnormal Nissl substance, and occasionally vacuolation (Fig. 6.20). Binucleation of ganglionic cells (Fig. 6.20A) can be seen in about 60 % of cases [159]. Increased reticulin deposition around ganglionic cells is frequent. The glial component is also heterogeneous. It can vary

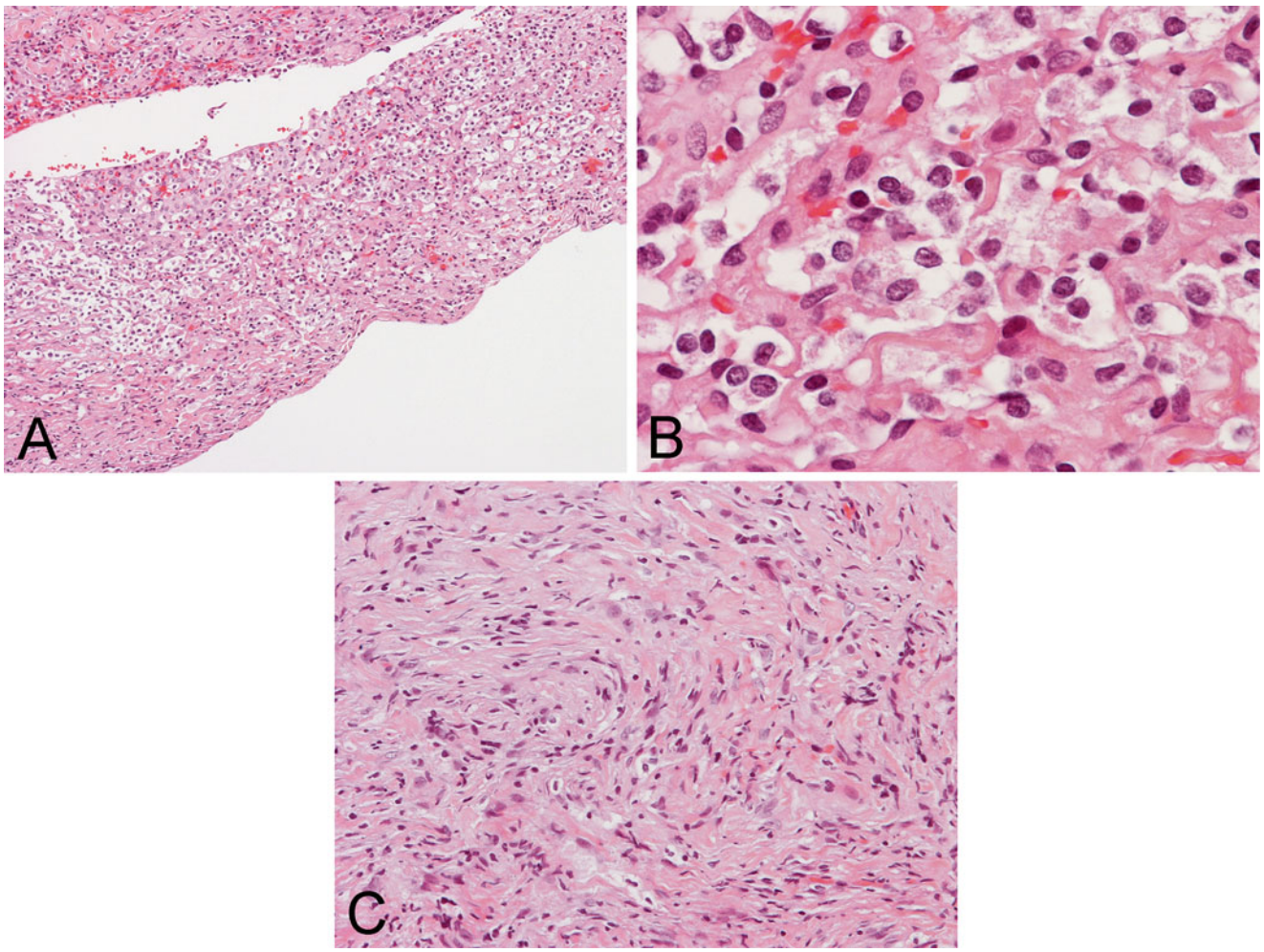

Fig. 6.18 Spinal leptomeningeal neurogliomatosis. (**a**) The typical area appears as an infiltrating tumor in a fibrous background. (**b**) On higher magnification, the tumor cells have perinuclear halo and round, monotonous nuclei resembling oligodendrogliocytes. (**c**) The amount of fibrosis can be quite variable and this image is taken from the same specimen in (a) and (b) and has a fibroblastic appearance suggestive of fibroblastic meningioma

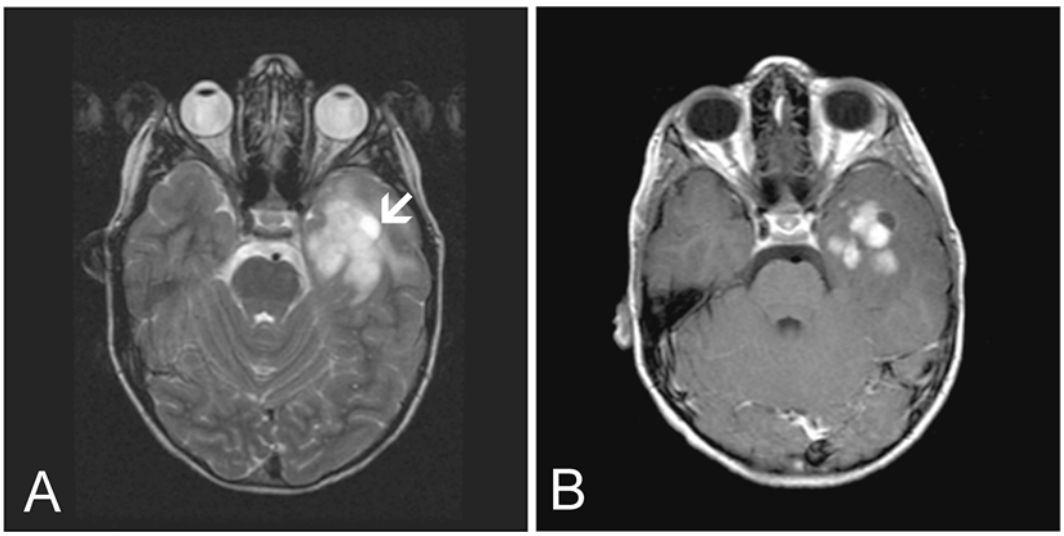

Fig. 6.19 MR-ganglioglioma. (**a**) Axial FSE-T2W MR image demonstrate a lobulated mass in the left temporal lobe with a small cystic component (*arrow*). (**b**) Axial post-contrast T1W MR image shows vivid enhancement of the solid component (8-year-old male)

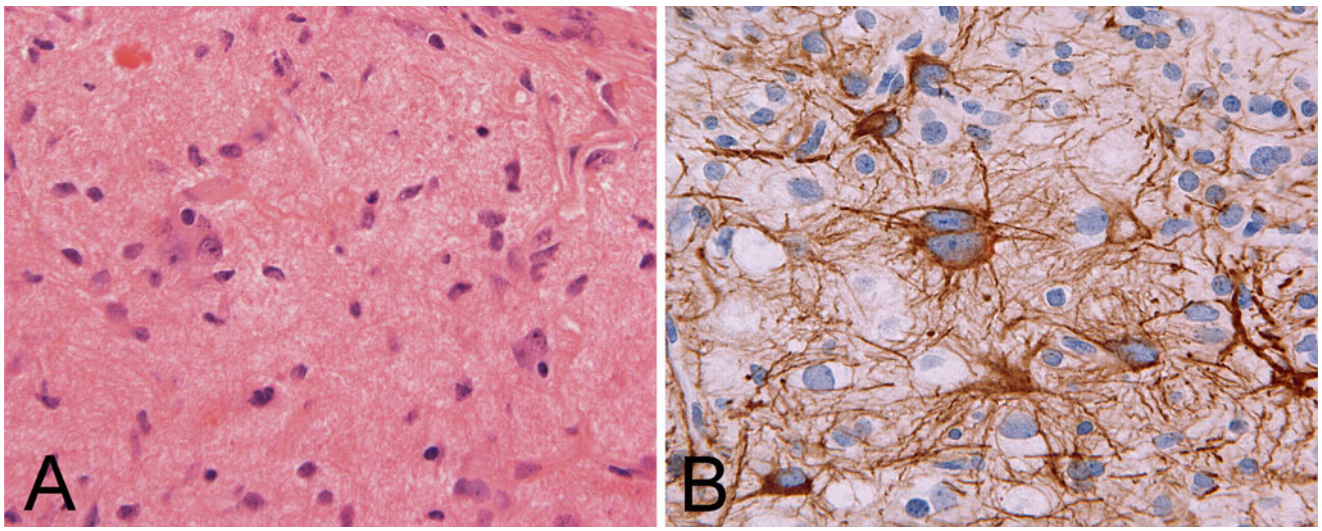

Fig. 6.20 Ganglioglioma: (**a**) Typical ganglioglioma is composed of a mixture of larger neurons and smaller neoplastic glial cells. The neurons often have dysplastic features, such as binucleation. (**b**) Immunohistochemistry for neurofilament proteins highlights the binucleated bizaare multipolar neurons within a background of proliferating glial cells

from low cellularity with only a few spindle cells to a cellularity closely resembling an astrocytic neoplasm. Calcifications, eosinophilic granular bodies, Rosenthal fibers, extensive perivascular lymphocytic infiltrations, and prominent capillary network are other common features. Mitotic figures are absent or rare, and necrosis should be absent. When a malignant component of anaplastic ganglioglioma is identified, it almost always involves the glial component.

Molecular pathology and Immunohistochemistry: *BRAF* V600E mutation has recently been demonstrated in ganglioglioma [160] and may represent a negative prognostic factor [161]. When the neuronal component is not obvious, immunohistochemistry for synaptophysin, neurofilament proteins, and NeuN are helpful adjuncts to highlight it. Neurofilament protein immunostain has the additional benefit of demonstrating the abnormal shape and processes of the ganglionic cells (Fig. 6.20b). Ganglionic cells typically demonstrate cytoplasmic surface immunoreactivity for synaptophysin [158]. Although CD34 are negative in adult neurons, it is positive in ganglionic cells in about three quarter of cases [162]. Silver-positive neurofibrillary tangles have been demonstrated in rare cases [163].

Associated lesions: Most gangliogliomas are sporadic, but about 5 % are associated with congenital abnormalities. In particular, cortical dysplasia has been demonstrated in about half the cases in one study [159].

Differential diagnosis: The major challenge in the diagnosis of ganglioglioma is to distinguish ganglioma with only focal ganglionic component from glioma. By the same token, it is also important not to mistake entrapped neurons in gliomas, particularly astrocytomas.

Dysplastic Gangliocytoma of the Cerebellum/ Lhermitte-Duclos Disease

Dysplastic gangliocytoma of the cerebellum/Lhermitte-Duclos disease is part of the PTEN hamartoma tumor syndrome that includes Bannayan–Riley–Ruvalcaba syndrome, and possibly Proteus syndrome, and Cowden syndrome [164, 165]. The disease is characterized by germline mutations of *PTEN*. Lhermitte-Duclos disease is usually discovered in the third or fourth decade and rarely seen in children. Radiographically, the lesion is a non-enhancing cerebellar mass with or without involvement of the vermis. It is hypointense on T1-weighted and hyperintense on T2-weighted sequences with alternating striations that follow the outline of the folia [166].

It is not certain whether this entity is a hamartoma, neoplastic growth, or a reaction to dysembryogenetic events. The signature gross feature is regional thickening of cerebellar folia with an unusual firmness but with preserved architecture. Histologically, it has the so-called inside-out architecture of the cerebellum. A layer of myelinated fibers with large diameter myelinated axons replaces the molecular layer. The internal granular layer is replaced by intermediate sized to large dysplastic neurons with some of them vaguely reminiscent to Purkinje cells. Scattered cells reminiscent of granule cells may be found in molecular layer or subpial locations. In some cases, granule cells persist in the deeper layer of the affected cortex. The native white matter of the folia is atrophic and rarefied.

Desmoplastic Infantile Ganglioglioma and Astrocytoma

Definition: Desmoplastic infantile ganglioglioma (DIG) and astrocytoma (DIA) (WHO grade I) are rare, slow growing, superficially located large, typically cystic tumor with desmoplastic changes that are often attached to the dura.

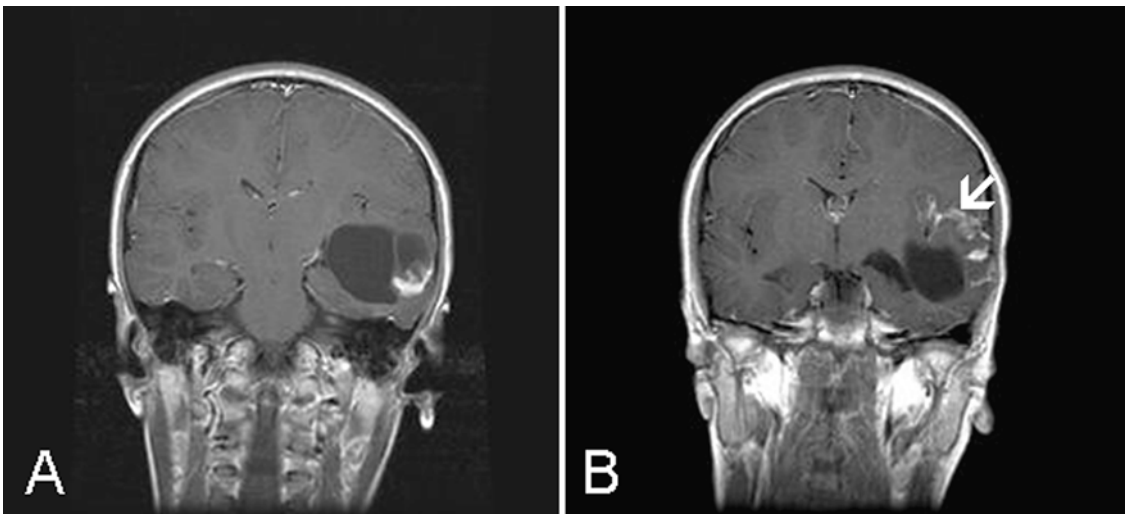

Fig. 6.21 MR-desmoplastic infantile ganglioglioma: post-contrast T1W coronal MR images demonstrate (**a**) a cystic mass with an enhancing, peripheral, solid component and (**b**) leptomeningeal enhancement (*arrow*) (9-year-old girl)

Clinical features: These tumors are seen almost exclusively within the first 2 years of life with exceptional cases in older children and young adults. Manifestations of increased cranial pressure and hydrocephalus are most common. Seizure and focal motor signs are only occasional.

Imaging findings: Imaging studies typically demonstrate a well-circumscribed, large, hypointense, uni- or multiloculated cystic mass with a superficially located nodule. The solid component reveals low signal intensity on T2-weighted sequences likely due to desmoplasia (Fig. 6.21). On post-contrast images, enhancement of the peripherally located nodule is avid [167].

Macroscopic pathology and histopathology: The tumor is often rubbery tough and cytologic preparation is often difficult to make. The peripherally located solid component often attaches to the leptomeninges and dura. Hemorrhage and necrosis should not be present. Histologically (Fig. 6.22) these tumors are sharply demarcated from the adjacent cortex. DIG contains both ganglionic and astrocytic component while DIA contains only astrocytic component. The desmoplastic component is featured by a mixture of collagen fibers, fibroblast like spindle cells and pleomorphic neuroepithelial cells with eosinophilic cytoplasm. These cells may arrange in whorls or fascicles. The ganglionic cells vary from small neuron to large, atypical ganglionic cells. Isolated ganglionic cells surrounded by desmoplastic changes are not uncommon. The collagenous deposition is well demonstrated by trichrome stain and reticulin deposition around individual cells is another diagnostic feature. Islands of poorly differentiated neuroepithelial cells with features of small blue cells reminiscent of primitive neuroectodermal tumor and without desmoplastic changes can be present and sometime as a prominent component. A non-desmoplastic cortical component can be found in the tumor adjacent to the cortex. While mitosis can be seen in the poorly differentiated component, they are not readily seen in the desmoplastic and cortical components.

Molecular pathology and immunohistochemistry: *BRAF* V600E mutation has been demonstrated in a small number of these tumors [168]. The ganglionic component can be demonstrated by neuronal markers including neurofilament proteins and synaptophysin. The fibroblast-like cells in the desmoplastic leptomeningeal component are often positive for vimentin and GFAP and also focally for smooth muscle actin. The astrocytic component is demonstrated by immunohistochemistry for GFAP.

Differential diagnosis: Tumors with the poorly differentiated component dominating the picture may raise a concern for primitive neuroectodermal tumor. The desmoplastic component, the spindle cells, and the large pleomorphic cells often raise a possibility of sarcoma. Both of situations are particularly challenging during intraoperative consultations.

Prognostic features: Despite the presence of poorly differentiated component, complete resection appears is an effective treatment. A rare case with anaplastic changes and dissemination through the CSF has been reported [169].

Dysembryoplastic Neuroepithelial Tumor (DNET)

Definition: Dysembryoplastic neuroepithelial tumor (DNET) (WHO grade 1) is a benign glial-neuronal tumor with a complex columnar and multinodular architecture and often associated with cortical dysplasia.

Clinical features: DNET is usually seen in infants, children, adolescent and young adults, and drug-resistant partial seizure is the most common presentation. Surgical treatment would lead to a cure and recurrence is uncommon.

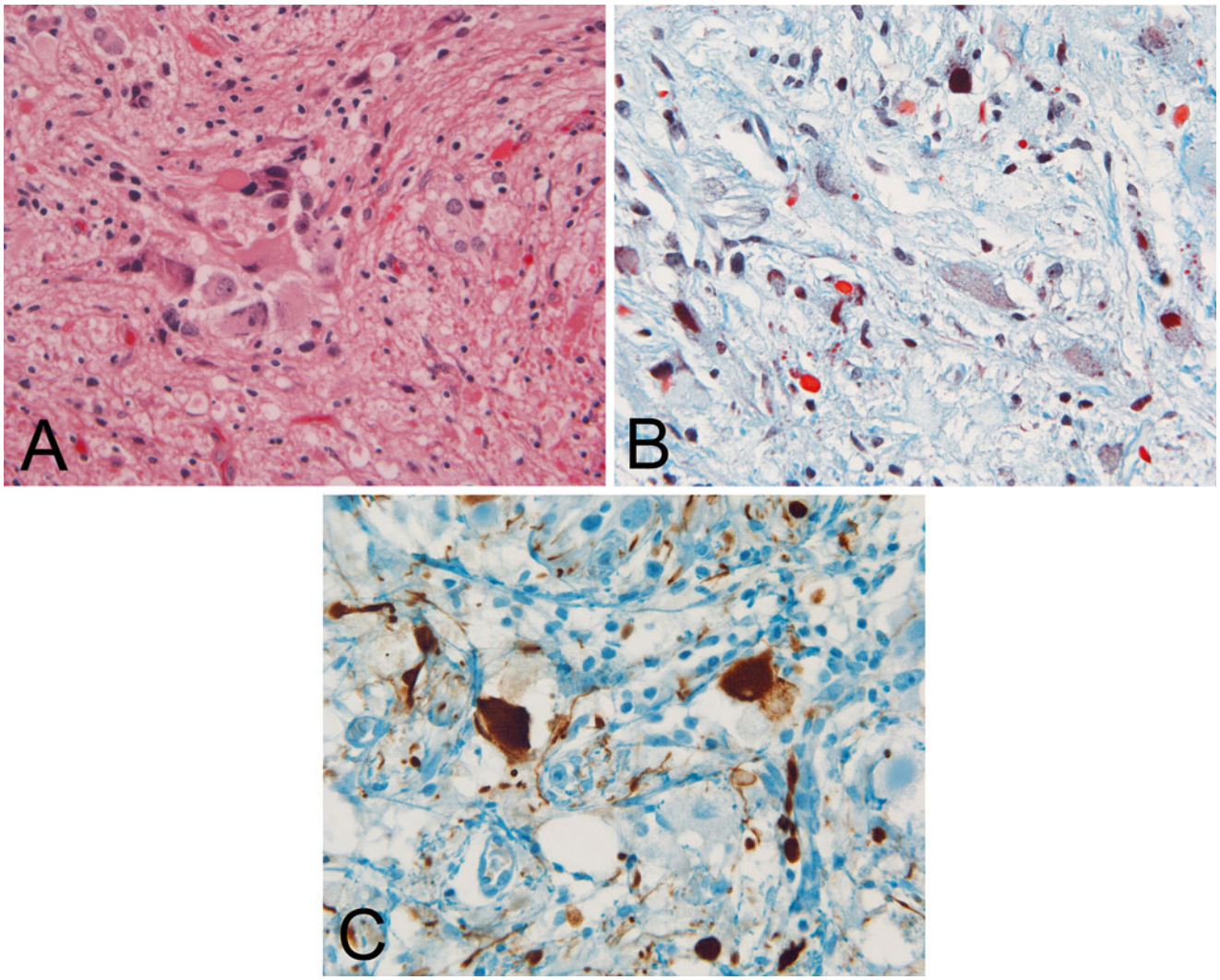

Fig. 6.22 Desmoplastic infantile ganglioglioma. (**a**) Note the large ganglionic cells cluster surrounded by a fibrillary component containing collagen fibers. (**b**) Note the ganglionic cells standing out in the collagenous background as demonstrated here with trichrome stain. (**c**) The neuronal component is well demonstrated by immunohistochemistry for neurofilament proteins

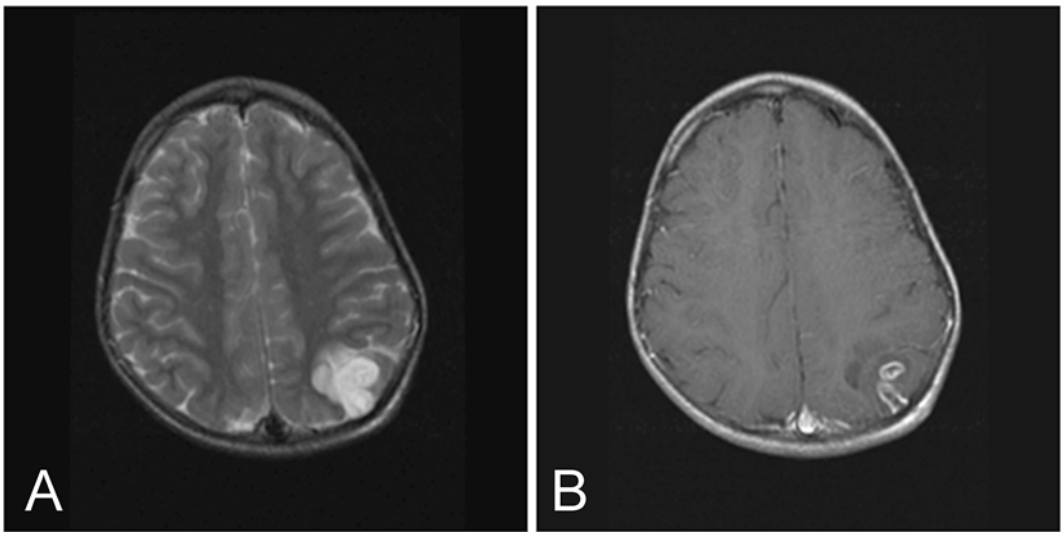

Fig. 6.23 MR-dysembryoplastic neuroepithelial tumor. (**a**) Axial FSE-T2W MR image demonstrates a cortically based, hyperintense mass in the left parietal lobe. (**b**) Axial post-contrast T1W MR image shows the tumor has focal enhancement. Only minimal edema is present around the tumor (10-year- old male). Note that the tumor illustrated here arises in an unusual location for this type of tumor

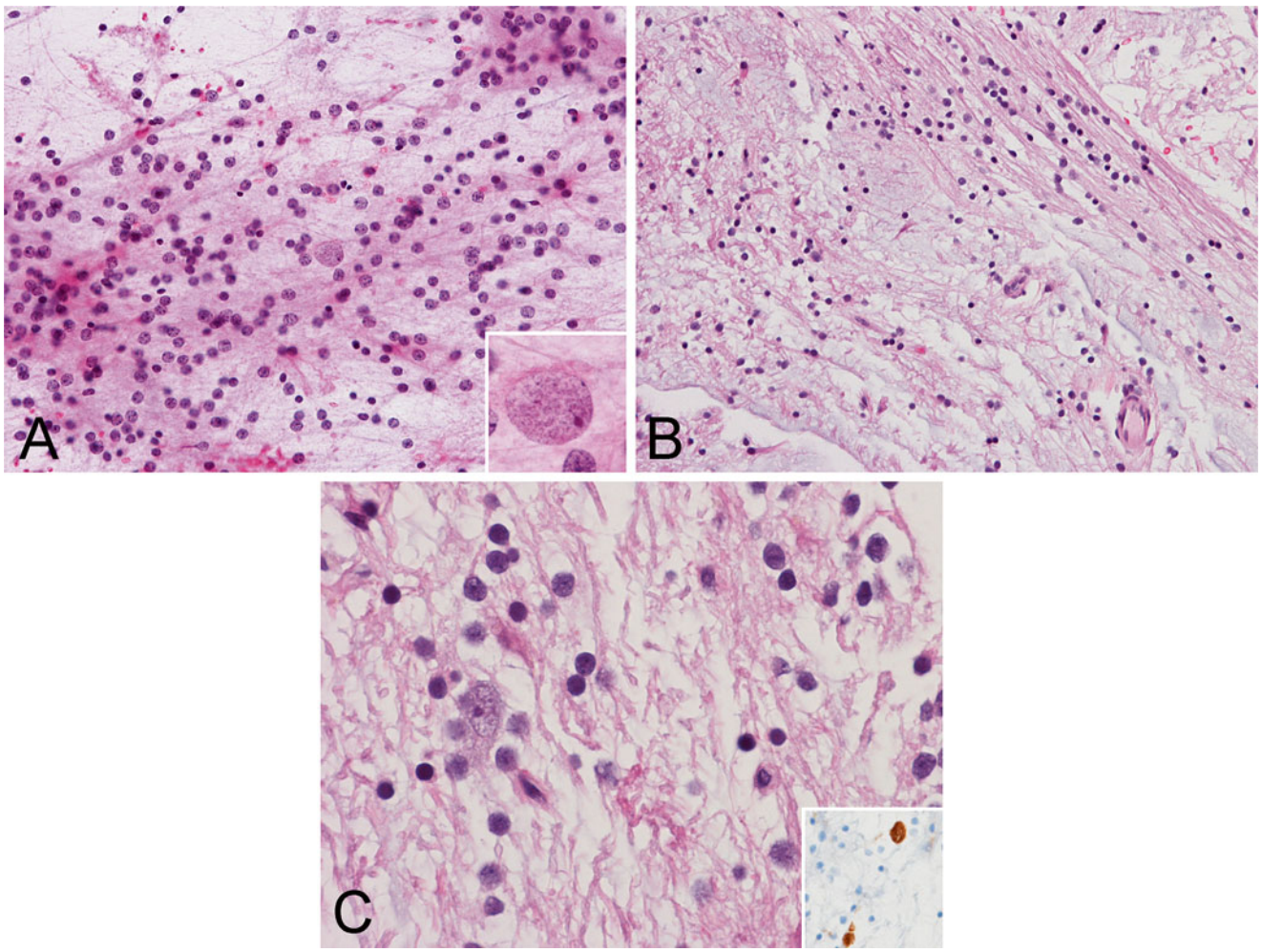

Fig. 6.24 Dysembryoplastic neuroepithelial tumor. (**a**) Cytologic preparation shows a meshwork of fine fibrillary neuropil-like processes. A naked nucleus from a neuronal cell is present and appears "floating" in the fibrillary background (inset). (**b**) This image is obtained from an area with substantial mucoid changes. (**c**) A ganglionic cell is shown here. Often these neurons are low in number but well demonstrated by immunohistochemistry to neuronal markers such as neurofilament proteins (Inset)

Imaging findings: This tumor typically presents as a well-circumscribed cortically based lesion without mass effect or peritumoral edema (Fig. 6.23). The size can vary from subcentimeter to several centimeters. These tumors are isointense or hypointense on T1-weighted images and hyperintense on T2-weighted images. A pseudocystic or multicystic appearance may be seen. If the tumor enhances the enhancement pattern is nodular [170].

Macroscopic pathology and histopathology: Surgical specimens of DNET typically consist of soft mucoid fragments. Cytologic preparation and frozen section would often demonstrate a mucoid background with small round, oligodendroglial-like cells and occasional neurons (Fig. 6.24). It should be noted that the amount of mucoid changes can be quite variable. The simple form of DNET contains the "specific glioneuronal element" featured by columnar alignment of small, oligodendrocyte-like cells along bundled axons and delicate capillaries in a mucoid background. Microcyst formation is common in cases that are markedly mucoid. In addition to the "specific glioneuronal element" the complex form of DNET contains sharply delineated nodular glial proliferations reminiscent of pilocytic astrocytoma, astrocytoma, oligodendroglioma or oligoastrocytoma. Cortical dysplasia can be found in the cortex surrounding the tumor.

Molecular pathology and immunohistochemistry: Neuronal cells are positive for CD34 in about 30 % of cases and *BRAF* (V600E) mutation has been demonstrated in about 25 % of the cases [171].

Papillary Glioneuronal Tumor

Papillary glioneuronal tumor (WHO grade I) is an uncommon tumor of young adult and adolescents that is uncommon in children and infants. It is typically seen in the cerebral hemispheres particularly the temporal lobe and the typical manifestation is seizure and headache. In the small number of reported cases, these tumors occur as cystic periventricular

lesion with mural nodules, enhancing borders, and septations [172, 173]. The tumor can be solid or cystic and shows the typical biphasic architecture. Histologically, hyalinized blood vessels form the backbone of the pseudopapillary architecture that is covered by a single or pseudostratified layer of small, cuboidal cells that has scant cytoplasm and round nuclei. In between the papillary structures are solid sheets of oligodendrogliocyte-like or neurocytic clear cells, medium sized "ganglioid" neurons, and large ganglionic cells in variable proportions. Minigemistocytes are occasionally present in the solid interpapillary areas. Rosenthal material and eosinophilic granular bodies can be found at the periphery of the tumor where they interface with the surrounding parenchyma. Perivascular glial cells are strongly positive for GFAP and Olig2. Solid areas are positive for synaptophysin and NeuN, but only larger ganglion-like cells are positive for neurofilament proteins. Microvascular proliferation and necrosis are generally absent. Mutations of *IDH1* and *IDH2*, deletion of chromosome 1p and 19q are not identified [174].

Rosette-Forming Glioneuronal Tumor of the Fourth Ventricle

Rosette-forming glioneuronal tumor of the fourth ventricle (WHO grade I) is a recently recognized uncommon benign tumor [175]. The lesion presents as well-defined mass with heterogeneous enhancement in fourth ventricle with cystic and solid components, potentially with hemorrhage and calcifications [176, 177]. It is essentially a tumor of young adults. Occasional cases can be seen in adolescents but are rare in children and infants. Due to its location, hydrocephalus is a typical manifestation [177]. Histologically, these tumors are biphasic. The superficial features mimic dysembryoplastic neuroepithelial tumor with a pilocytic astrocytoma-like growth pattern [178]. The tumor contains perivascular pseudorosettes lined by delicate cells with delicate cell process radiating towards the vessel. In between these pseudorosettes are monotonous small neurocytic cells that form neurocytic rosettes characterized by a core of eosinophilic neuropils rimmed by neurocytic cells.

Central Neurocytoma and Cerebellar Liponeurocytoma

Central neurocytoma (WHO grade II) is commonly seen in young adults but uncommon in adolescents and children. They occur most frequently as intraventricular tumor in the lateral and/or third ventricle. Extraventricular tumors can occur. Central neurocytoma present as a well marginated, lobulated mass, often with cystic changes and hemorrhage. On MR imaging the lesion is isointense on T1-weighted, hyperintense on T2-weighted sequences and shows inhomogeneous moderate enhancement [176, 179].

Histologically, neurocytoma is composed of monotonous round to polygonal cells with centrally located nuclei and formation of neuropil islands [180]. Calcifications are seen in half of the cases. With all these features considered, they can be mistaken as oligodendroglioma. The neuronal differentiation is best testified by strong and diffuse staining for synaptophysin in both tumor cells and neuropils. NeuN is often positive [181]. It should be noted that central neurocytoma can also be focally positive for Olig2 [182]. Ultrastructural examination shows a neuronal tumor with distinctive features [180].

Cerebellar liponeurocytoma is essentially a tumor of older adults. Histologically, it is similar to central neurocytoma, but a lipomatous component is present. Gene expression studies suggest that it is related to central neurocytoma [183].

Spinal Paraganglioma

This is a tumor of older adults and is rarely seen in the pediatric age group. They occur typically at the cauda equina and they are histologically identical to paraganglioma arising in other part of the body. On MR imaging, spinal paraganglioma appears as a well-marginated mass, isointense on T1-weighted images, iso to hyperintense on T2-weighted sequences, with avid enhancement following contrast administration. Hemorrhage may be seen within the mass [6].

Ependymal Family of Tumors

In the current WHO classification, ependymal tumors are found in grade I (subependymoma and myxopapillary ependymoma), grade II (ependymoma), and grade III (anaplastic ependymoma) categories. Together, they comprise one of the most frequent tumors in the pediatric age group.

Subependymoma

Subependymoma is a benign, slow growing glial neoplasm typically attached to the ventricular wall. It is almost unknown to the pediatric age group. Subependymoma is most often encountered in the fourth ventricle followed by the lateral ventricle typically as a well-circumscribed hypo to isointense on T1-weighted and relatively hyperintense on T2-weighted sequences mass without enhancement [176]. Histologically, it is characterized by clusters of bland appearing neoplastic glial cells embedded within a dense background of fibrillary matrix of glial processes reminiscent of bouquet of flowers scattered within a lawn. Microcystic changes are common. Because of their slow growing, subependymoma is an uncommon surgical specimen but they can present as incidental finding in autopsy.

Ependymoma and Anaplastic Ependymoma

Definition: Ependymoma (WHO grade II) and anaplastic ependymoma (WHO grade III) are tumors with phenotypic features of ependymal cells and are typically found in areas with ependymal cells. While ependymoma is slow-growing and indolent, anaplastic ependymoma is aggressive.

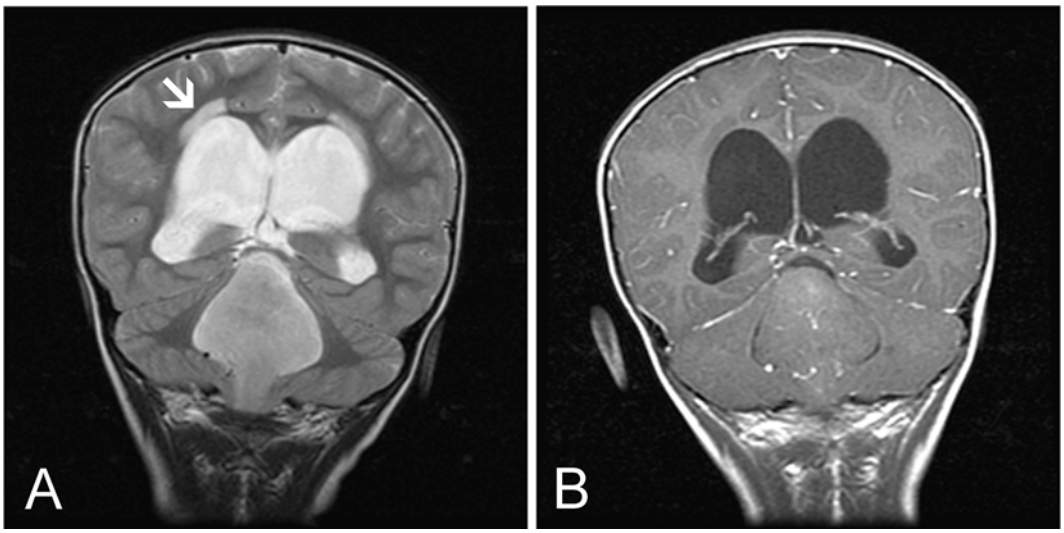

Fig. 6.25 MR-ependymoma. (**a**) Coronal FSE-T2W MR image demonstrates a large, well-demarcated mass of intermediate to high signal intensity that filled and dilated the fourth ventricle causing hydrocephalus and CSF edema (*arrow*). (**b**) Coronal T1W post-contrast MR image show minimal enhancement of the tumor (5-year-old male)

Incidence: Ependymoma is a childhood tumor and comprises up to 6–12 % of all pediatric intracranial tumors and up to 30 % of intracranial tumors in children younger than 3 years old. In contrast to those arising in adult patients, pediatric ependymomas and anaplastic ependymomas occur more commonly in the posterior fossa than in spinal cord. Interestingly, rare congenital cases have been described [8].

Clinical features: With its typical association with the ventricular lining and involvement of the fourth ventricle, symptoms are typically caused by hydrocephalus and increased intracranial pressure. Head enlargement secondary to hydrocephalus can be seen in patients under 2 years of age. Tumors arising in the posterior fossa can also cause cerebellar ataxia, visual disturbance, and other symptoms. As surgical resection remains the mainstay of treatment for ependymoma, correct recognition of these entities particularly during intraoperative consultation is crucial.

Imaging findings: Ependymoma in younger children occurs most frequently in the posterior fossa as a well-circumscribed intraventricular mass with variable enhancement. Associated ventricular obstruction and hydrocephalus are common. This tumor commonly demonstrates cystic change and calcification. Intraventricular ependymomas may insinuate and even exit through the foramina of Luschka and Magenti. Spinal dissemination may occur. Intratumoral hemorrhage can rapidly expand the tumor leading to compression of the brain stem that requires urgent neurosurgical intervention. The tumor reveals hypo to isointense signal characteristics on T1-weighted imaging and iso to hyperintense signal on T2-weighted sequences (Fig. 6.25). The presence of calcifications and hemorrhage is associated with "blooming artifact" on MRI while both are readily demonstrated on CT [176, 184]. Ependymomas in older children or young adults are often supratentorial. Supratentorial tumors may be intraventricular or intraparenchymal. While they share common imaging features with infratentorial ependymomas, they tend to be larger in size [184].

Macroscopic pathology and histopathology: These tumors can occur in any location along the ventricular lining. Rare extraneural ependymoma can be found in the sacrococcygeal area where the filum inserts. When compared to diffuse astrocytomas, ependymomas are well circumscribed. Necrosis and hemorrhage are uncommon. Ependymomas can also fill the fourth ventricle and extend through the foramina of Luschka and Magendie into the subarachnoid space. Both ependymoma and anaplastic ependymoma have a tendency for craniospinal dissemination through the CSF.

Classic ependymomas (Fig. 6.26) typically have a well-delineated interface with the surrounding parenchymal tissue. Ependymomas are characterized by a moderately cellular proliferation with small to moderately sized, monotonous, nuclei with "salt and pepper" speckling of the chromatin and small nucleoli. Mitotic activities are not readily seen. These cells typically arrange in a perivascular pseudorosettes around a blood vessel associated with a signature paucinuclear zone around the blood vessel.

In addition, true ependymal rosettes or ependymal canals featured by ependymal cells in circular arrangement forming a lumen can be seen but are not common features. Focal papillary changes can also be seen (see below). Secondary changes including myxoid background, calcifications, hemorrhage, and hyalinization of blood vessels can also occur.

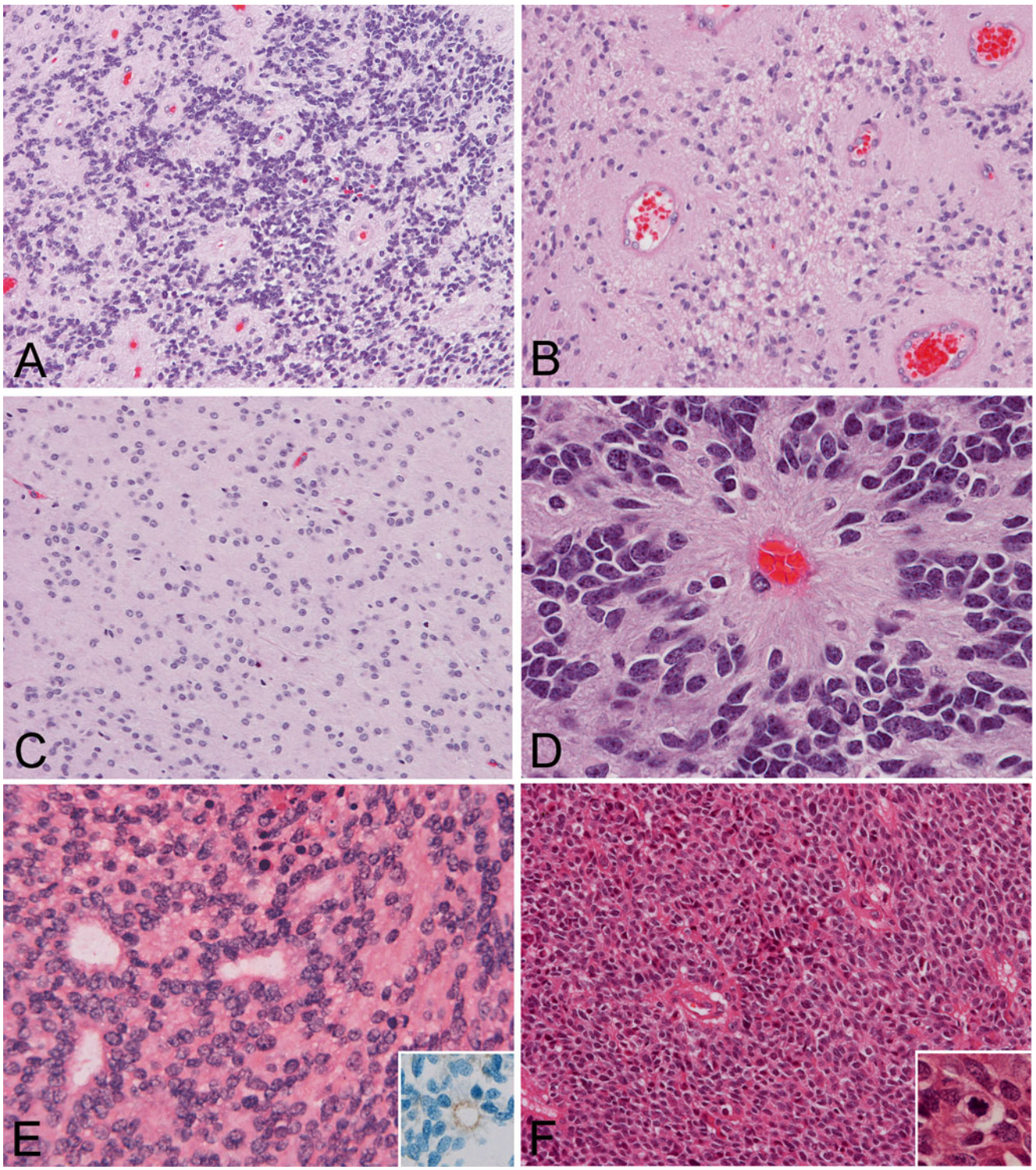

Fig. 6.26 Ependymoma: (**a**) and (**b**) show two ependymomas with significant variation in cellularity. Note that the perivascular pseudorosettes can be well appreciated. (**c**) is obtained from the same case as (**b**) in a location where perivascular pseudorosettes are subtle. (**d**) is a classic perivascular pseudorosettes in ependymoma. (**e**) shows ependymal canals in an ependymoma. These structures are reminiscent of the central canal of spinal cord. Immunohistochemistry for epithelial membrane antigen would demonstrate positive immunoreactivity at the luminal border of these canals (inset in (**e**)). (**f**) shows a cellular ependymoma. Note the increase in cellularity in comparison to classic ependymoma and increase in mitotic figure (Inset). Necrosis is not readily seen in this tumor

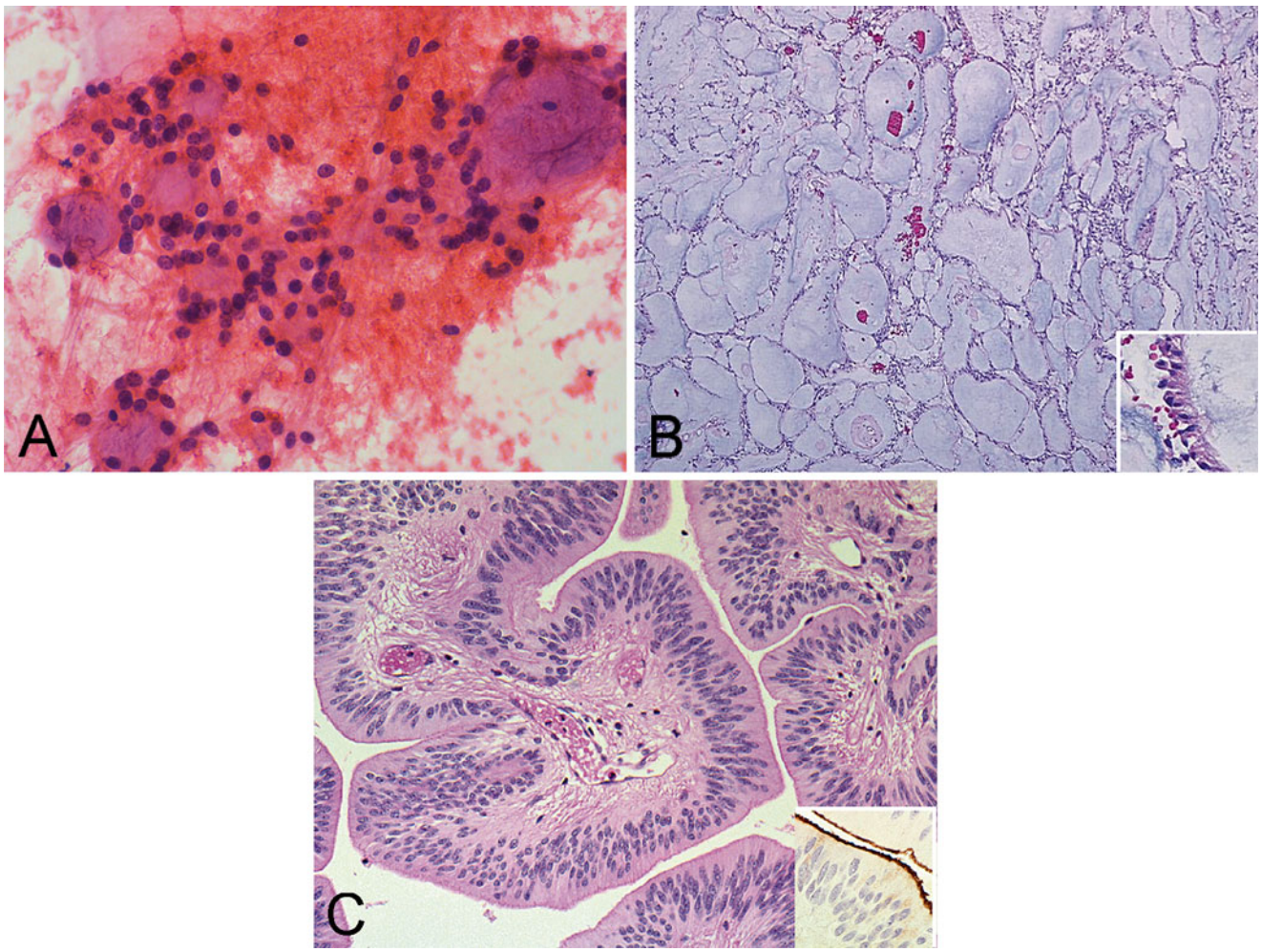

Fig. 6.27 Myxopapillary ependymoma and papillary ependymoma: (**a**) is a cytologic preparation of a myxopapillary ependymoma. Note the large globes of myxoid substance and the monotonous nuclei. (**b**) is myxopapillary ependymoma. Note the attenuated ependymal cells in inset. (**c**) is a papillary ependymoma. Note that there are no myxoid changes in comparison to myxopapillary ependymoma and no basement membrane in comparison to choroid plexus papilloma. EMA immunoreactivity can often be demonstrated at the luminal border but not cytoplasm of the lining cells (inset in (**c**))

Mitotic figures and necrosis are typically absent in ependymoma. However, occasional mitoses and occasional nonpalisading, geographic foci of necrosis are allowed in ependymoma. It should also be noted that histologic features of ependymoma do not always faithfully reflect the biological potential of an ependymoma. Anaplastic ependymomas are characterized by cellular pleomorphism, brisk mitotic activity and high proliferative index, pseudopalisading necrosis, and microvascular proliferation.

Variants of ependymoma: *Cellular ependymoma* is characterized by a substantial increase in cellularity without increase in mitotic rate or other features of anaplastic changes; they are often extraventricular. While papillary formations can be identified focally in classical ependymoma, they are characteristically extensive in *papillary ependymoma* (Fig. 6.27c). The finger-like projections are covered by a layer of ependymal cells with characteristic fibrillary processes extending to the fibrovascular stalk and lacking a basement membrane, a critical feature that distinguishes these tumors from choroid plexus tumors. *Clear cell ependymoma* is often a supratentorial tumors of young patients and are associated with extraneural metastases and early recurrence [185]. *Tanycytic ependymoma* usually involve the spinal cord and are characterized by tumor cells arranged in poorly intertwined fascicles of variable width. Nuclei maintain the classic "salt and pepper" speckling of ependymoma and provide a diagnostically helpful feature.

Immunohistochemistry and electron microscopy: Ependymomas and anaplastic ependymomas are typically immunoreactive for GFAP. Cytokeratin can be focally positive but is usually not as extensive as choroid plexus

tumors. EMA is typically positive at the luminal surface of the ependymal canals or areas with papilla formation. Intracytoplasmic immunoreactivities are far less common and often appear as dot like immunoreactivity. Ependymomas are also positive for S100, vimentin, and rare cases express thyroid transcription factor-1 (TTF-1) [186]. Ki67 labeling index for ependymoma is low and in the range of 2–5 %; a higher level might be indicative of a more adverse biology.

Ependymal tumors possess highly diagnostic ultrastructural features including microvilli (9 + 2 cilia, with their basal blepharoplasts), zonulae adherents (long "zipper' like" and extensive junctional complexes), and luminal cilia. These electron microscopic features are particularly helpful in distinguishing clear cell ependymoma from mimicking tumors such as gliomas under some circumstances.

Differential diagnosis: Classic ependymoma is usually not a diagnostic challenge. However, the cellularity of an ependymoma may be high enough to suggest a small blue cell tumor such as medulloblastoma. On the other extreme, the cellularity may be low enough to suggest a pilocytic astrocytoma. A small intraoperative biopsy may become a diagnostic challenge particularly when it is obtained from the posterior fossa of a child. Clear cell ependymoma is particularly easy to be confused with other tumors with clear cell features such as oligodendroglioma and central neurocytoma. Tanycytic astrocytoma may be confused with pilocytic astrocytoma.

Molecular genetics: Although multiple genetic aberrations have been demonstrated in ependymoma, no definitive genetic pathways have been related to biological behavior of ependymomas [187].

Myxoependymoma

Myxopapillary ependymoma (WHO grade I) is seen predominantly in young adults and sometime children. It arises almost exclusively in the most distal part of the spinal cord including the conus medullaris, cauda equine, and filum terminale. Incomplete resection is associated with late recurrence and distant metastases. Back pain is a common presentation.

Radiographically, the tumor is typically a mass around the filum terminale that is isointense, occasionally hyperintense, to the spinal cord on T1-weighted sequences and hyperintense on T2-weighted sequences [6].

Grossly, myxoependymoma is well demarcated and does not invade surrounding structures. Histologically, tumors display a characteristic pattern with lobules of myxoid material lined by a thin and attenuated layer of ependymal cells that lacks nuclear atypia (Fig. 6.27a, b). These tumors are positive for GFAP, EMA, and S100 but negative for cytokeratin.

Miscellaneous Neuroepithelial Tumors and Tumor-Like Lesions

Astroblastoma

Astroblastoma is a rare glial tumor that has not been assigned a WHO grade. It occurs mainly in cerebral hemispheres of children, adolescents, and young adults and its biological behavior is variable. Radiographically, astroblastoma usually present as a large, supratentorial tumor with solid and cystic components. The solid component has been described as "bubbly" in appearance and is mostly isointense on T2-sequences with inhomogeneous enhancement [188]. The cystic component demonstrates peripheral enhancement. The tumor may calcify. Astroblastomas are well-circumscribed, non-calcifying, often cystic changes, and associated with little edema [189]. Histologically, they are well delineated and have a pushing margin. The tumor is characterized by perivascular arrangement of tumor cells similar to that of ependymoma. In contrast to ependymoma where fine perivascular cytoplasmic processes are seen, astroblastoma has stout columnar cells anchoring to the blood vessels with broad processes. The blood vessels are often sclerotic. The tumor cells are reactive for GFAP, S100, and vimentin. Limited reactivities for EMA [190] cytokeratin have also been reported. In general, tumors with low-grade histology have better prognosis than high-grade tumors. Comparative genomic hybridization [190] and cytogenetic studies [191] reveal change that are not typical for ependymoma and argue against astroblastoma being a variant of ependymoma.

Angiocentric Glioma

Angiocentric glioma (WHO grade I) [192] is a rare tumor that is mostly found in children, adolescents, and young adults. Tumors are located superficially in the cerebral hemispheres and on MRI appear as a well-defined, non-enhancing mass that is hypointense on T1-weighted images and hyperintense on T2-weighted sequences [193]. Epilepsy is the most common presentation. In general, surgical treatment is effective for these tumors although a rare case of recurrence and malignant progression in an adult [192] and a case with combined features of angiocentric glioma and glioblastoma [194] have been reported. Histologically, the tumor is characterized by mono- or multilayered sleeves of monomorphic, bipolar spindle cells with radial arrangement reminiscent of pseudorosettes of ependymomas. The tumor cells extend lengthwise along blood vessels and may aggregate beneath the pia-arachnoid in horizontal streams. Areas with solid growth may also be present. The nuclei are generally bland in appearance. Eosinophilic intracytoplasmic density abutting the nuclei can be seen and these structures are immunoreactive for EMA and these structures correspond ultrastructurally to microlumens.

Perivascular tumor cells are variably positive for GFAP. The major differential diagnosis is ependymoma. Cortical dysplasia has been reported to be associated with this entity [195]. The *IDH1 R132H* mutation has not been demonstrated in three cases studied [196].

Chordoid Glioma

Chordoid glioma (WHO grade II) is a tumor of adulthood and are rarely seen in adolescence. This is a slow growing, noninvasive glial tumor that occurs in the third ventricle. On imaging, the lesion has been described as a well defined, oblong mass located in the anterior third ventricle or hypothalamus. The tumor is usually isointense on T1W sequences, iso to slightly hyperintense on T2W sequences and exhibits uniform dense enhancement. Cystic changes may be observed in the center of the mass [197]. Histologically, it is composed of epithelioid GFAP-positive glial cells arranged in cords and islands embedded within a mucinous background. Lymphoplasmacytic infiltration is typical [197].

Hypothalamic Neuronal Hamartoma

The majority of cases occur as a mass hanging from the floor of the third ventricle. They may be sporadic or associated with syndromes such as Pallister-Hall (congenital hypothalamic hamartoblastoma syndrome). Precocious puberty is the most common clinical manifestation. On MRI the lesion presents as an exophytic or pedunculated, well-circumscribed, nonenhancing mass in the region of the tuber cinereum. It is isointense on T1-weighted sequences and slightly hyperintense on T2-weighted sequences [198]. Histologically, these hamartomas contain neurons of variable size similar to neurons in the adjacent normal tuber cinereum and hypothalamic nuclei. Typically lesions are composed of abnormally distributed but cytologically normal neurons and glia, including fibrillary astrocytes and oligodendrocytes [199].

Choroid Plexus Tumors

Definition: The choroid plexus give rise to choroid plexus papilloma (WHO grade I), atypical choroid plexus papilloma (WHO grade II), and choroid plexus carcinoma (WHO grade III).

Clinical features: Although choroid plexus tumor is an uncommon tumor, it is common in children and represents 10–20 % of tumors within the first year of life. Choroid plexus papilloma has been reported to be associated with Aicardi syndrome [200–202] and Li-Fraumeni syndrome [203]. In the pediatric age group, the lateral ventricles are the most common sites followed by the fourth ventricle and the cerebellar pontine angle. Due to their location, manifestations of CSF blockage and hydrocephalus are common. Choroid plexus papilloma, although benign, can produce drop metastases. Choroid plexus carcinoma is one of the very few carcinomas that occurs almost exclusively in children under 3 years of age and often results in malignant invasion and metastases. This entity has been associated with rhabdoid predisposition syndrome and proposed to represent AT/RT [204]. However, as the spectrum of INI1-deficient tumors is expanding [82, 83] such an association remains to be confirmed.

Imaging findings: On MRI (Fig. 6.28) choroid plexus papilloma typically appears as a well delineated, lobulated, intraventricular mass that is isointense on T1-weighted imaging,

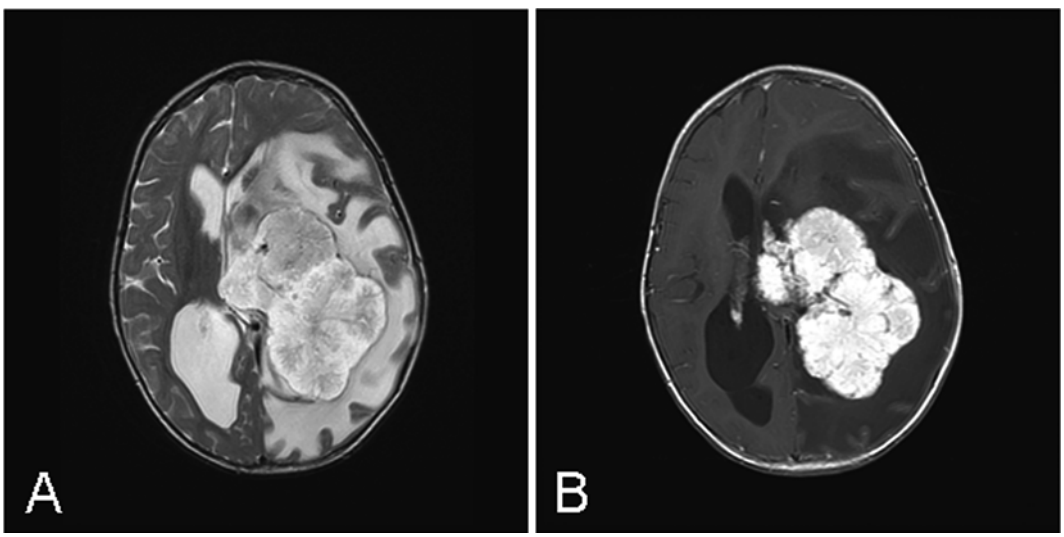

Fig. 6.28 MR-choroid plexus papilloma. (**a**) Axial FSE-T2W MR image demonstrates a large, well-defined mass arising from the left lateral ventricle. The tumor has mixed, intermediate intensity and increased signal intensity. (**b**) Axial post-contrast T1W MR image shows the mass has vivid enhancement. Significant edema is also present in the surrounding brain (15-month-old male)

iso- to hyperintense on T2-weighted sequences and enhances avidly on post-contrast imaging. Occasionally there may be T2-weighted hyperintensity in the surrounding brain parenchyma due to edema [176]. Leptomeningeal dissemination may occur [205].

Macroscopic pathology and histopathology: Choroid plexus papillomas are cauliflower-like exophytic growths that are well-circumscribed from the ventricular wall. Histologically, choroid plexus papilloma appears as papillary proliferation with a fibrovascular core lined by a single layer of monotonous cuboidal to columnar epithelium with a basement membrane. Mitotic figures are typically absent. Some tumors may have focal necrosis, increased cellularity, pleomorphism, brain invasion, and focal loss of papillary arrangement.

Atypical choroid plexus papilloma: On imaging, atypical choroid plexus papilloma is indistinguishable from typical choroid plexus papilloma. Mitotic figures are extremely rare in choroid plexus papilloma and when the mitotic rate is over two or more per ten randomly selected high powered fields, a diagnosis of atypical choroid plexus papilloma can be established [206]. Up to two of the following features may be present in atypical choroid plexus papilloma but their presence is not required for the diagnosis: increased cellularity, nuclear pleomorphism, areas of solid growth (blurring of the papillary pattern), and areas of necrosis.

Choroid plexus carcinoma: These are malignant tumor with at least four of the five following features: mitotic rate of over five per ten high powered fields, increased cellularity, increased nuclear pleomorphism, solid growth pattern (solid sheets of tumor cells), and necrosis. Diffuse brain invasion is also common, but it is not a required diagnostic criterion [206]. Spinal dissemination may be present at the time of diagnosis. On MRI studies, choroid plexus carcinoma may have more irregular margins than papillomas but they share the same signal characteristics. Therefore, MRI cannot reliably distinguish between these two choroid plexus malignancies [176].

Immunohistochemistry: Choroid plexus papillomas are positive for vimentin and podoplanin (D2-40) [207]. It should be noted that podoplanin is also positive in glioblastoma, and anaplastic astrocytomas. These tumors are positive for cytokeratins and often, but now always, positive for cytokeratin 7 and negative for cytokeratin 20. Choroid plexus papillomas are variably positive for S100, synaptophysin [208, 209], transthyretin, synaptophysin, and EMA. Although GFAP is negative in normal choroid plexus, it is positive in choroid plexus papilloma.

Differential diagnosis: In the pediatric age group, choroid plexus carcinoma needs to be distinguished from other high grade tumors such as medulloblastoma and AT/RT. Endolymphatic sac tumor is an uncommon tumor associated with von Hippel-Lindau syndrome and is mostly seen in adults. These tumors morphologically recapitulate the features of choroid plexus papilloma and are a close mimicker of choroid plexus papilloma. Rare pediatric cases have been reported [210, 211]. In contrast to choroid plexus papilloma, bone invasion is common in endolymphatic sac tumors. EAAT-1 and Kir7.1 are positive in choroid plexus papilloma but negative in endolymphatic sac tumors [212].

Tumor of the Pineal Region

Clinical presentation of different kinds of pineal lesion is very similar. About half of pineal parenchymal tumors occur in children [213]. It includes manifestations due to increase in intracranial pressure, changes in mental status, or due to compression of tectum and associated midbrain structures (Parinaud syndrome), brainstem, and cerebellum.

Pineocytoma

Pineocytoma (WHO grade I) occurs mainly in adults but it can also be seen in the pediatric age group. Pineocytoma usually presents as round, well-demarcated mass on imaging. Histologically, it is moderately cellular tumor consists of small, monotonous, mature cells with round to oval nuclei containing finely dispersed chromatin and without prominent nucleoli resembling pineocytes. Mitotic figures are typically rare or absent. One of the diagnostic features is short, conspicuous club shaped cytoplasmic processes that are further demonstrated by immunohistochemistry for neurofilament proteins or silver stains. Pineocytomatous rosette is another diagnostic feature. The tumor cells are strongly positive for synaptophysin, neurofilament proteins and variably for other neuronal markers and markers of photoreceptors such as S-antigen. Ultrastructural features of normal pineocytes can also be found in pineocytomas.

Pineal Parenchymal Tumor of Intermediate Differentiation

Depending on histologic features, pineal parenchymal tumor of intermediate differentiation (PPTID) is of WHO grade II or III. It is most common in young adults but it occurs in all ages including childhood. Dissemination through the CSF is limited to a small number of cases. On MRI, pineocytoma and pineal parenchymal tumor of intermediate differentiation share similar features. Both present as well demarcated masses, hypo to isointense on T1-weighted images and

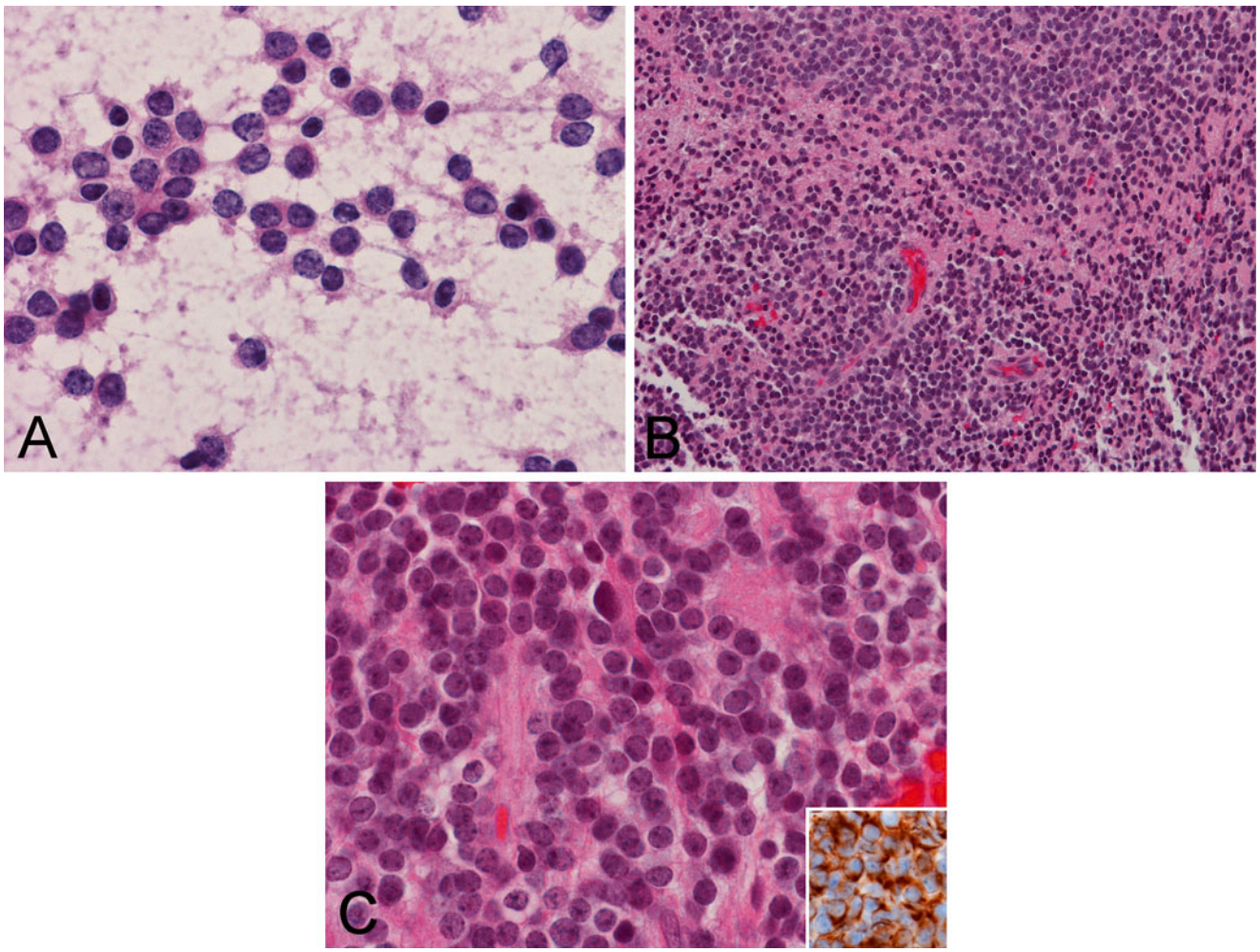

Fig. 6.29 Pineal parenchymal tumor of intermediate differentiation. What is shown here is a WHO grade II tumor. (**a**) On cytologic smear preparation, the tumor is composed of small blue cells with minimal cytoplasm. The nuclei have a "salt and pepper" appearance, a typical feature of neuroendocrine tumor. (**b**) The tumor cells are packed in solid sheets without specific pattern of arrangement. (**c**) Close view of the tumor showing monotonous, round nuclei with small islands of neuropils. The tumor cells are strongly positive for neurofilament proteins (Inset)

hyperintense on T2-weighted sequences. Homogenous, avid enhancement is seen on post-contrast imaging. Pineoblastoma presents as a large mass with signal characteristics similar to the more benign tumors of pineal tissue origin although enhancement may be in homogenous and areas of necrosis may be present. CSF dissemination may occur [214].

Histologically, it varies from neurocytoma-like solid sheets of tumor cells to lobulated arrangement with moderate to high cellularity (Fig. 6.29). There is mild to moderate atypia and low to moderate mitotic activity. Occasionally Homer Wright rosettes or giant tumor cells can be seen. The less aggressive tumors (WHO grade II) have mitoses less than six per ten high powered fields and strong neurofilament protein staining. Grade III tumors has either six or more mitoses per ten high powered fields or fewer than six mitoses but without immunoreactivity for neurofilament proteins [215].

Pineoblastoma

Pineoblastoma (WHO grade IV) represents the most primitive of pineal parenchymal tumor [216]. It is a highly aggressive primitive embryonal tumor that is seen mostly in the first two decades of life followed by young adults and older adults. Pineoblastoma can occur in patients with bilateral retinoblastoma as what has been designated "trilateral retinoblastoma" and these tumors are usually associated with *RB1* gene mutation [217]. Due to its aggressiveness interval between initial presentation and diagnosis can be short. On MRI, it is hypo- to isointense on T1-weighted images with heterogeneous enhancement (Fig. 6.30). In general, pineal germinoma and pineoblastoma has lower ADC value and higher Choline/NAA ratio than pineal glioma and teratoma [218]. Cranial spinal dissemination through CSF is not

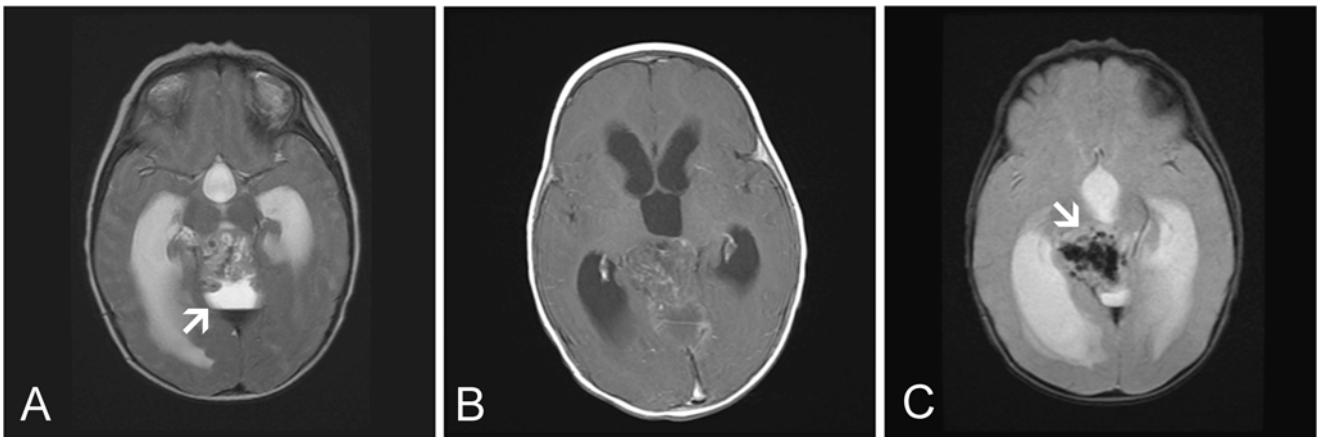

Fig. 6.30 MR-pineoblastoma. (**a**) Axial Sequence MR image shows a large solid and cystic pineal mass causing obstructive hydrocephalus. A fluid–fluid level (*arrow*) is likely due to hemorrhage in the posterior aspect of the mass. (**b**) Axial T1W post-contrast enhanced MR image shows the mass is poorly defined and has heterogeneous enhancement. (**c**) Axial GRE MR image shows additional areas of hemorrhage in the solid component of the mass (*arrow*) (8-month-old female)

uncommon. Surgical specimens are usually composed of fragments of friable tissue. Histologically, they are comparable to PNETs and medulloblastomas and are composed of solid sheets of small blue cells with minimal amount of cytoplasm. Although Homer Wright rosettes and Flexner-Wintersteiner rosettes may be present, pineocytomatous rosette is lacking. These tumors are mitotically active and often necrotic. These tumors are immunoreactive for synaptophysin and variably with S-100 antigen but non-reactive for neurofilament proteins [215]. The major differential diagnoses of pineoblastoma include germ cell tumor, atypical teratoid/rhabdoid tumor, pineal parenchymal tumor of intermediate differentiation, and medulloblastoma.

Papillary Tumor of the Pineal Region

Papillary tumor of the pineal region is a rare tumor of WHO grade II or grade III but the criteria for distinction are not well established. The small number of reported cases includes both adults and children. In the two reported pediatric cases with radiographic studies, these tumors had solid and cystic components, obstructed the third ventricle and demonstrated moderate, inhomogeneous enhancement after administration of gadolinium [219, 220]. These tumors generally present as a relatively large (2.5–4 cm) well-circumscribed mass. Histologically, it contains fibrovascular cores lined by amphophilic to eosinophilic columnar cells. Some tumors are mitotically active. Ependymal-like differentiation such as true rosette and ependymal tubules can be found in the more densely areas. Tumor cells can also be vacuolated and contain an eosinophilic PAS-positive cytoplasmic mass. Necrosis is common. In contrast to ependymoma, immunoreactivity for GFAP is usually focal. Immunohistochemistry for cytokeratins is more likely to be positive in the papillary areas. Ultrastructural studies have demonstrated features of ependymal differentiation [221, 222].

Tumor and Tumor-Like Lesions of the Sellar Region

The sellar region is a complex structure which includes the anterior and posterior pituitary, dura, and surrounding bone. Several tumors and tumor-like lesions can arise from this area. Craniopharyngioma and germ cell tumors are more common in the pediatric age group.

Tumor and Tumor-Like Condition of the Meninges

Meningeal space occupying lesion is uncommon in children. Dural or leptomeningeal mass and neoplastic meningitis are the most common presentations. The major categories [223] of this family include meningothelial proliferations, particularly meningiomatosis and meningioma, primary melanocytic tumors, benign mesenchymal tumors and sarcomas, poorly differentiated/embryonal tumors, inflammatory tumors, secondary and metastasis of primary tumor of the CNS. Meningioma is uncommon in the pediatric age group particularly in young children. When this is compounded by the rich diversity of meningiomas and other meningeal lesions, meningeal lesions in children pose diagnostic challenges.

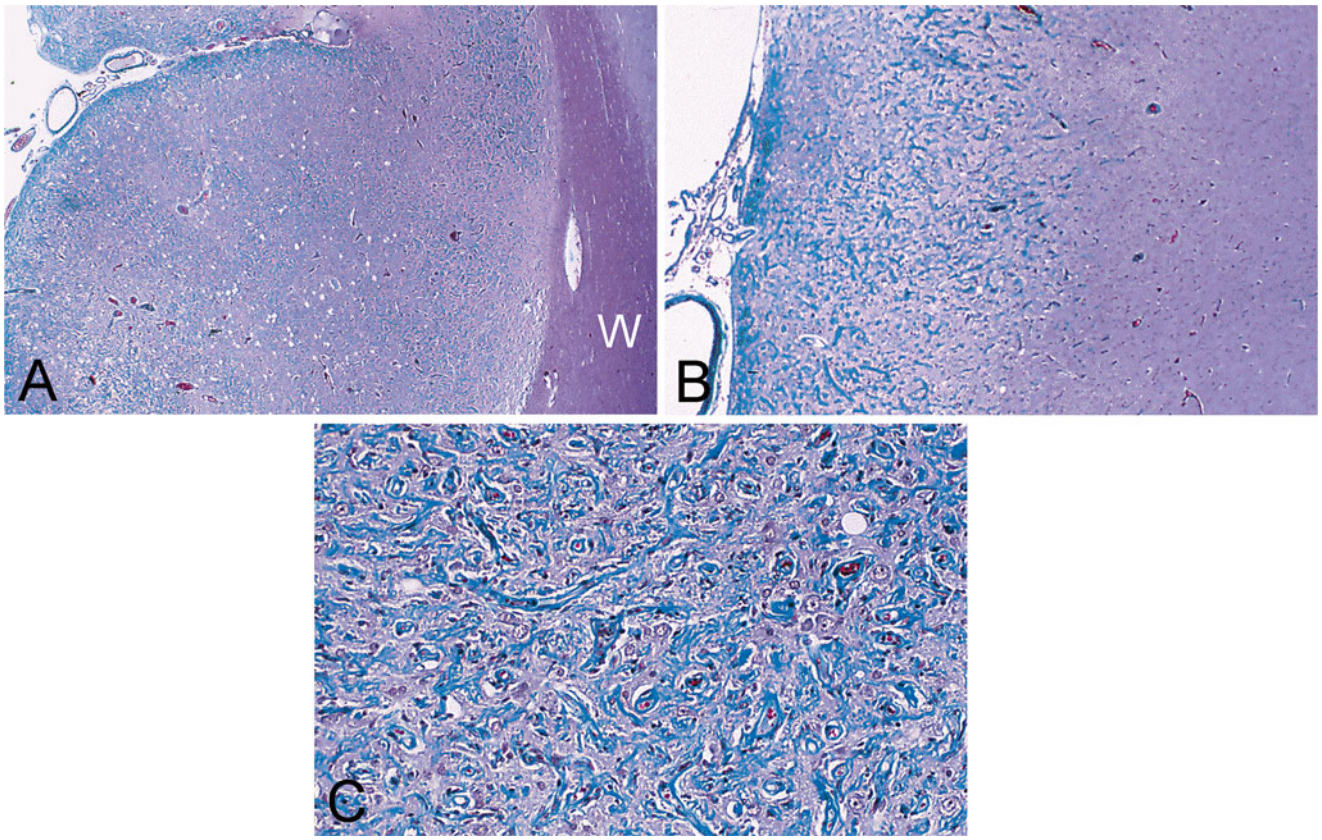

Fig. 6.31 Meningioangiomatosis. (**a**) Trichrome stain demonstrates an "en plaque" proliferation along the cerebral cortex that is well demarcated from the white matter (*W*). (**b**) At the periphery of the lesion, the lesion has an infiltrative margin that interfaces with the adjacent cortex. (**c**) The proliferation is composed of whorls of cells and the blood vessels in this particular case are markedly sclerotic (Trichrome stain)

Meningioangiomatosis

Meningioangiomatosis is believed to be hamartomatous, developmental, or reactive in nature. It typically presents as an "en plaque" leptomeningeal proliferation along the cerebral cortex with seizure as the most common manifestation [224, 225]. It can present in pediatric and adult patients; it can be sporadic or associated with neurofibromatosis type 2 (NF-2). Cases associated with NF-2 are often multifocal and clinically asymptomatic. A single case associated with sudden death has been reported [226]. In rare occasions, meningioma may arise from meningiomatosis. Although these tumors are intraparenchymal, they should not be viewed as brain invasion [227]. These tumors radiographically and pathologically mimic invasive meningiomas [227]. The meningioangiomatosis component in cases associated with meningioma appears to be neoplastic in nature in comparison to cases of pure meningioangiomatosis [227].

On MRI, meningioangiomatosis is usually plaque-like, hypo- to isointense on T1-weighted sequences, iso- to hyperintense on T2-weighted sequences, and demonstrates heterogeneous enhancement. Intratumoral calcifications are common. Gyriform hyperintensity seen on FLAIR sequences, reflects proliferating microvessels with perivascular cuffs of spindle-cell proliferation [228]. Due to its rarity meningioangiomatosis is often misdiagnosed as meningioma, vascular malformation, or other low grade tumors [228, 229].

Grossly, meningioangiomatosis appears as a firm plaque that is adhered to the brain. In contrast to meningiomas, they cannot be peeled off from the brain. An infiltrative interface with the brain parenchyma explains its firm adhesion (Fig. 6.31). Psammoma bodies can be seen. Histologically, meningiomatosis is characterized by a perivascular spindle-cell proliferation that is separated by a variable amount of brain parenchyma. In sporadic cases, vimentin is consistently positive in spindle cells but immunoreactivity for EMA and CD34 is variable [230]. The Ki67 labeling index is typically low [230, 231].

Meningioma

Meningiomas can be sporadic or associated with NF-2. These tumors are uncommon in adolescents and almost

unheard of during infancy. Seizure and increased intracranial pressure are the most frequent sign at presentation [232, 233]. However, meningiomas are the most common dural tumor in the pediatric age group. Pediatric meningiomas tend to be larger, intraparenchymal, and more aggressive [232, 233]. Clear cell meningioma (WHO grade II) and papillary meningioma (WHO grade III) are more common than the adult spectrum.

The imaging characteristics of the tumor in children are similar to those in adults. The tumor is usually large, well demarcated, isointense on T1-weighted sequences, with variable intensity on T2-sequences and avid enhancement. Meningiomas are usually extra-axial; a feature that may be reflected by the presence of a cleft of CSF on T2-weighted images. A small number of tumors are intra-axial or intraventricular. Radiation induced meningiomas may develop years after radiation of the brain [233].

The histologic grading is the same as in adult cases, pediatric meningiomas are predominantly leptomeningeal or intracerebral [234], with occasional association with meningiomatosis. These tumors should not be viewed as meningioma with brain invasion corresponding to WHO grade II [227]. Although a correlation of prognosis with WHO histologic grade exists, the correlation is not is strong as in adult cases. These tumors tend to occur in uncommon locations such as the spinal canal, posterior fossa, and ventricles [223]. Meningiomas, particularly those with high-grade histology, can pose a diagnostic challenge and must be distinguished form mimickers including other high grade tumors such as undifferentiated poorly differentiated and undifferentiated small blue cell tumor, secondary hematopoietic and histiocytic tumors, and primary CNS tumors such as AT/RT and gliosarcomas. Sarcomatoid meningioma should be carefully distinguished from bone/soft tissue sarcoma.

Leptomeningeal Tumor Dissemination ("Neoplastic Meningitis")

Widespread leptomeningeal dissemination of a primary CNS or systemic tumor typically would give rise to a meningitis-like clinical and neuroimaging picture. In some cases, a conspicuous primary tumor cannot be identified. Such dissemination includes meningeal gliomatosis, oligodendrogliomatosis, sarcomatosis, lymphomatosis, histiocytosis, and melanomatosis. In contrast to adult patients, carcinomatosis, other than those caused by choroid plexus carcinoma, is rare in pediatric patients. On the other hand, primary CNS tumors that tend to give rise to CSF dissemination including medulloblastoma/PNET, AT/RT, and less commonly ependymomas do not usually pose a diagnostic challenge as a tumor mass is almost always present.

Imaging studies play an important role in the diagnosis of disseminated tumor because a mass is not always present. The diagnosis of leptomeningeal dissemination of a primary CNS tumor requires post-contrast imaging showing enhancement of tumor coating the leptomeninges. In addition, drop metastatic lesions, manifested as enhancing nodules, can be seen along the spinal cord, predominantly along the cauda equine [235].

Miscellaneous Tumors and Tumor-Like Lesions

Intracranial germ cell tumor is a rather common tumor in the pediatric age group. They are most common in the pineal gland followed by the pituitary. A significant proportion of these tumors is seminoma dominated by a seminomatous component (Fig. 6.32). The pathologic features are similar to germ cell tumors arising in other locations (please see corresponding chapter for details). It should be noted that the pineal biopsy is usually small endoscopic specimens and granulomatous changes may mask the tumor cells (Fig. 6.32c).

Epidermoid cysts can be found in all age groups and they are most commonly seen in the cerebellopontine angle followed by para-pituitary area and other locations. A small number can be paraspinal or intraspinal and seen in the sacral region. Histology is identical to epidermoid cysts in other locations.

Chordoma and chondrosarcoma are typically tumor of adults. Other than patients with prior radiation, intracranial osteosarcoma is uncommon.

Langerhans histiocytosis is a common entity in the cranial bone in the pediatric age group but intra-axial ones are rare. Grois et al. have identified three main types: circumscribed granuloma in the meninges and choroid plexus; granulomas involving the brain parenchyma, usually as an extension from the meninges or Virchow-Robin spaces; and neurodegenerative lesions without granuloma that affects mainly the cerebellum and the brainstem [236, 237]. Isolated involvement of the CNS by juvenile granulomatosis is rare but systemic juvenile granulomatosis with involvement of the CNS is not uncommon.

Primary lymphoma of the CNS is extremely rare in the pediatric age group with non-Hodgkin B-cell lymphoma being most common. Patients with congenital or acquired immune deficiencies are associated with increased risk [238] of primary CNS lymphoma. The outcome seems to be better than in adult cases with an overall survival of 86 % [239]. Secondary involvement of the CNS by lymphoma and leukemia often takes the form of leptomeningeal involvement, which makes cytologic examination of the CSF an important diagnostic procedure.

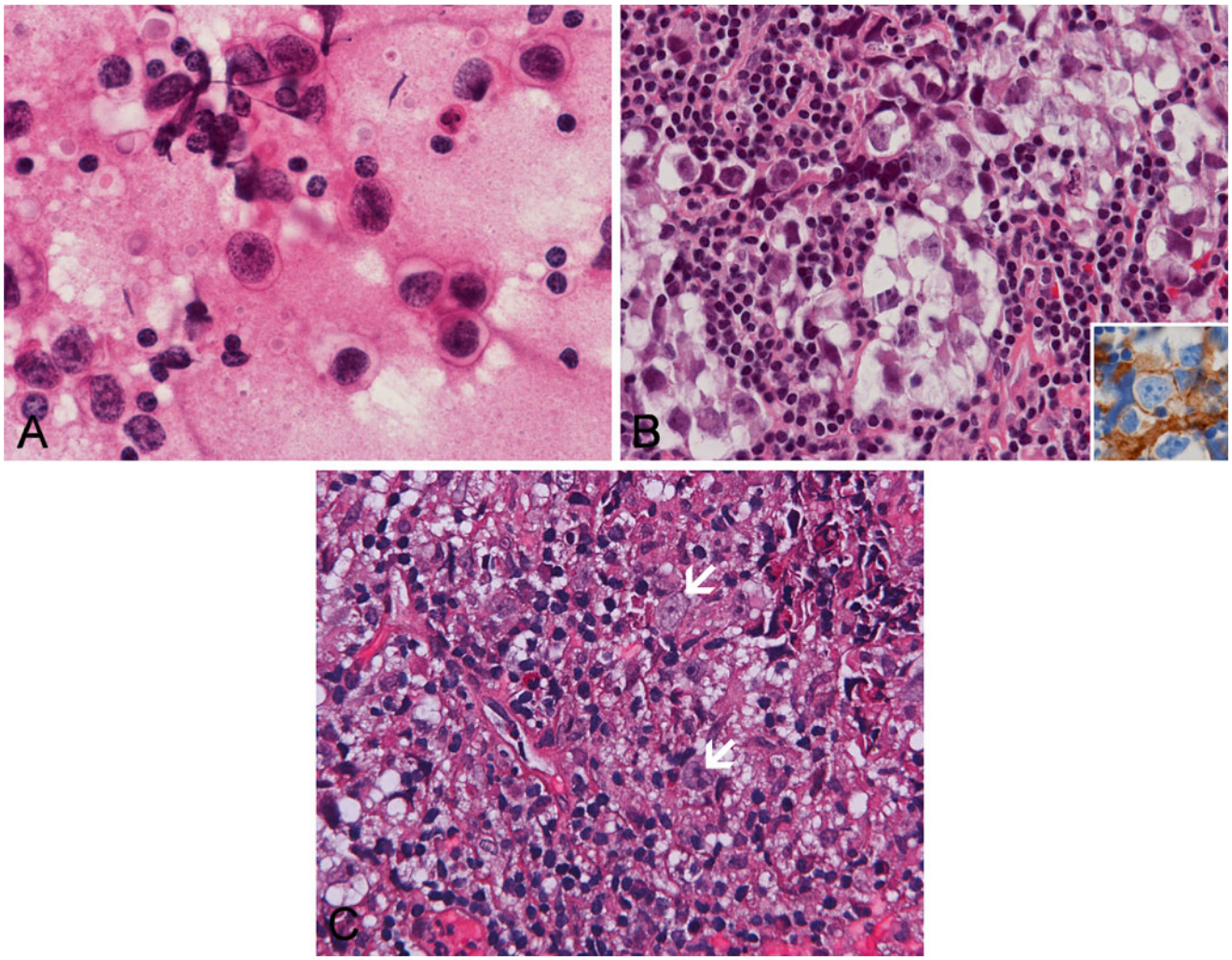

Fig. 6.32 Germinoma of pineal. (**a**) Smeared cytologic preparation shows a mixture of large tumor cells with large nuclei and prominent nucleoli admixed with small lymphocytes in the background. (**b**) A classic germinoma with small clusters of tumor cells embedded in a background of normal appearing lymphocytes. The tumor cells have large nuclei with prominent nucleoli and abundant, clear cytoplasm. The tumor cells show positive staining for placental alkaline phosphatase (inset). (**c**) Extensive granulomatous changes in this particular case raise the question of infection. The scant atypical cells (*arrows*) indicate germinoma with granulomatous changes

References

1. Louis DN, Ohgaki H, Wiesteler OD, Cavenee WK. WHO classification of tumours of the central nervous system. Lyon: International Agency for Research on Cancer; 2007.
2. Ries LAGSM, Gurney JG, Linet M, Tamra T, Young JL, Bunin GR, editors. Cancer incidence and survival among children and adolescents: United States SEER Program 1975–1995, National Cancer Institute, SEER Program. Bethesda, MD: National Institutes of Health; 1999. NIH Pub. No. 99-4649. Bethesda, MD, 1999.
3. Colosimo C, di Lella GM, Tartaglione T, et al. Neuroimaging of thalamic tumors in children. Childs Nerv Syst. 2002;18:426–39.
4. Cuccia V, Monges J. Thalamic tumors in children. Childs Nerv Syst. 1997;13:514–20. Discussion 521.
5. Rosemberg S, Fujiwara D. Epidemiology of pediatric tumors of the nervous system according to the WHO 2000 classification: a report of 1,195 cases from a single institution. Childs Nerv Syst. 2005;21:940–4.
6. Koeller KK, Rosenblum RS, Morrison AL. Neoplasms of the spinal cord and filum terminale: radiologic-pathologic correlation. Radiographics. 2000;20:1721–49.
7. Janisch W, Haas JF, Schreiber D, et al. Primary central nervous system tumors in stillborns and infants. Epidemiological considerations. J Neurooncol. 1984;2:113–6.
8. Rickert CH. Neuropathology and prognosis of foetal brain tumours. Acta Neuropathol. 1999;98:567–76.
9. Panigrahy A, Krieger MD, Gonzalez-Gomez I, et al. Quantitative short echo time 1H-MR spectroscopy of untreated pediatric brain tumors: preoperative diagnosis and characterization. AJNR Am J Neuroradiol. 2006;27:560–72.
10. Tzika AA, Vajapeyam S, Barnes PD. Multivoxel proton MR spectroscopy and hemodynamic MR imaging of childhood brain tumors: preliminary observations. AJNR Am J Neuroradiol. 1997;18:203–18.

11. Hwang JH, Egnaczyk GF, Ballard E, et al. Proton MR spectroscopic characteristics of pediatric pilocytic astrocytomas. AJNR Am J Neuroradiol. 1998;19:535–40.
12. Kan P, Liu JK, Hedlund G, et al. The role of diffusion-weighted magnetic resonance imaging in pediatric brain tumors. Childs Nerv Syst. 2006;22:1435–9.
13. Rumboldt Z, Camacho DL, Lake D, et al. Apparent diffusion coefficients for differentiation of cerebellar tumors in children. AJNR Am J Neuroradiol. 2006;27:1362–9.
14. Borja MJ, Plaza MJ, Altman N, et al. Conventional and advanced MRI features of pediatric intracranial tumors: supratentorial tumors. AJR Am J Roentgenol. 2013;200:W483–503.
15. Lefranc M, Monet P, Desenclos C, et al. Perfusion MRI as a neurosurgical tool for improved targeting in stereotactic tumor biopsies. Stereotact Funct Neurosurg. 2012;90:240–7.
16. Barajas Jr RF, Chang JS, Segal MR, et al. Differentiation of recurrent glioblastoma multiforme from radiation necrosis after external beam radiation therapy with dynamic susceptibility-weighted contrast-enhanced perfusion MR imaging. Radiology. 2009;253:486–96.
17. Liwnicz BH, Rubinstein LJ. The pathways of extraneural spread in metastasizing gliomas: a report of three cases and critical review of the literature. Hum Pathol. 1979;10:453–67.
18. Buhren J, Christoph AH, Buslei R, et al. Expression of the neurotrophin receptor p75NTR in medulloblastomas is correlated with distinct histological and clinical features: evidence for a medulloblastoma subtype derived from the external granule cell layer. J Neuropathol Exp Neurol. 2000;59:229–40.
19. Chelliah D, Mensah Sarfo-Poku C, Stea BD, et al. Medulloblastoma with extensive nodularity undergoing post-therapeutic maturation to a gangliocytoma: a case report and literature review. Pediatr Neurosurg. 2010;46:381–4.
20. Pillai S, Singhal A, Byrne AT, et al. Diffusion-weighted imaging and pathological correlation in pediatric medulloblastomas: "They are not always restricted!". Childs Nerv Syst. 2011;27:1407–11.
21. Koeller KK, Rushing EJ. From the archives of the AFIP: medulloblastoma: a comprehensive review with radiologic-pathologic correlation. Radiographics. 2003;23:1613–37.
22. Bourgouin PM, Tampieri D, Grahovac SZ, et al. CT and MR imaging findings in adults with cerebellar medulloblastoma: comparison with findings in children. AJR Am J Roentgenol. 1992;159:609–12.
23. Yeom KW, Mobley BC, Lober RM, et al. Distinctive MRI features of pediatric medulloblastoma subtypes. AJR Am J Roentgenol. 2013;200:895–903.
24. Koci TM, Chiang F, Mehringer CM, et al. Adult cerebellar medulloblastoma: imaging features with emphasis on MR findings. AJNR Am J Neuroradiol. 1993;14:929–39.
25. Fruehwald-Pallamar J, Puchner SB, Rossi A, et al. Magnetic resonance imaging spectrum of medulloblastoma. Neuroradiology. 2011;53:387–96.
26. Kalimo H, Paljarvi L, Ekfors T, et al. Pigmented primitive neuroectodermal tumor with multipotential differentiation in cerebellum (pigmented medullomyoblastoma). A case with light- and electron-microscopic, and immunohistochemical analysis. Pediatr Neurosci. 1987;13:188–95.
27. Gottardo NG, Hansford JR, McGlade JP, et al. Medulloblastoma down under 2013: a report from the third annual meeting of the International Medulloblastoma Working Group. Acta Neuropathol. 2014;127:189–201.
28. Taylor RE, Bailey CC, Robinson KJ, et al. Impact of radiotherapy parameters on outcome in the International Society of Paediatric Oncology/United Kingdom Children's Cancer Study Group PNET-3 study of preradiotherapy chemotherapy for M0-M1 medulloblastoma. Int J Radiat Oncol Biol Phys. 2004;58:1184–93.
29. Northcott PA, Korshunov A, Witt H, et al. Medulloblastoma comprises four distinct molecular variants. J Clin Oncol. 2011;29:1408–14.
30. Kool M, Korshunov A, Remke M, et al. Molecular subgroups of medulloblastoma: an international meta-analysis of transcriptome, genetic aberrations, and clinical data of WNT, SHH, Group 3, and Group 4 medulloblastomas. Acta Neuropathol. 2012;123:473–84.
31. Thompson MC, Fuller C, Hogg TL, et al. Genomics identifies medulloblastoma subgroups that are enriched for specific genetic alterations. J Clin Oncol. 2006;24:1924–31.
32. Ellison DW. Childhood medulloblastoma: novel approaches to the classification of a heterogeneous disease. Acta Neuropathol. 2010;120:305–16.
33. Katsetos CD, Del Valle L, Legido A, et al. On the neuronal/neuroblastic nature of medulloblastomas: a tribute to Pio del Rio Hortega and Moises Polak. Acta Neuropathol. 2003;105:1–13.
34. Maraziotis T, Perentes E, Karamitopoulou E, et al. Neuron-associated class III beta-tubulin isotype, retinal S-antigen, synaptophysin, and glial fibrillary acidic protein in human medulloblastomas: a clinicopathological analysis of 36 cases. Acta Neuropathol. 1992;84:355–63.
35. Korf HW, Korf B, Schachenmayr W, et al. Immunocytochemical demonstration of interphotoreceptor retinoid-binding protein in cerebellar medulloblastoma. Acta Neuropathol. 1992;83:482–7.
36. Ellison D. Classifying the medulloblastoma: insights from morphology and molecular genetics. Neuropathol Appl Neurobiol. 2002;28:257–82.
37. Schiffer D, Cavalla P, Chio A, et al. Tumor cell proliferation and apoptosis in medulloblastoma. Acta Neuropathol. 1994;87:362–70.
38. Buczynski J, Jesionek-Kupnicka D, Kordek R, et al. Apoptosis in non-astrocytic brain tumours in children. Folia Neuropathol. 2002;40:155–9.
39. Fattet S, Haberler C, Legoix P, et al. Beta-catenin status in paediatric medulloblastomas: correlation of immunohistochemical expression with mutational status, genetic profiles, and clinical characteristics. J Pathol. 2009;218:86–94.
40. Matakas F, Cervos-Navarro J, Gullotta F. The ultrastructure of medulloblastomas. Acta Neuropathol. 1970;16:271–84.
41. Packer RJ, Sutton LN, Elterman R, et al. Outcome for children with medulloblastoma treated with radiation and cisplatin, CCNU, and vincristine chemotherapy. J Neurosurg. 1994;81:690–8.
42. Fan X, Wang Y, Kratz J, et al. hTERT gene amplification and increased mRNA expression in central nervous system embryonal tumors. Am J Pathol. 2003;162:1763–9.
43. Fernandez-Teijeiro A, Betensky RA, Sturla LM, et al. Combining gene expression profiles and clinical parameters for risk stratification in medulloblastomas. J Clin Oncol. 2004;22:994–8.
44. Grotzer MA, Hogarty MD, Janss AJ, et al. MYC messenger RNA expression predicts survival outcome in childhood primitive neuroectodermal tumor/medulloblastoma. Clin Cancer Res. 2001;7:2425–33.
45. Grotzer MA, Janss AJ, Fung K, et al. TrkC expression predicts good clinical outcome in primitive neuroectodermal brain tumors. J Clin Oncol. 2000;18:1027–35.
46. Karch SB, Urich H. Medulloepithelioma: definition of an entity. J Neuropathol Exp Neurol. 1972;31:27–53.
47. Molloy PT, Yachnis AT, Rorke LB, et al. Central nervous system medulloepithelioma: a series of eight cases including two arising in the pons. J Neurosurg. 1996;84:430–6.
48. Priest JR, Williams GM, Manera R, et al. Ciliary body medulloepithelioma: four cases associated with pleuropulmonary blastoma—a report from the International Pleuropulmonary Blastoma Registry. Br J Ophthalmol. 2011;95:1001–5.
49. Donner LR, Teshima I. Peripheral medulloepithelioma: an immunohistochemical, ultrastructural, and cytogenetic study of a rare, chemotherapy-sensitive, pediatric tumor. Am J Surg Pathol. 2003;27:1008–12.
50. Bruggers CS, Welsh CT, Boyer RS, et al. Successful therapy in a child with a congenital peripheral medulloepithelioma and disruption of hindquarter development. J Pediatr Hematol Oncol. 1999;21:161–4.

51. Kleinman GM, Young RH, Scully RE. Primary neuroectodermal tumors of the ovary: a report of 25 cases. Am J Surg Pathol. 1993;17:764–78.
52. Michael H, Hull MT, Ulbright TM, et al. Primitive neuroectodermal tumors arising in testicular germ cell neoplasms. Am J Surg Pathol. 1997;21:896–904.
53. Davies RP, Lee CS. Medulloepithelioma: MRI appearances. Australas Radiol. 1988;32:503–5.
54. Auer RN, Becker LE. Cerebral medulloepithelioma with bone, cartilage, and striated muscle. Light microscopic and immunohistochemical study. J Neuropathol Exp Neurol. 1983;42:256–67.
55. Scheithauer BW, Rubinstein LJ. Cerebral medulloepithelioma. Report of a case with multiple divergent neuroepithelial differentiation. Childs Brain. 1979;5:62–71.
56. Sharma MC, Mahapatra AK, Gaikwad S, et al. Pigmented medulloepithelioma: report of a case and review of the literature. Childs Nerv Syst. 1998;14:74–8.
57. Troost D, Jansen GH, Dingemans KP. Cerebral medulloepithelioma: electron microscopy and immunohistochemistry. Acta Neuropathol. 1990;80:103–7.
58. Korshunov A, Sturm D, Ryzhova M, et al. Embryonal tumor with abundant neuropil and true rosettes (ETANTR), ependymoblastoma, and medulloepithelioma share molecular similarity and comprise a single clinicopathological entity. Acta Neuropathol. 2013;128(2):279–89.
59. Khoddami M, Becker LE. Immunohistochemistry of medulloepithelioma and neural tube. Pediatr Pathol Lab Med. 1997;17:913–25.
60. Caccamo DV, Herman MM, Rubinstein LJ. An immunohistochemical study of the primitive and maturing elements of human cerebral medulloepitheliomas. Acta Neuropathol. 1989;79:248–54.
61. Korshunov A, Ryzhova M, Jones DT, et al. LIN28A immunoreactivity is a potent diagnostic marker of embryonal tumor with multilayered rosettes (ETMR). Acta Neuropathol. 2012;124:875–81.
62. Horten BC, Rubinstein LJ. Primary cerebral neuroblastoma. A clinicopathological study of 35 cases. Brain. 1976;99:735–56.
63. Gould VE, Jansson DS, Molenaar WM, et al. Primitive neuroectodermal tumors of the central nervous system. Patterns of expression of neuroendocrine markers, and all classes of intermediate filament proteins. Lab Invest. 1990;62:498–509.
64. Rhodes RH, Cole M, Takaoka Y, et al. Intraventricular cerebral neuroblastoma. Analysis of subtypes and comparison with hemispheric neuroblastoma. Arch Pathol Lab Med. 1994;118:897–911.
65. McCabe MG, Ichimura K, Liu L, et al. High-resolution array-based comparative genomic hybridization of medulloblastomas and supratentorial primitive neuroectodermal tumors. J Neuropathol Exp Neurol. 2006;65:549–61.
66. Russo C, Pellarin M, Tingby O, et al. Comparative genomic hybridization in patients with supratentorial and infratentorial primitive neuroectodermal tumors. Cancer. 1999;86:331–9.
67. Lorentzen M, Hagerstrand I. Congenital ependymoblastoma. Acta Neuropathol. 1980;49:71–4.
68. Langford LA. The ultrastructure of the ependymoblastoma. Acta Neuropathol. 1986;71:136–41.
69. Cruz-Sanchez FF, Haustein J, Rossi ML, et al. Ependymoblastoma: a histological, immunohistological and ultrastructural study of five cases. Histopathology. 1988;12:17–27.
70. Ehret M, Jacobi G, Hey A, et al. Embryonal brain neoplasms in the neonatal period and early infancy. Clin Neuropathol. 1987; 6:218–23.
71. Mannoji H, Becker LE. Ependymal and choroid plexus tumors. Cytokeratin and GFAP expression. Cancer. 1988;61:1377–85.
72. Rickert CH, Paulus W. Epidemiology of central nervous system tumors in childhood and adolescence based on the new WHO classification. Childs Nerv Syst. 2001;17:503–11.
73. Biegel JA. Molecular genetics of atypical teratoid/rhabdoid tumor. Neurosurg Focus. 2006;20:E11.
74. Las Heras F, Pritzker KP. Adult variant of atypical teratoid/rhabdoid tumor: immunohistochemical and ultrastructural confirmation of a rare tumor in the sella tursica. Pathol Res Pract. 2010;206:788–91.
75. Raisanen J, Biegel JA, Hatanpaa KJ, et al. Chromosome 22q deletions in atypical teratoid/rhabdoid tumors in adults. Brain Pathol. 2005;15:23–8.
76. Makuria AT, Rushing EJ, McGrail KM, et al. Atypical teratoid rhabdoid tumor (AT/RT) in adults: review of four cases. J Neurooncol. 2008;88:321–30.
77. Takahashi K, Nishihara H, Katoh M, et al. Case of atypical teratoid/rhabdoid tumor in an adult, with long survival. Brain Tumor Pathol. 2011;28:71–6.
78. Samaras V, Stamatelli A, Samaras E, et al. Atypical teratoid/rhabdoid tumor of the central nervous system in an 18-year-old patient. Clin Neuropathol. 2009;28:1–10.
79. Meyers SP, Khademian ZP, Biegel JA, et al. Primary intracranial atypical teratoid/rhabdoid tumors of infancy and childhood: MRI features and patient outcomes. AJNR Am J Neuroradiol. 2006;27: 962–71.
80. Koral K, Gargan L, Bowers DC, et al. Imaging characteristics of atypical teratoid-rhabdoid tumor in children compared with medulloblastoma. AJR Am J Roentgenol. 2008;190:809–14.
81. Fleming AJ, Hukin J, Rassekh R, et al. Atypical teratoid rhabdoid tumors (ATRTs): the British Columbia's Children's Hospital's experience, 1986–2006. Brain Pathol. 2012;22:625–35.
82. Haberler C, Laggner U, Slavc I, et al. Immunohistochemical analysis of INI1 protein in malignant pediatric CNS tumors: Lack of INI1 in atypical teratoid/rhabdoid tumors and in a fraction of primitive neuroectodermal tumors without rhabdoid phenotype. Am J Surg Pathol. 2006;30:1462–8.
83. Bourdeaut F, Freneaux P, Thuille B, et al. hSNF5/INI1-deficient tumours and rhabdoid tumours are convergent but not fully overlapping entities. J Pathol. 2007;211:323–30.
84. Biegel JA, Rorke LB, Packer RJ, et al. Monosomy 22 in rhabdoid or atypical tumors of the brain. J Neurosurg. 1990;73:710–4.
85. Rorke LB, Packer RJ, Biegel JA. Central nervous system atypical teratoid/rhabdoid tumors of infancy and childhood: definition of an entity. J Neurosurg. 1996;85:56–65.
86. Roberts CW, Biegel JA. The role of SMARCB1/INI1 in development of rhabdoid tumor. Cancer Biol Ther. 2009;8:412–6.
87. Biegel JA, Zhou JY, Rorke LB, et al. Germ-line and acquired mutations of INI1 in atypical teratoid and rhabdoid tumors. Cancer Res. 1999;59:74–9.
88. Bruggers CS, Bleyl SB, Pysher T, et al. Clinicopathologic comparison of familial versus sporadic atypical teratoid/rhabdoid tumors (AT/RT) of the central nervous system. Pediatr Blood Cancer. 2011;56:1026–31.
89. Donner LR, Wainwright LM, Zhang F, et al. Mutation of the INI1 gene in composite rhabdoid tumor of the endometrium. Hum Pathol. 2007;38:935–9.
90. Perry A, Fuller CE, Judkins AR, et al. INI1 expression is retained in composite rhabdoid tumors, including rhabdoid meningiomas. Mod Pathol. 2005;18:951–8.
91. Wang W, Cote J, Xue Y, et al. Purification and biochemical heterogeneity of the mammalian SWI-SNF complex. Embo J. 1996; 15:5370–82.
92. Judkins AR, Burger PC, Hamilton RL, et al. INI1 protein expression distinguishes atypical teratoid/rhabdoid tumor from choroid plexus carcinoma. J Neuropathol Exp Neurol. 2005;64:391–7.
93. Judkins AR, Mauger J, Ht A, et al. Immunohistochemical analysis of hSNF5/INI1 in pediatric CNS neoplasms. Am J Surg Pathol. 2004;28:644–50.
94. Savage N, Linn D, McDonough C, et al. Molecularly confirmed primary malignant rhabdoid tumor of the urinary bladder: implications of accurate diagnosis. Ann Diagn Pathol. 2012;16:504–7.

95. Trobaugh-Lotrario AD, Finegold MJ, Feusner JH. Rhabdoid tumors of the liver: rare, aggressive, and poorly responsive to standard cytotoxic chemotherapy. Pediatr Blood Cancer. 2011;57:423–8.
96. Hollmann TJ, Hornick JL. INI1-deficient tumors: diagnostic features and molecular genetics. Am J Surg Pathol. 2011;35:e47–63.
97. Kreiger PA, Judkins AR, Russo PA, et al. Loss of INI1 expression defines a unique subset of pediatric undifferentiated soft tissue sarcomas. Mod Pathol. 2009;22:142–50.
98. Rieske P, Zakrzewska M, Piaskowski S, et al. Molecular heterogeneity of meningioma with INI1 mutation. Mol Pathol. 2003;56:299–301.
99. Schmitz U, Mueller W, Weber M, et al. INI1 mutations in meningiomas at a potential hotspot in exon 9. Br J Cancer. 2001;84:199–201.
100. Tsai CY, Wong TT, Lee YH, et al. Intact INI1 gene region with paradoxical loss of protein expression in AT/RT: implications for a possible novel mechanism associated with absence of INI1 protein immunoreactivity. Am J Surg Pathol. 2012;36:128–33.
101. Biggs PJ, Garen PD, Powers JM, et al. Malignant rhabdoid tumor of the central nervous system. Hum Pathol. 1987;18:332–7.
102. Burger PC, Yu IT, Tihan T, et al. Atypical teratoid/rhabdoid tumor of the central nervous system: a highly malignant tumor of infancy and childhood frequently mistaken for medulloblastoma: a Pediatric Oncology Group study. Am J Surg Pathol. 1998;22:1083–92.
103. Antonelli M, Cenacchi G, Modena P, et al. Ultrastructural evidence of ependymal differentiation in a genetically proven atypical teratoid/rhabdoid tumor. Childs Nerv Syst. 2009;25:1627–31.
104. Gessi M, Giangaspero F, Lauriola L, et al. Embryonal tumors with abundant neuropil and true rosettes: a distinctive CNS primitive neuroectodermal tumor. Am J Surg Pathol. 2009;33:211–7.
105. Dunham C, Sugo E, Tobias V, et al. Embryonal tumor with abundant neuropil and true rosettes (ETANTR): report of a case with prominent neurocytic differentiation. J Neurooncol. 2007;84:91–8.
106. Al-Hussaini M, Abuirmeileh N, Swaidan M, et al. Embryonal tumor with abundant neuropil and true rosettes: a report of three cases of a rare tumor, with an unusual case showing rhabdomyoblastic and melanocytic differentiation. Neuropathology. 2011;31:620–5.
107. Paulus W, Kleihues P. Genetic profiling of CNS tumors extends histological classification. Acta Neuropathol. 2010;120:269–70.
108. Neelima R, Easwer HV, Kapilamoorthy TR, et al. Embryonal tumor with multilayered rosettes: Two case reports with a review of the literature. Neurol India. 2012;60:96–9.
109. Schindler G, Capper D, Meyer J, et al. Analysis of BRAF V600E mutation in 1,320 nervous system tumors reveals high mutation frequencies in pleomorphic xanthoastrocytoma, ganglioglioma and extra-cerebellar pilocytic astrocytoma. Acta Neuropathol. 2011;121:397–405.
110. Rodriguez FJ, Perry A, Gutmann DH, et al. Gliomas in neurofibromatosis type 1: a clinicopathologic study of 100 patients. J Neuropathol Exp Neurol. 2008;67:240–9.
111. Burkhard C, Di Patre PL, Schuler D, et al. A population-based study of the incidence and survival rates in patients with pilocytic astrocytoma. J Neurosurg. 2003;98:1170–4.
112. Dirks PB, Jay V, Becker LE, et al. Development of anaplastic changes in low-grade astrocytomas of childhood. Neurosurgery. 1994;34:68–78.
113. Tomlinson FH, Scheithauer BW, Hayostek CJ, et al. The significance of atypia and histologic malignancy in pilocytic astrocytoma of the cerebellum: a clinicopathologic and flow cytometric study. J Child Neurol. 1994;9:301–10.
114. Fulham MJ, Melisi JW, Nishimiya J, et al. Neuroimaging of juvenile pilocytic astrocytomas: an enigma. Radiology. 1993;189:221–5.
115. Lee YY, Van Tassel P, Bruner JM, et al. Juvenile pilocytic astrocytomas: CT and MR characteristics. AJR Am J Roentgenol. 1989;152:1263–70.
116. Fisher PG, Breiter SN, Carson BS, et al. A clinicopathologic reappraisal of brain stem tumor classification. Identification of pilocystic astrocytoma and fibrillary astrocytoma as distinct entities. Cancer. 2000;89:1569–76.
117. Takeuchi H, Kubota T, Sato K, et al. Ultrastructure of capillary endothelium in pilocytic astrocytomas. Brain Tumor Pathol. 2004;21:23–6.
118. Perilongo G, Garre ML, Giangaspero F. Low-grade gliomas and leptomeningeal dissemination: a poorly understood phenomenon. Childs Nerv Syst. 2003;19:197–203.
119. Tihan T, Fisher PG, Kepner JL, et al. Pediatric astrocytomas with monomorphous pilomyxoid features and a less favorable outcome. J Neuropathol Exp Neurol. 1999;58:1061–8.
120. Fernandez C, Figarella-Branger D, Girard N, et al. Pilocytic astrocytomas in children: prognostic factors—a retrospective study of 80 cases. Neurosurgery. 2003;53:544–53. Discussion 554-545.
121. French PJ, Barlow A, Barlow P, et al. A case of pilomyxoid astrocytoma presenting with CSF rhinorrhoea in a 15-year-old. Br J Neurosurg. 2009;23:545–7.
122. Alimohamadi M, Bidabadi MS, Ayan Z, et al. Pilomyxoid astrocytoma with involvement of the sella turcica in an adolescent. J Clin Neurosci. 2009;16:1648–9.
123. Paraskevopoulos D, Patsalas I, Karkavelas G, et al. Pilomyxoid astrocytoma of the cervical spinal cord in a child with rapid progression into glioblastoma: case report and literature review. Childs Nerv Syst. 2011;27:313–21.
124. van der Wal EJ, Azzarelli B, Edwards-Brown M. Malignant transformation of a chiasmatic pilocytic astrocytoma in a patient with diencephalic syndrome. Pediatr Radiol. 2003;33:207–10.
125. Lee IH, Kim JH, Suh YL, et al. Imaging characteristics of pilomyxoid astrocytomas in comparison with pilocytic astrocytomas. Eur J Radiol. 2011;79:311–6.
126. Johnson MW, Eberhart CG, Perry A, et al. Spectrum of pilomyxoid astrocytomas: intermediate pilomyxoid tumors. Am J Surg Pathol. 2010;34:1783–91.
127. Jeon YK, Cheon JE, Kim SK, et al. Clinicopathological features and global genomic copy number alterations of pilomyxoid astrocytoma in the hypothalamus/optic pathway: comparative analysis with pilocytic astrocytoma using array-based comparative genomic hybridization. Mod Pathol. 2008;21:1345–56.
128. Amatya VJ, Akazawa R, Sumimoto Y, et al. Clinicopathological and immunohistochemical features of three pilomyxoid astrocytomas: comparative study with 11 pilocytic astrocytomas. Pathol Int. 2009;59:80–5.
129. Goldman JE, Corbin E. Rosenthal fibers contain ubiquitinated alpha B-crystallin. Am J Pathol. 1991;139:933–8.
130. Katsetos CD, Krishna L. Lobar pilocytic astrocytomas of the cerebral hemispheres: I. Diagnosis and nosology. Clin Neuropathol. 1994;13:295–305.
131. Machen SK, Prayson RA. Cyclin D1 and MIB-1 immunohistochemistry in pilocytic astrocytomas: a study of 48 cases. Hum Pathol. 1998;29:1511–6.
132. Matsumoto T, Fujii T, Yabe M, et al. MIB-1 and p53 immunocytochemistry for differentiating pilocytic astrocytomas and astrocytomas from anaplastic astrocytomas and glioblastomas in children and young adults. Histopathology. 1998;33:446–52.
133. Tihan T, Ersen A, Qaddoumi I, et al. Pathologic characteristics of pediatric intracranial pilocytic astrocytomas and their impact on outcome in 3 countries: a multi-institutional study. Am J Surg Pathol. 2012;36:43–55.
134. Lewis RA, Gerson LP, Axelson KA, et al. von Recklinghausen neurofibromatosis. II. Incidence of optic gliomata. Ophthalmology. 1984;91:929–35.
135. Fuller CE, Frankel B, Smith M, et al. Suprasellar monomorphous pilomyxoid neoplasm: an ultrastructural analysis. Clin Neuropathol. 2001;20:256–62.
136. Jeuken JW, Wesseling P. MAPK pathway activation through BRAF gene fusion in pilocytic astrocytomas; a novel oncogenic

fusion gene with diagnostic, prognostic, and therapeutic potential. J Pathol. 2010;222:324–8.
137. Tian Y, Rich BE, Vena N, et al. Detection of KIAA1549-BRAF fusion transcripts in formalin-fixed paraffin-embedded pediatric low-grade gliomas. J Mol Diagn. 2011;13:669–77.
138. Hawkins C, Walker E, Mohamed N, et al. BRAF-KIAA1549 fusion predicts better clinical outcome in pediatric low-grade astrocytoma. Clin Cancer Res. 2011;17:4790–8.
139. Rodriguez EF, Scheithauer BW, Giannini C, et al. PI3K/AKT pathway alterations are associated with clinically aggressive and histologically anaplastic subsets of pilocytic astrocytoma. Acta Neuropathol. 2011;121:407–20.
140. Cheng Y, Pang JC, Ng HK, Ding M, Zhang SF, Zheng J, Liu DG, Poon WS. HYPERLINK "/pubmed/11119125"Pilocytic astrocytomas do not show most of the genetic changes commonly seen in diffuse astrocytomas. Histopathology. 2000 Nov;37(5):437-44. PMID: 11119125.
141. Rosenblum MK, Erlandson RA, Budzilovich GN. The lipid-rich epithelioid glioblastoma. Am J Surg Pathol. 1991;15:925–34.
142. Suri V, Jha P, Agarwal S, et al. Molecular profile of oligodendrogliomas in young patients. Neuro Oncol. 2011;13:1099–106.
143. Kreiger PA, Okada Y, Simon S, et al. Losses of chromosomes 1p and 19q are rare in pediatric oligodendrogliomas. Acta Neuropathol. 2005;109:387–92.
144. Lipper MH, Eberhard DA, Phillips CD, et al. Pleomorphic xanthoastrocytoma, a distinctive astroglial tumor: neuroradiologic and pathologic features. AJNR Am J Neuroradiol. 1993;14:1397–404.
145. Lach B, Duggal N, DaSilva VF, et al. Association of pleomorphic xanthoastrocytoma with cortical dysplasia and neuronal tumors. A report of three cases. Cancer. 1996;78:2551–63.
146. Im SH, Chung CK, Kim SK, et al. Pleomorphic xanthoastrocytoma: a developmental glioneuronal tumor with prominent glioproliferative changes. J Neurooncol. 2004;66:17–27.
147. Giannini C, Scheithauer BW, Burger PC, et al. Pleomorphic xanthoastrocytoma: what do we really know about it? Cancer. 1999;85:2033–45.
148. Pahapill PA, Ramsay DA, Del Maestro RF. Pleomorphic xanthoastrocytoma: case report and analysis of the literature concerning the efficacy of resection and the significance of necrosis. Neurosurgery. 1996;38:822–8. Discussion 828-829.
149. Hirose T, Giannini C, Scheithauer BW. Ultrastructural features of pleomorphic xanthoastrocytoma: a comparative study with glioblastoma multiforme. Ultrastruct Pathol. 2001;25:469–78.
150. Martinez-Diaz H, Kleinschmidt-DeMasters BK, Powell SZ, et al. Giant cell glioblastoma and pleomorphic xanthoastrocytoma show different immunohistochemical profiles for neuronal antigens and p53 but share reactivity for class III beta-tubulin. Arch Pathol Lab Med. 2003;127:1187–91.
151. Dougherty MJ, Santi M, Brose MS, et al. Activating mutations in BRAF characterize a spectrum of pediatric low-grade gliomas. Neuro Oncol. 2010;12:621–30.
152. Yang S, Wetzel S, Law M, et al. Dynamic contrast-enhanced T2*-weighted MR imaging of gliomatosis cerebri. AJNR Am J Neuroradiol. 2002;23:350–5.
153. Armao DM, Stone J, Castillo M, et al. Diffuse leptomeningeal oligodendrogliomatosis: radiologic/pathologic correlation. AJNR Am J Neuroradiol. 2000;21:1122–6.
154. Rodriguez FJ, Perry A, Rosenblum MK, et al. Disseminated oligodendroglial-like leptomeningeal tumor of childhood: a distinctive clinicopathologic entity. Acta Neuropathol. 2012;124:627–41.
155. Schniederjan MJ, Alghamdi S, Castellano-Sanchez A, et al. Diffuse leptomeningeal neuroepithelial tumor: 9 pediatric cases with chromosome 1p/19q deletion status and IDH1 (R132H) immunohistochemistry. Am J Surg Pathol. 2013;37:763–71.
156. Ko MW, Turkeltaub PE, Lee EB, et al. Primary diffuse leptomeningeal gliomatosis mimicking a chronic inflammatory meningitis. J Neurol Sci. 2009;278:127–31.
157. Koeller KK, Henry JM. From the archives of the AFIP: superficial gliomas—radiologic-pathologic correlation. Armed Forces Institute of Pathology. Radiographics. 2001;21:1533–56.
158. Miller DC, Lang FF, Epstein FJ. Central nervous system gangliogliomas. Part 1: pathology. J Neurosurg. 1993;79:859–66.
159. Prayson RA, Khajavi K, Comair YG. Cortical architectural abnormalities and MIB1 immunoreactivity in gangliogliomas: a study of 60 patients with intracranial tumors. J Neuropathol Exp Neurol. 1995;54:513–20.
160. Donson AM, Kleinschmidt-Demasters BK, Aisner DL, et al. Pediatric brainstem gangliogliomas show BRAF mutation in a high percentage of cases. Brain Pathol. 2013;24(2):173–83.
161. Dahiya S, Haydon DH, Alvarado D, et al. BRAF (V600E) mutation is a negative prognosticator in pediatric ganglioglioma. Acta Neuropathol. 2013;125:901–10.
162. Blumcke I, Giencke K, Wardelmann E, et al. The CD34 epitope is expressed in neoplastic and malformative lesions associated with chronic, focal epilepsies. Acta Neuropathol. 1999;97:481–90.
163. Soffer D, Umansky F, Goldman JE. Ganglioglioma with neurofibrillary tangles (NFTs): neoplastic NFTs share antigenic determinants with NFTs of Alzheimer's disease. Acta Neuropathol. 1995;89:451–3.
164. Blumenthal GM, Dennis PA. PTEN hamartoma tumor syndromes. Eur J Hum Genet. 2008;16:1289–300.
165. Pilarski R, Burt R, Kohlman W, et al. Cowden syndrome and the PTEN hamartoma tumor syndrome: systematic review and revised diagnostic criteria. J Natl Cancer Inst. 2013;105:1607–16.
166. Shin JH, Lee HK, Khang SK, et al. Neuronal tumors of the central nervous system: radiologic findings and pathologic correlation. Radiographics. 2002;22:1177–89.
167. Tenreiro-Picon OR, Kamath SV, Knorr JR, et al. Desmoplastic infantile ganglioglioma: CT and MRI features. Pediatr Radiol. 1995;25:540–3.
168. Koelsche C, Sahm F, Paulus W, et al. BRAF V600E expression and distribution in desmoplastic infantile astrocytoma/ganglioglioma. Neuropathol Appl Neurobiol. 2014;40:337–44.
169. De Munnynck K, Van Gool S, Van Calenbergh F, et al. Desmoplastic infantile ganglioglioma: a potentially malignant tumor? Am J Surg Pathol. 2002;26:1515–22.
170. Fernandez C, Girard N, Paz Paredes A, et al. The usefulness of MR imaging in the diagnosis of dysembryoplastic neuroepithelial tumor in children: a study of 14 cases. AJNR Am J Neuroradiol. 2003;24:829–34.
171. Chappe C, Padovani L, Scavarda D, et al. Dysembryoplastic neuroepithelial tumors share with pleomorphic xanthoastrocytomas and gangliogliomas BRAF (V600E) mutation and expression. Brain Pathol. 2013;23:574–83.
172. Stosic-Opincal et al. Papillary glioneuronal tumor. AJR Am J Roentgenol. 2005;185(1):265–7.
173. Xiao H et al. Papillary glioneuronal tumor: radiological evidence of a newly established tumor entity. J Neuroimaging. 2011;21(3):297–302.
174. Agarwal S, Sharma MC, Singh G, et al. Papillary glioneuronal tumor: a rare entity—report of four cases and brief review of literature. Childs Nerv Syst. 2012;28:1897–904.
175. Rosenblum MK. The 2007 WHO classification of nervous system tumors: newly recognized members of the mixed glioneuronal group. Brain Pathol. 2007;17:308–13.
176. Smith AB, Smirniotopoulos JG, Horkanyne-Szakaly I. From the radiologic pathology archives: intraventricular neoplasms: radiologic-pathologic correlation. Radiographics. 2013;33:21–43.
177. Marhold F, Preusser M, Dietrich W, et al. Clinicoradiological features of rosette-forming glioneuronal tumor (RGNT) of the fourth

ventricle: report of four cases and literature review. J Neurooncol. 2008;90:301–8.
178. Komori T, Scheithauer BW, Hirose T. A rosette-forming glioneuronal tumor of the fourth ventricle: infratentorial form of dysembryoplastic neuroepithelial tumor? Am J Surg Pathol. 2002;26: 582–91.
179. Kerkovsky M, Zitterbart K, Svoboda K, et al. Central neurocytoma: the neuroradiological perspective. Childs Nerv Syst. 2008; 24:1361–9.
180. Kubota T, Hayashi M, Kawano H, et al. Central neurocytoma: immunohistochemical and ultrastructural study. Acta Neuropathol. 1991;81:418–27.
181. Preusser M, Laggner U, Haberler C, et al. Comparative analysis of NeuN immunoreactivity in primary brain tumours: conclusions for rational use in diagnostic histopathology. Histopathology. 2006;48:438–44.
182. Preusser M, Budka H, Rossler K, et al. OLIG2 is a useful immunohistochemical marker in differential diagnosis of clear cell primary CNS neoplasms. Histopathology. 2007;50:365–70.
183. Horstmann S, Perry A, Reifenberger G, et al. Genetic and expression profiles of cerebellar liponeurocytomas. Brain Pathol. 2004; 14:281–9.
184. Yuh EL, Barkovich AJ, Gupta N. Imaging of ependymomas: MRI and CT. Childs Nerv Syst. 2009;25:1203–13.
185. Fouladi M, Helton K, Dalton J, et al. Clear cell ependymoma: a clinicopathologic and radiographic analysis of 10 patients. Cancer. 2003;98:2232–44.
186. Zamecnik J, Chanova M, Kodet R. Expression of thyroid transcription factor 1 in primary brain tumours. J Clin Pathol. 2004;57:1111–3.
187. Yao Y, Mack SC, Taylor MD. Molecular genetics of ependymoma. Chin J Cancer. 2011;30:669–81.
188. Bell JW, Osborn AG, Salzman KL, et al. Neuroradiologic characteristics of astroblastoma. Neuroradiology. 2007;49:203–9.
189. Port JD, Brat DJ, Burger PC, et al. Astroblastoma: radiologic-pathologic correlation and distinction from ependymoma. AJNR Am J Neuroradiol. 2002;23:243–7.
190. Brat DJ, Hirose Y, Cohen KJ, et al. Astroblastoma: clinicopathologic features and chromosomal abnormalities defined by comparative genomic hybridization. Brain Pathol. 2000;10:342–52.
191. Jay V, Edwards V, Squire J, et al. Astroblastoma: report of a case with ultrastructural, cell kinetic, and cytogenetic analysis. Pediatr Pathol. 1993;13:323–32.
192. Wang M, Tihan T, Rojiani AM, et al. Monomorphous angiocentric glioma: a distinctive epileptogenic neoplasm with features of infiltrating astrocytoma and ependymoma. J Neuropathol Exp Neurol. 2005;64:875–81.
193. Osborn AG, Salzman KL, Thurnher MM, et al. The new World Health Organization classification of central nervous system tumors: what can the neuroradiologist really say? AJNR Am J Neuroradiol. 2012;33:795–802.
194. Lu JQ, Patel S, Wilson BA, et al. Malignant glioma with angiocentric features. J Neurosurg Pediatr. 2013;11:350–5.
195. Marburger T, Prayson R. Angiocentric glioma: a clinicopathologic review of 5 tumors with identification of associated cortical dysplasia. Arch Pathol Lab Med. 2011;135:1037–41.
196. Raghunathan A, Olar A, Vogel H, et al. Isocitrate dehydrogenase 1 R132H mutation is not detected in angiocentric glioma. Ann Diagn Pathol. 2012;16:255–9.
197. Pomper MG, Passe TJ, Burger PC, et al. Chordoid glioma: a neoplasm unique to the hypothalamus and anterior third ventricle. AJNR Am J Neuroradiol. 2001;22:464–9.
198. Mittal S, Mittal M, Montes JL, et al. Hypothalamic hamartomas. Part 1. Clinical, neuroimaging, and neurophysiological characteristics. Neurosurg Focus. 2013;34:E6.
199. Coons SW, Rekate HL, Prenger EC, et al. The histopathology of hypothalamic hamartomas: study of 57 cases. J Neuropathol Exp Neurol. 2007;66:131–41.
200. Frye RE, Polling JS, Ma LC. Choroid plexus papilloma expansion over 7 years in Aicardi syndrome. J Child Neurol. 2007;22:484–7.
201. Taggard DA, Menezes AH. Three choroid plexus papillomas in a patient with Aicardi syndrome. A case report. Pediatr Neurosurg. 2000;33:219–23.
202. Trifiletti RR, Incorpora G, Polizzi A, et al. Aicardi syndrome with multiple tumors: a case report with literature review. Brain Dev. 1995;17:283–5.
203. Gozali AE, Britt B, Shane L, et al. Choroid plexus tumors; management, outcome, and association with the Li-Fraumeni syndrome: the Children's Hospital Los Angeles (CHLA) experience, 1991–2010. Pediatr Blood Cancer. 2012;58:905–9.
204. Schittenhelm J, Nagel C, Meyermann R, et al. Atypical teratoid/rhabdoid tumors may show morphological and immunohistochemical features seen in choroid plexus tumors. Neuropathology. 2011;31:461–7.
205. Irsutti M, Thorn-Kany M, Arrue P, et al. Suprasellar seeding of a benign choroid plexus papilloma of the fourth ventricle with local recurrence. Neuroradiology. 2000;42:657–61.
206. Jeibmann A, Hasselblatt M, Gerss J, et al. Prognostic implications of atypical histologic features in choroid plexus papilloma. J Neuropathol Exp Neurol. 2006;65:1069–73.
207. Shibahara J, Kashima T, Kikuchi Y, et al. Podoplanin is expressed in subsets of tumors of the central nervous system. Virchows Arch. 2006;448:493–9.
208. Kepes JJ, Collins J. Choroid plexus epithelium (normal and neoplastic) expresses synaptophysin. A potentially useful aid in differentiating carcinoma of the choroid plexus from metastatic papillary carcinomas. J Neuropathol Exp Neurol. 1999;58:398–401.
209. Carlotti Jr CG, Salhia B, Weitzman S, et al. Evaluation of proliferative index and cell cycle protein expression in choroid plexus tumors in children. Acta Neuropathol. 2002;103:1–10.
210. Ferreira MA, Feiz-Erfan I, Zabramski JM, et al. Endolymphatic sac tumor: unique features of two cases and review of the literature. Acta Neurochir (Wien). 2002;144:1047–53.
211. Kupferman ME, Bigelow DC, Carpentieri DF, et al. Endolymphatic sac tumor in a 4-year-old boy. Otol Neurotol. 2004;25:782–6.
212. Schittenhelm J, Roser F, Tatagiba M, et al. Diagnostic value of EAAT-1 and Kir7.1 for distinguishing endolymphatic sac tumors from choroid plexus tumors. Am J Clin Pathol. 2012;138:85–9.
213. Al-Hussaini M, Sultan I, Abuirmileh N, et al. Pineal gland tumors: experience from the SEER database. J Neurooncol. 2009;94:351–8.
214. Smith AB, Rushing EJ, Smirniotopoulos JG. From the archives of the AFIP: lesions of the pineal region—radiologic-pathologic correlation. Radiographics. 2010;30:2001–20.
215. Jouvet A, Saint-Pierre G, Fauchon F, et al. Pineal parenchymal tumors: a correlation of histological features with prognosis in 66 cases. Brain Pathol. 2000;10:49–60.
216. Dahiya S, Perry A. Pineal tumors. Adv Anat Pathol. 2010; 17:419–27.
217. Plowman PN, Pizer B, Kingston JE. Pineal parenchymal tumours: II. On the aggressive behaviour of pineoblastoma in patients with an inherited mutation of the RB1 gene. Clin Oncol (R Coll Radiol). 2004;16:244–7.
218. Tong T, Zhenwei Y, Xiaoyuan F. MRI and 1H-MRS on diagnosis of pineal region tumors. Clin Imaging. 2012;36:702–9.
219. Buffenoir K, Rigoard P, Wager M, et al. Papillary tumor of the pineal region in a child: case report and review of the literature. Childs Nerv Syst. 2008;24:379–84.
220. Abela L, Rushing EJ, Ares C, et al. Pediatric papillary tumors of the pineal region: to observe or to treat following gross total resection? Childs Nerv Syst. 2013;29:307–10.

221. Cykowski MD, Wartchow EP, Mierau GW, et al. Papillary tumor of the pineal region: ultrastructural study of a case. Ultrastruct Pathol. 2012;36:68–77.
222. Jouvet A, Fauchon F, Liberski P, et al. Papillary tumor of the pineal region. Am J Surg Pathol. 2003;27:505–12.
223. Perry A, Dehner LP. Meningeal tumors of childhood and infancy. An update and literature review. Brain Pathol. 2003;13:386–408.
224. Wiebe S, Munoz DG, Smith S, et al. Meningioangiomatosis. A comprehensive analysis of clinical and laboratory features. Brain. 1999;122(Pt 4):709–26.
225. Kim NR, Choe G, Shin SH, et al. Childhood meningiomas associated with meningioangiomatosis: report of five cases and literature review. Neuropathol Appl Neurobiol. 2002;28:48–56.
226. Wixom C, Chadwick AE, Krous HF. Sudden, unexpected death associated with meningioangiomatosis: case report. Pediatr Dev Pathol. 2005;8:240–4.
227. Perry A, Kurtkaya-Yapicier O, Scheithauer BW, et al. Insights into meningioangiomatosis with and without meningioma: a clinicopathologic and genetic series of 24 cases with review of the literature. Brain Pathol. 2005;15:55–65.
228. Yao Z, Wang Y, Zee C, et al. Computed tomography and magnetic resonance appearance of sporadic meningioangiomatosis correlated with pathological findings. J Comput Assist Tomogr. 2009;33:799–804.
229. Arcos A, Serramito R, Santin JM, et al. Meningioangiomatosis: clinical-radiological features and surgical outcome. Neurocirugia (Astur). 2010;21:461–6.
230. Wang Y, Gao X, Yao ZW, et al. Histopathological study of five cases with sporadic meningioangiomatosis. Neuropathology. 2006;26:249–56.
231. Prayson RA. Meningioangiomatosis. A clinicopathologic study including MIB1 immunoreactivity. Arch Pathol Lab Med. 1995;119:1061–4.
232. Thuijs NB, Uitdehaag BM, Van Ouwerkerk WJ, et al. Pediatric meningiomas in The Netherlands 1974–2010: a descriptive epidemiological case study. Childs Nerv Syst. 2012;28:1009–15.
233. Mehta N, Bhagwati S, Parulekar G. Meningiomas in children: a study of 18 cases. J Pediatr Neurosci. 2009;4:61–5.
234. Legius E, Vles JS, Casaer P, et al. Intraparenchymal meningioma in a 14-month-old infant: case report. Brain Dev. 1985;7:622–4.
235. Rippe DJ, Boyko OB, Friedman HS, et al. Gd-DTPA-enhanced MR imaging of leptomeningeal spread of primary intracranial CNS tumor in children. AJNR Am J Neuroradiol. 1990;11:329–32.
236. Grois N, Prayer D, Prosch H, et al. Neuropathology of CNS disease in Langerhans cell histiocytosis. Brain. 2005;128:829–38.
237. Grois N, Prosch H, Waldhauser F, et al. Pineal gland abnormalities in Langerhans cell histiocytosis. Pediatr Blood Cancer. 2004;43:261–6.
238. Schabet M. Epidemiology of primary CNS lymphoma. J Neurooncol. 1999;43:199–201.
239. Abla O, Weitzman S, Blay JY, et al. Primary CNS lymphoma in children and adolescents: a descriptive analysis from the International Primary CNS Lymphoma Collaborative Group (IPCG). Clin Cancer Res. 2011;17:346–52.
240. Fukushima S, Terasaki M, Sakata K, et al. Sensitivity and usefulness of anti-phosphohistone-H3 antibody immunostaining for counting mitotic figures in meningioma cases. Brain Tumor Pathol. 2009;26:51–7.
241. Lu QR, Yuk D, Alberta JA, et al. Sonic hedgehog-regulated oligodendrocyte lineage genes encoding bHLH proteins in the mammalian central nervous system. Neuron. 2000;25:317–29.
242. Zhou Q, Wang S, Anderson DJ. Identification of a novel family of oligodendrocyte lineage-specific basic helix-loop-helix transcription factors. Neuron. 2000;25:331–43.
243. Yokoo H, Nobusawa S, Takebayashi H, et al. Anti-human Olig2 antibody as a useful immunohistochemical marker of normal oligodendrocytes and gliomas. Am J Pathol. 2004;164:1717–25.
244. Otero JJ, Rowitch D, Vandenberg S. OLIG2 is differentially expressed in pediatric astrocytic and in ependymal neoplasms. J Neurooncol. 2011;104:423–38.
245. Mokhtari K, Paris S, Aguirre-Cruz L, et al. Olig2 expression, GFAP, p53 and 1p loss analysis contribute to glioma subclassification. Neuropathol Appl Neurobiol. 2005;31:62–9.
246. Ligon KL, Alberta JA, Kho AT, et al. The oligodendroglial lineage marker OLIG2 is universally expressed in diffuse gliomas. J Neuropathol Exp Neurol. 2004;63:499–509.
247. Wolf HK, Buslei R, Schmidt-Kastner R, et al. NeuN: a useful neuronal marker for diagnostic histopathology. J Histochem Cytochem. 1996;44:1167–71.
248. Koperek O, Gelpi E, Birner P, et al. Value and limits of immunohistochemistry in differential diagnosis of clear cell primary brain tumors. Acta Neuropathol. 2004;108:24–30.
249. Hamilton SR, Liu B, Parsons RE, et al. The molecular basis of Turcot's syndrome. N Engl J Med. 1995;332:839–47.
250. Hirsch B, Shimamura A, Moreau L, et al. Association of biallelic BRCA2/FANCD1 mutations with spontaneous chromosomal instability and solid tumors of childhood. Blood. 2004;103:2554–9.
251. Offit K, Levran O, Mullaney B, et al. Shared genetic susceptibility to breast cancer, brain tumors, and Fanconi anemia. J Natl Cancer Inst. 2003;95:1548–51.
252. Evans DG, Farndon PA, Burnell LD, et al. The incidence of Gorlin syndrome in 173 consecutive cases of medulloblastoma. Br J Cancer. 1991;64:959–61.
253. Schofield D, West DC, Anthony DC, et al. Correlation of loss of heterozygosity at chromosome 9q with histological subtype in medulloblastomas. Am J Pathol. 1995;146:472–80.
254. Aszterbaum M, Rothman A, Johnson RL, et al. Identification of mutations in the human PATCHED gene in sporadic basal cell carcinomas and in patients with the basal cell nevus syndrome. J Invest Dermatol. 1998;110:885–8.
255. Hahn H, Wicking C, Zaphiropoulous PG, et al. Mutations of the human homolog of Drosophila patched in the nevoid basal cell carcinoma syndrome. Cell. 1996;85:841–51.
256. Malkin D, Li FP, Strong LC, et al. Germ line p53 mutations in a familial syndrome of breast cancer, sarcomas, and other neoplasms. Science. 1990;250:1233–8.
257. Taylor MD, Mainprize TG, Rutka JT, et al. Medulloblastoma in a child with Rubenstein-Taybi syndrome: case report and review of the literature. Pediatr Neurosurg. 2001;35:235–8.
258. Rogers L, Pattisapu J, Smith RR, et al. Medulloblastoma in association with the Coffin-Siris syndrome. Childs Nerv Syst. 1988;4:41–4.
259. Fleck BJ, Pandya A, Vanner L, et al. Coffin-Siris syndrome: review and presentation of new cases from a questionnaire study. Am J Med Genet. 2001;99:1–7.
260. Osterling WL, Boyer RS, Hedlund GL, et al. MPPH syndrome: two new cases. Pediatr Neurol. 2011;44:370–3.
261. Slade I, Bacchelli C, Davies H, et al. DICER1 syndrome: clarifying the diagnosis, clinical features and management implications of a pleiotropic tumour predisposition syndrome. J Med Genet. 2011;48:273–8.
262. van Slegtenhorst M, de Hoogt R, Hermans C, Nellist M, Janssen B, Verhoef S, et al. Identification of the tuberous sclerosis gene TSC1 on chromosome 9q34. Science. 1997;277(5327):805–8.
263. Pollack IF, Mulvihill JJ. Neurofibromatosis 1 and 2. Brain Pathol. 1997;7(2):823–36.
264. von Deimling A, Fimmers R, Schmidt MC, Bender B, Fassbender F, Nagel J, et al. Comprehensive allelotype and genetic anaysis of

466 human nervous system tumors. J Neuropathol Exp Neurol. 2000;59(6):544–58.
265. Maddock IR, Moran A, Maher ER, Teare MD, Norman A, Payne SJ, et al. A genetic register for von Hippel-Lindau disease. J Med Genet. 1996;33(2):120–7
266. Vorechovsky et al. (1997) et al. Patched (ptch)-associated preferential expression of smoothened (smoh) in human basal cell carcinoma of the skin. Cancer Res. 1997;57(21):4731–5.
267. Sutphen R, Diamond TM, Minton SE, Peacocke M, Tsou HC, Root AW. Severe Lhermitte-Duclos disease with unique germline mutation of PTEN. Am J Med Genet. 1999;82(4):290–3.
268. Robinson S, Cohen AR. Cowden disease and Lhermitte-Duclos disease: characterization of a new phakomatosis. Neurosurgery. 2000;46(2):371–83.
269. Cavenee WK, Burger PC, Leung SY, van Meir EG. Turcot syndrome. In: Louis DN, Ohgaki H, Wiestler OD, Cavenee WK, editors. WHO classification of tumours of the central nervous system. Lyon, France: International Agency for Research on Cancer (IARC); 2007. p. 229–31.
270. Laberge-le Couteulx S, Jung HH, Labauge P, Houtteville JP, Lescoat C, Cecillon M, et al. Truncating mutations in CCM1, encoding KRIT1, cause hereditary cavernous angiomas. Nat Genet. 1999;23(2):189–93.
271. Taylor MD, Gokgoz N, Andrulis IL, Mainprize TG, Drake JM, Rutka JT. Familial posterior fossa brain tumors of infancy secondary to germline mutation of the hSNF5 gene. Am J Hum Genet. 2000;66(4):1403–6.
272. Sopta M, Gallie BL, Gill RM, Hamel PA, Muncaster M, Zacksenhaus E, et al. The retinoblastoma protein and the cell cycle. Semin Cancer Biol. 1992;3(3):107–13.
273. Pratt CB, Raimondi SC, Kaste SC, Heaton DM, Mounce KG, Mandrell B, et al. Outcome for patients with constitutional 13q chromosomal abnormalities and retinoblastoma. Pediatr Hematol Oncol. 1994;11(5):541–7.
274. Tachibana I, Smith JS, Sato K, Hosek SM, Kimmel DW, Jenkins RB. Investigation of germline PTEN, p53, p16(INK4A)/p14(ARF), and CDK4 alterations in familial glioma. Am J Med Genet. 2000;92(2):136–41.